

Technische Universität Dresden
Fakultät Maschinenwesen

Development of Novel Blends based on Rubber and
in-situ Synthesized Polyurethane-urea

Von der Fakultät Maschinenwesen der Technischen Universität Dresden

zur

Erlangung des akademischen Grades
Doktoringenieur (Dr.-Ing.)
angenommene Dissertation

vorgelegt von

M.Sc. Tahir, Muhammad

geboren am 17.03.1982 in Lahore, Pakistan

Tag der Einreichung: 18.08.2017

Tag der Verteidigung: 08.12.2017

Gutachter: Prof. Dr. rer. nat. habil. Gert Heinrich
Prof. Dr. Dr. h.c. József Karger-Kocsis

Prof. Dr.rer.medic. Hans-Peter Wiesmann
Vorsitzender der Promotionskommission

Dedicated to my Töchter
Kanwal and Ayesha

Acknowledgements

First of all, I would like to thank Dr. Nasir Mahmood for his valuable guidance, which paved my way to the PhD studies at the Technische Universität Dresden, Germany. His consistent suggestions through all the stages of my doctoral research were quite helpful. I am highly indebted to Dr. Klaus Werner Stöckelhuber for the intellectual ideas, suggestions and discussions, which helped me a lot to successfully challenge the doctoral research project at the Leibniz-Institut für Polymerforschung Dresden (IPF). I am thankful to Jun.-Prof. Dr. Sven Wießner for his interest, necessary support and suggestions. I am grateful to Dr. Amit Das for his words of encouragement and motivation. I appreciate Mr. René Jurk for the operational demonstrations of lab equipment, without which the lab sessions may not be so pleasant and great.

This research work could have never been realized without the helpful, envisaged and thoughtful supervision of Prof. Dr. rer. nat. habil. Gert Heinrich.

I am grateful to the talented and skillful coworkers at IPF. In particular, I am thankful to Dr. Mikhail Malanin for FTIR measurements, Dr. Hartmut Komber for ^1H NMR spectroscopy, Dr. Petr Formanek and Mrs. Uta Reuter for TEM measurements, Dr. Regine Boldt for SEM measurements, Dr. Dieter Jehnichen for XRD, Dr. Roland Vogel for rheological testing, Dr. Dieter Fischer for RAMAN measurements and Mr. Holger Scheibner for tensile testing.

Lastly, I shall remain indebted to my parents, Mrs. Azra Parveen and Mr. Muhammad Sadiq, for their encouraging words and well wishes. I would extend heartiest appreciation to my wife, Mubsharah Rashid, for her persistence support and patience during my PhD studies. My daughters, Kanwal and Ayesha, are my source of continuous strength, which greatly contributed to successfully accomplish this challenging task of my doctoral dissertation.

Eidesstattliche Erklärung

Hiermit versichere ich, dass ich die vorliegende Arbeit ohne unzulässige Hilfe Dritter und ohne Benutzung anderer als der angegebenen Hilfsmittel angefertigt habe; die aus fremden Quellen direkt oder indirekt übernommenen Gedanken sind als solche kenntlich gemacht.

Dresden, 18.08.2017

Tahir, Muhammad

Abstract

Polyurethane and the analogous 'polyurethane-urea' are high performance polymeric materials having remarkable properties such as high stiffness, abrasion and tear strengths. In many studies, the low strength rubbers have been blended with various types of polyurethanes for new and improved materials. However, until now, the reported heterogeneous blends offer only a narrow temperature range of application due to the high temperature softening of their polyurethane (-urea) phase. In addition, the conventional solution-or melt-blending methods are time and energy intensive, which tend to forfeit the economical realization of the reported blends. In contrast to earlier studies, a simplified reactive blending process is suggested to synthesize polyurethane-urea via a prepolymer route during blending with rubbers to obtain novel elastomeric materials having extended performance characteristics.

The reactive blending process is opted to prepare blends based on nitrile butadiene rubber (NBR) and *in-situ* synthesized polyurethane-urea (PUU). The blending is carried out in an internal mixer at a preset temperature of 100°C. The critical temperatures of the reactive blending process are determined from the chemo-rheological analysis of a premix, composed of a 4,4'-diphenylmethane diisocyanate (MDI)/polyether (PTMEG) based prepolymer admixed with 1,3-phenylene diamine (mPD). The prepared NBR/PUU blends exhibit highly improved mechanical properties. Contrary to previous reports, the reinforced dynamic-mechanical responses of the novel blends remain stable till very high temperatures ($\geq 180^\circ\text{C}$).

The influence of diamine type on the *in-situ* synthesized polyurethane-urea and the performance of prepared blends are investigated. Four different diamines, namely 1,3-Phenylene diamine, 1,4-Bis(aminomethyl)benzene, 4,4'-Methylene-bis(2-chloroaniline) and 4,4'-(1,3-Phenylenediisopropylidene)bisaniline, are selected to chain extend the prepolymer to PUU during blending with NBR. The chemical and domain structure of the PUUs are found to greatly

influence the reinforced tensile and dynamic-mechanical responses of the NBR/PUU 70/30 blends.

The PUU (based on MDI/PTMEG prepolymer and mPD) is blended with polar (CR, XNBR) and nonpolar (NR, EPDM, sSBR) rubbers. PUU compatibilizes with all the rubbers irrespective of their polarity and reinforces their tensile and dynamic-mechanical characteristics.

The use of blends in industrial applications, for example, in a truck tire tread compound and as a roller covering material, is examined. In a simplified tire tread formulation, the carbon black for NR-CB composite is partially replaced with an equivalent quantity of PUU for NR/PUU-CB composite of similar hardness. The dynamic mechanical investigations reveal that the energy dissipation and strain dependent softening is high in NR-CB as compared to the NR/PUU-CB composite. In another application, NBR/PUU blend is successfully tested as a rubber roller covering material. The tested blend-covered roller retains its structural integrity and develops less heat build-up as compared to the silica filled NBR-covered roller. This shows a substantial suitability of the blend-covered rollers for film, printing and textile processing machinery.

These novel blends are considered to be the promising new materials for many commercial applications including wheels, rubber rollers, belts or pump impellers.

Kurzfassung

Polyurethane und das analoge "Polyurethan-Urea" sind Hochleistungs-Polymermaterialien mit bemerkenswerten Eigenschaften wie hoher Steifigkeit, Abrieb- und Reißfestigkeit. In mehreren Studien wurden bisher Elastomere geringer Festigkeit mit verschiedenen Arten von Polyurethanen verblendet, mit dem Ziel neue und verbesserte Werkstoffe zu entwickeln. Bisher sind diese heterogenen Blends jedoch aufgrund der Erweichung ihrer Polyurethan-(Urea)-Phase bei höheren Temperaturen nur in einem engen Temperaturbereich einsatzfähig. Darüber hinaus sind die konventionellen Lösungs- oder Schmelzmischverfahren zeit- und energieintensiv, was eine ökonomische Realisierung der so hergestellten Blends fraglich macht. Im Gegensatz zu früheren Studien wird ein vereinfachtes reaktives Mischverfahren vorgeschlagen, um Polyurethan-Urea über eine Prepolymer-Route während des Mischens mit Kautschuken zu synthetisieren, um neue elastomere Materialien mit deutlich verbesserten Leistungsmerkmalen zu erhalten.

Dieser reaktive Mischprozess wurde zur Herstellung von Blends auf Basis von Nitril-Butadien-Kautschuk (NBR) und in situ synthetisiertem Polyurethan-Urea (PUU) gewählt. Das Verblenden erfolgt in einem Innenmischer bei einer voreingestellten Temperatur von 100 °C. Die kritischen Temperaturen des reaktiven Mischprozesses werden mit Hilfe einer chemo-rheologischen Analyse der Vormischung bestimmt, bestehend aus einem auf 4,4'-Diphenylmethyldiisocyanat (MDI) / Polyether (PTMEG) basierten Prepolymer, gemischt mit 1,3-Phenylendiamin (mPD). Die so hergestellte NBR / PUU-Blends weisen stark verbesserte mechanische Eigenschaften auf. Im Gegensatz zu den konventionell gemischten Systemen bleibt die dynamisch-mechanische Verstärkung dieser neuartigen Blends bis zu sehr hohen Temperaturen (≥ 180 °C) stabil.

Der Einfluss des Diamin-Typs auf das in situ-synthetisierte Polyurethan-Urea und die Eigenschaftsprofile der damit hergestellten Mischungen wurde ebenfalls untersucht. Vier verschiedene Diamine, nämlich 1,3-Phenylendiamin, 1,4-Bis(aminomethyl)benzol, 4,4'-Methylen-bis(2-chloranilin) und 4,4'-(1,3-Phenylendiisopropyliden)bisanilin, wurden als chain-extender für die in-situ Reaktion während der Verblendens mit NBR ausgewählt. Es zeigte sich, dass sowohl die chemische Zusammensetzung, als auch die Domänenstruktur des PUU starken Einfluss auf die statische Zugfestigkeit und die dynamisch-mechanische Eigenschaften der NBR / PUU 70/30-Blends aufweisen.

PUU (basierend auf MDI / PTMEG-Prepolymer und mPD) wurde auch mit verschiedenen polaren (CR, XNBR) und unpolaren (NR, EPDM, sSBR) Kautschuken verblendet. Dabei zeigte sich, dass PUU kompatibel mit allen untersuchten Kautschuktypen, unabhängig von deren Polarität ist, und zu einer Verbesserung deren statischen- und dynamisch-mechanischen Eigenschaften führt.

Der Einsatz der elastomeren PUU-Blends wurde auch in industrierelevanten Anwendungen untersucht, so wurden z.B. Modellmischungen für den Einsatz in LKW-Reifenlaufstreifen oder als Walzenbezüge für die Textilindustrie hergestellt. In der vereinfachten LKW-Reifenlaufflächenmischung wird der verstärkende Füllstoff Ruß in der Naturkautschukmischung teilweise durch eine äquivalente Menge an PUU ersetzt, um ein Reifenmaterial mit ähnlicher Härte zu erhalten. Dynamisch-mechanische Untersuchungen zeigen, dass die Energiedissipation und die Spannungserweichung der Laufstreifenmischung durch den partiellen Einsatz von PUU anstelle von Ruß deutlich verbessert werden. In einer anderen Anwendung wurde der NBR / PUU-Blend erfolgreich als Gummiwalzenbezug getestet. Die getestete mit PUU-Blend-bezogene Walze behält im Prüfstandsversuch ihre strukturelle Integrität und zeigt einen geringeren

Wärmeaufbau im Vergleich zu der herkömmlichen Walze aus mit Silika gefüllten NBR. Dies zeigt eine grundsätzliche Eignung der PUU-Blends als Walzenmaterial für Folien-, Druck- und Textilverarbeitungsmaschinen.

Die neuartigen elastomeren PUU-Blends zeigen großes Potential als vielversprechende neue Werkstoffe für viele kommerzielle Anwendungen wie z.B. Reifenmaterialien, Gummiwalzen, Treibriemen oder Pumpenlaufräder.

Abbreviations

NBR	Nitrile butadiene rubber
XNBR	Carboxylated nitrile butadiene rubber
CR	Chloroprene rubber
NR	Natural rubber
SSBR	Solution Styrene butadiene rubber
EPDM	Ethylene propylene diene monomer
PUU	Polyurethane-urea
PTMEG	Poly (tetramethylene ether) glycol, Polytetrahydrofuran
SS	Soft segment
HS	Hard segment
PP	Prepolymer
MDI	4, 4'-diphenylmethane diisocyanate
mPD	1,3-phenylenediamine
pXD	1,4-Bis(aminomethyl)benzene
MBCA	4,4'-Methylene-bis(2-chloroaniline)
BisAM	4,4'-(1,3-Phenylenediisopropylidene)bisaniline
CB	Carbon black
NMR	Nuclear magnetic resonance
TEM	Transmission electron microscopy
SEM	Scanning electron microscopy
EDX	Energy dispersive X-ray spectroscopy
DMA	Dynamic mechanical analysis
WAXS	Wide angle X-ray scattering
GPC	Gel permeation chromatography

DMSO Dimethyl sulfoxide

DMAc Dimethylacetamide

OsO₄ Osmium tetroxide

Symbols

T_{premix} Temperature of premixing

T_{RB} Temperature of reactive blending

G' Storage modulus (shear mode)

G'' Loss modulus (shear mode)

E' Storage modulus (tensile mode)

E'' Loss modulus (tensile mode)

$\tan \delta$ Loss factor

T_o Onset temperature

T_c Crossover temperature

T_m Melting temperature

T_f Inflection point temperature

T_{soft} Softening temperature

M_L Minimum torque

M_H Maximum torque

T_g Glass transition temperature

M_n Number average molar mass

M_w Weight average molar mass

E'_0 Storage modulus at low strain

E'_∞ Storage modulus at high strain

$\Delta E'$ Payne effect

TABLE OF CONTENTS

1 INTRODUCTION	1
1.1 CHALLENGES	2
1.2 AIMS, OBJECTIVES AND APPROACH	3
1.3 SCHEME OF RESEARCH WORK	4
2 LITERATURE SURVEY	7
2.1 FUNDAMENTALS OF POLYURETHANES	7
2.2 OVERVIEW OF BLENDS BASED ON RUBBER AND POLYURETHANES	11
3 EXPERIMENTAL: MATERIALS, BLENDING PROCESS AND CHARACTERIZATION TECHNIQUES	17
3.1 MATERIALS	17
3.2 REACTIVE BLENDING PROCESS.....	20
3.3 CHARACTERIZATION TECHNIQUES	22
3.3.1 Chemo-rheological measurements.....	22
3.3.2 Proton nuclear magnetic resonance spectroscopy	23
3.3.3 Curing study.....	24
3.3.4 Transmission electron microscopy	24
3.3.5 Scanning electron microscopy with energy dispersive X-ray analysis	25
3.3.6 Mechanical testing.....	26
3.3.7 Dynamic mechanical measurements.....	27
3.3.8 Wide angle X-ray scattering	28
3.3.9 Raman spectroscopy	29
4 RESULTS AND DISCUSSION.....	30
4.1 REACTIVE BLENDING OF NBR AND <i>IN-SITU</i> SYNTHESIZED PUU	30
4.1.1 Chemo-rheological investigation.....	31
4.1.2 Torque-time response of the reactive blending procedure	33
4.1.3 Structural characterization of in-situ PUU	34
4.1.4 Energy-filtered transmission electron microscopy	36
4.1.5 SEM-EDX analysis.....	38
4.1.6 Curing behavior	39
4.1.7 Mechanical properties	40
4.1.8 Dynamic-mechanical analysis	41

4.1.9	<i>Wide angle X-ray scattering</i>	45
4.2	ROLE OF DIAMINE STRUCTURE	47
4.2.1	<i>Chemo-rheological investigation</i>	47
4.2.2	<i>Reactive blending and torque-time profiles</i>	53
4.2.3	<i>Structural characterization by ¹H NMR</i>	57
4.2.4	<i>Curing study</i>	61
4.2.5	<i>Morphology of hetero-phase blend-vulcanizates</i>	63
4.2.6	<i>Stress-strain curves</i>	66
4.2.7	<i>Dynamic-mechanical behavior</i>	67
4.2.8	<i>Wide angle X-ray scattering</i>	69
4.3	BLENDS OF POLAR/NON-POLAR RUBBERS AND <i>IN-SITU</i> PUU	71
4.3.1	<i>Curing behavior</i>	72
4.3.2	<i>Tensile testing</i>	74
4.3.3	<i>Dynamic mechanical analysis</i>	77
4.3.4	<i>Structural characterization by Raman spectroscopy</i>	80
4.3.5	<i>SEM-EDX analysis</i>	84
4.4	APPLICATIONS OF RUBBER/PUU BLENDS	87
4.4.1	<i>NR/PUU blend as tire tread material</i>	87
4.4.1.1	<i>Preparation of composites</i>	87
4.4.1.2	<i>Morphological investigation by TEM</i>	89
4.4.1.3	<i>Dynamic mechanical analysis</i>	90
4.4.1.3.1	<i>Temperature sweep test</i>	90
4.4.1.3.2	<i>Amplitude sweep test-Payne effect</i>	93
4.4.2	<i>NBR/PUU blend as roller covering material</i>	94
4.4.2.1	<i>Experimental set-up and heat build-up test</i>	96
	CONCLUSIONS	99
	RECOMMENDATIONS AND OUTLOOK	102
	REFERENCES	103
	LIST OF FIGURES	111
	LIST OF TABLES	117
	PUBLICATIONS	118

1 Introduction

Blending of polymers to obtain novel materials, offering new application possibilities and performance benefits, has attracted significant scientific interest. Polymer blends, mixtures of two or more polymers, can be based on condensation polymers (silicon rubber, polyesters etc.) and/or addition polymers including homopolymers (polyisoprene, polychloroprene etc.) and copolymers (polyurethanes, styrene butadiene rubber, nitrile butadiene rubber etc.). These polymers can be blended by methods, namely melt, solution, reactive, latex and fine powder blending as well as interpenetrating polymer network (IPN) technology to obtain miscible or immiscible and thermosetting or thermoplastic materials [1-3]. Melt blending predominates due to the benefits of simple mechanical mixing of blend components; however, it mostly requires high blending temperatures. Solution blending requires an additional step of evaporating the used solvent. Latex blending is limited to a few commercially available rubber latexes (Taktene-Lanxess, Natural latex-Thaitex). Fine powder blending is confined to polymers; sensitive to temperature, time and high shear rate of mechanical mixing [4]. The IPN technology is challenging and susceptible to processing parameters [5] and the reactive blending method is primarily opted to compatibilize immiscible polymer blends [6].

Immiscible blends produce heterogeneous morphologies as compared to the miscible blends that are homogeneous down to their molecular level. For example, blends of styrene butadiene rubber with acrylonitrile butadiene rubber and polybutadiene rubber are reported to be immiscible [7] and miscible [8], respectively. In the immiscible blends, the interfacial region is characterized by a large interfacial tension and weak adhesion between blend components. The compatibilization process, i.e. reduction in interfacial tension and promotion of interfacial adhesion can be achieved by using a physical or reactive compatibilization technique. In the case of physical

compatibilization, a pre-formed graft or block copolymer (interfacial agents) is added to stay preferentially at the interface of immiscible components of polymer blend. In the case of reactive compatibilization, the copolymer is created by a chemical reaction at the interfacial region between immiscible blend components. When the immiscible components are compatibilized by an interfacial modification, the resulting blend is termed as a polymer alloy [9-10].

Immiscible components of polymer blends can also be compatibilized without using any interfacial agent. This can be achieved by realizing the mutual interpenetration and entanglement of polymer chains at the interface between the immiscible blend components. The synthesis of a polymer from its precursors during blending with other polymers offers an attractive way to realize compatibilization. This approach is opted here by synthesizing polyurethane-urea via a prepolymer route during reactive blending with rubbers [11-12].

1.1 Challenges

The broad spectrum of the useful properties of polyurethane (-urea) relies on their immense structural diversity and thermodynamic incompatibility between the soft and hard segments obtained from the polyol and diisocyanate-chain extender, respectively [13-17]. The blending of polyurethanes with other polymeric materials is continuously being investigated to obtain materials offering new performance benefits. The blending of a range of polyurethanes with different rubbers has also been investigated and certain improvements in mechanical and dynamic-mechanical properties of blends have been reported. Unfortunately, the reported blends possess a narrow temperature range of application due to the softening of the polyurethane (-urea) phase. Additionally, the time and energy consuming solution- or high temperature melt-blending methods have mainly been opted to blend either the pre-synthesized thermoplastic

polyurethane or the solid polyurethane precursors (polyol and blocked polyisocyanate) or the in-solution synthesized polyurethane with rubbers [18-30].

Surprisingly, blending of polyurethane-ureas with rubber has never been attempted until recently via the solution blending method by Nasir *et al.* [24, 25]. The study concluded that the role of polyurethane-urea phase changes from a highly reinforcing to a softener above the melting temperature of crystalline domains within the polyurethane-urea phase of the heterogeneous blends. It is interesting to mention that the melt blending of rubber with a pre-formed high hard segment polyurethane-urea has never been reported due to the high melting temperature of polyurethane-urea polymer, which may cause thermo-oxidative degradation of the rubber matrix during blending.

Contrary to the conventional solution- and melt-blending methods, the challenge is to develop a new, simple and efficient method to blend polyurethane-ureas with rubber(s). In addition, the obtained novel blends should offer extended performance benefits for practical applications.

1.2 Aims, objectives and approach

Considering the diversified chemistry of polyurethane-ureas, the aim of this work is to develop a reactive blending process to generate the polyurethane-urea phase in rubber matrix, thus obtaining compatibilized, reinforced and useful blends. The process should be simple, efficient and flexible enough in utilizing the available structural components of polyurethane-urea to prepare blends with any polar or nonpolar rubber. The incorporation of fillers (carbon black, silica etc.), compounding of curatives and crosslinking of rubber phase should be conveniently achieved with conventional equipment of rubber technology. To achieve these objectives, a polyurethane-urea with high hard segment contents is synthesized from the polyaddition reactions of a diamine chain extender with the isocyanate-terminated urethane prepolymer in presence of a

rubber in an internal mixer at pre-determined processing conditions. The proposed process of reactive blending is shown in Fig. 1.1 and is explained in section 3.2.

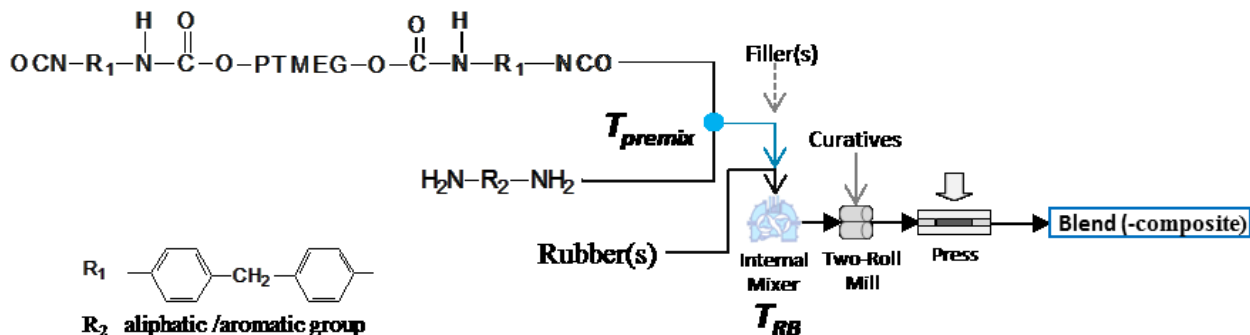


Figure 1.1 Process of reactive blending to obtain blend (-composite) based on rubber and *in-situ* synthesized PUU. Temperatures of premixing (T_{premix}) and reactive blending (T_{RB}) are obtained from the chemo-rheological measurements.

1.3 Scheme of research work

In order to obtain rubber/polyurethane-urea blends of unprecedented mechanical and dynamic-mechanical properties, blending of rubber with the *in-situ* synthesized polyurethane-urea is realized by exploiting the temperature-dependent reactivity of an aliphatic or aromatic diamine with a linear bifunctional isocyanate end-capped polyether prepolymer. For this purpose, a reactive blending process, expediting the conventional rubber equipment, is proposed and opted for the research work presented in this thesis. The chapter-by-chapter synopsis is as following:

Chapter 2 presents the relevant polyurethane chemistry and a thorough review of earlier studies of blending different kinds of polyurethanes with rubbers. The reported blending methodologies and characteristics of blend materials are also provided.

Chapter 3 provides details about materials, specific description of the proposed process of reactive blending and characterization techniques for the stepwise analysis of the polymeric materials.

Chapter 4 presents, in detail, the experimental results and discussions.

The detailed description about blending the *in-situ* synthesized polyurethane-urea (PUU) with nitrile butadiene rubber (NBR) is given in subchapter 4.1. The chemo-rheological analysis of the premix (mixture of prepolymer and diamine) and selection of temperatures for the reactive blending process are presented. A structural analysis of the *in-situ* synthesized PUU is elaborated by using ^1H NMR spectroscopy. The results of mechanical and dynamic-mechanical temperature sweep tests are shown. A morphological investigation of blends is performed by TEM and the SEM measurements, which show existence of interpenetrated interfacial region i.e. the interphase between the *in-situ* synthesized PUU and NBR phases.

In subchapter 4.2, the influence of diamine structure on the chemo-rheological response of a premix, the reactive blending procedure in an internal mixer, structural, morphological and performance characteristics of the prepared blends is studied. A chemo-rheological analysis of the reactive PUU premixes, comprising of a prepolymer admixed with 1,3-phenylenediamine (mPD), 1,4-Bis(aminomethyl)benzene (pXD), 4,4'-Methylene-bis(2-chloroaniline) (MBCA) and 4,4'-(1,3-Phenylenediisopropylidene)bisaniline (Bisaniline-M, BisAM), is presented. The detailed ^1H NMR spectroscopic analysis of PUU-mPD, PUU-pXD, PUU-MBCA and PUU-BisAM, synthesized *in-situ* during reactive blending with NBR, is given. The structural and morphological aspects of *in-situ* PUUs are shown to influence remarkably the tensile and dynamic-mechanical properties of heterogeneous blends. SEM analyses of the cryofractured surfaces of four different kinds of blends are presented. X-ray measurements are shown to reveal that the hard segment domains of PUU are always disorderly structured, which seems intrinsic to the opted process of reactive blending.

In subchapter 4.3, the PUU (based on MDI/PTMEG prepolymer and mPD) is reactively blended with polar (CR, XNBR) and nonpolar (NR, EPDM, sSBR) rubbers. The Raman spectroscopic investigation structurally identifies the micro-sized irregular domains of the *in-situ* synthesized PUU in the rubber matrix of blends. The *in-situ* generated PUU is shown to reinforce the tensile and dynamic-mechanical response of all kind of rubber matrices. SEM micrographs of the cryofractured specimens are presented to observe failure (if any) at the interface.

In subchapter 4.4, the blends are examined for commercial applications including a truck tire tread compound and a rubber roller covering material. The PUU is incorporated in a model truck tire tread formulation. The CB (N330) in NR-CB composite has partially been replaced with an equivalent quantity of *in-situ* synthesized PUU for NR/PUU-CB composite of similar hardness. The NR-CB and NR/PUU-CB composites are compared with respect to their dynamic-mechanical behavior. In another application, a NBR/PUU blend based prototype roller is successfully examined on a lab-scale test rig and the test results are shown.

In chapter 5, a summary of the research work is presented.

Chapter 6 presents recommendations and outlook regarding commercialization and future utilization of the proposed reactive blending process.

2 Literature Survey

2.1 Fundamentals of polyurethanes

The wide spectrum of polyurethane (-urea) properties arises from the structural diversities of the constituent components, i.e. isocyanates, polyols and chain extenders. The pure and modified components may be bifunctional or polyfunctional for linear or crosslinked structures of polyurethane (-urea) polymers. In general, the polyurethane (-urea) polymers are formed from the exothermic polyaddition reaction of isocyanates with polyols and, additionally, with hydroxyl or amine terminated chain extender(s) to introduce urethane or urea groups in polymer chains. The urea groups generate a high hydrogen-bond density in order to get a polymer with high temperature sustainability and structural integrity. The macrodiols, diisocyanates and diamine are opted in this study to obtain linear macromolecules of the *in-situ* synthesized polyurethane-urea polymer.

The most common polyols are hydroxyl-terminated polyether or polyester macrodiols. In applications requiring low temperature flexibility, higher rebound and lesser heat build-up, polyether polyols like poly (tetramethylene ether) glycol (PTMEG) are preferred over polyester polyols like poly (ethylene glycol) adipate. The toluene diisocyanate (TDI) and 4,4'-diphenylmethane diisocyanate (MDI) are of greater industrial importance as compared to other commercially available diisocyanates. However, the industrial consumption of MDI is growing due to a relatively high volatility and inhalation toxicity of TDI. A bifunctional, low molecular weight, aliphatic or aromatic diamine is used for the linear extension of the prepolymer chains. Aromatic diamines provide better control over reactivity with diisocyanates and are preferred over highly reactive aliphatic diamine in this investigation.

The polyols render flexibility to polymer chains and constitute soft segments (SS). The combination of diisocyanate and diamine imparts rigidity to polymer chains and constitutes hard segments (HS). The thermodynamic incompatibility tends to phase separate soft and hard segments into soft and hard domains. The soft domains act as a matrix for the rigid hard domains in order to produce a unique structural morphology, which defines the macroscopic mechanical behavior of the polyurethane-urea polymer [13-17].

The synthesis of polyurethane-urea polymer can be realized by one-shot and pre-polymer polymerization techniques. The one-shot route involves a simultaneous mixing of the three main components i.e. diisocyanate, macrodiol and diamine. In the prepolymer route, the liquid polyol is reacted with an excess of diisocyanate to get isocyanate-terminated urethane prepolymer. The prepolymer is either a viscous fluid or a solid with low melting temperature [31]. Subsequently, the prepolymer is reacted with a low molecular weight diamine to obtain polyurethane-urea polymer. The one-shot and prepolymer routes to polyurethane-urea formation are shown in Fig. 2.1.

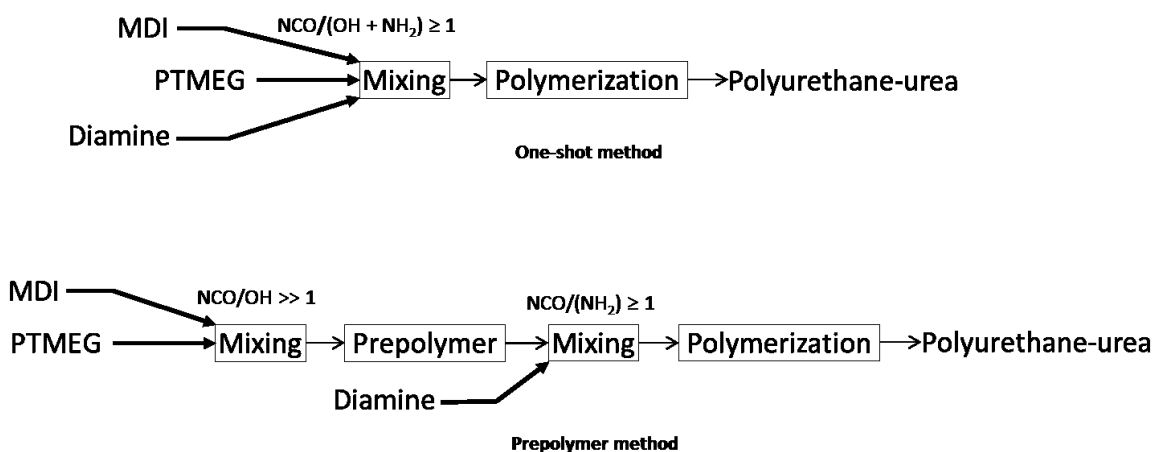


Figure 2.1 A simplified representation of polymerization routes to polyurethane-urea: One-shot and prepolymer method [31]

The prepolymer method produces a more regular sequence of soft and hard segments along the polymer chain, whereas this sequence is relatively random in one-shot method [32]. The simplicity and structural reproducibility emphasizes the use of prepolymer route for the *in-situ* synthesized polyurethane-urea during reactive blending with rubbers for the herein presented research work. The synthesis of polyurethane-urea polymer via the prepolymer route is shown in Fig. 2.2.

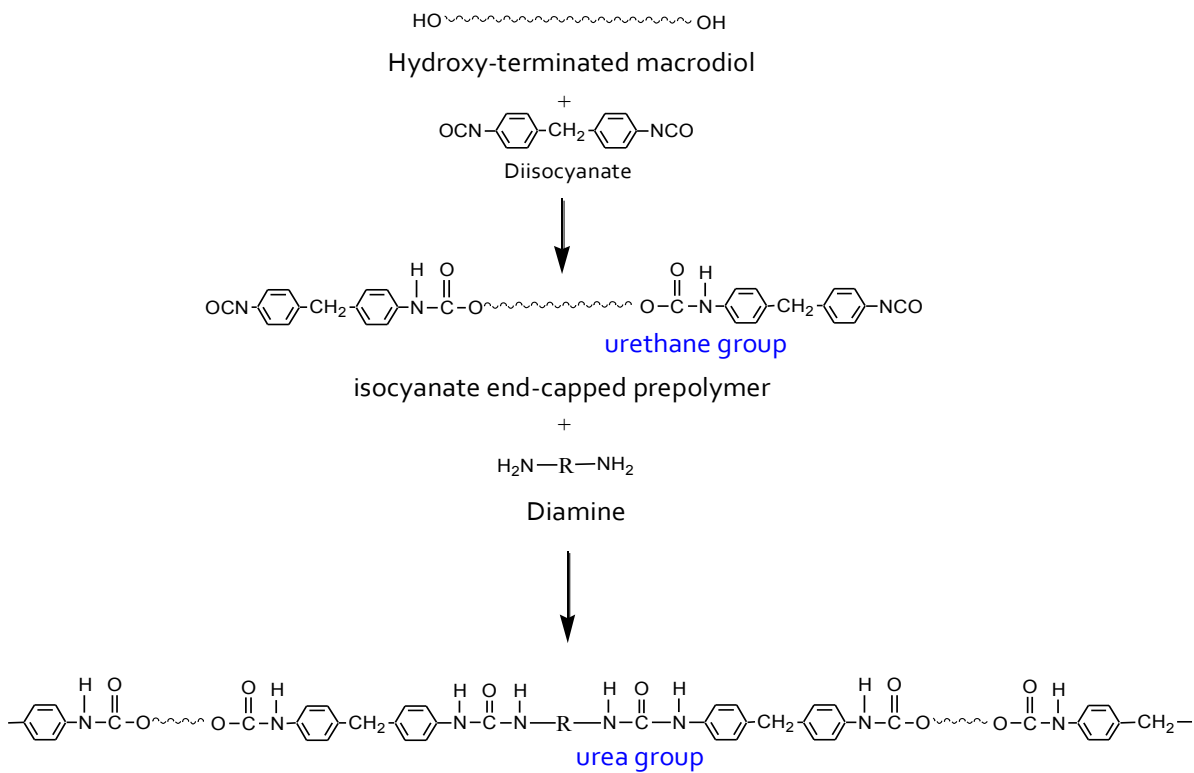


Figure 2.2 Main reactions of isocyanate with polyol and diamine to form polyurethane-urea via the prepolymer route

Figure 2.3 provides a modular representation of structure and morphology of soft and hard segments/domains of polyurethane-urea polymer. The phase separated and phase mixed structural morphologies are shown. For the formation of polyurethane-urea polymer, the isocyanate index (ratio of isocyanate to amino groups) is taken from 0.95 to 1.1. A higher than 1.0 value of

isocyanate index leads to the crosslinking of polymer chains via allophanate and biuret formation, and thus influences the performance of the polyurethane-urea polymer (see Fig. 2.4).

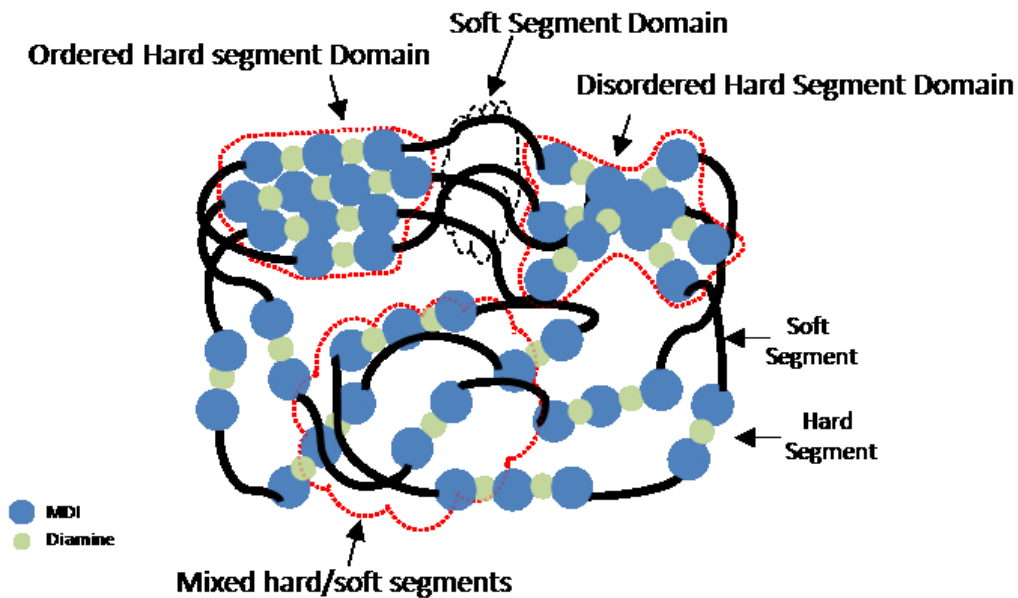


Figure 2.3 Graphical representation of morphologically diversified polyurethane-urea

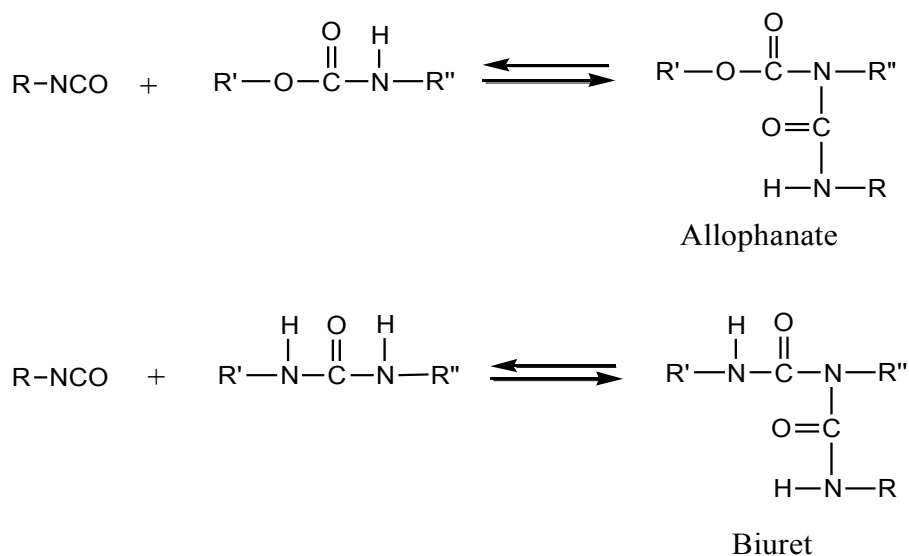


Figure 2.4 Secondary addition reactions of isocyanate group with urethane- and urea-linkages of polyurethane-urea chains

2.2 Overview of blends based on rubber and polyurethanes

A reasonable number of studies have been published on blending polyurethane (-urea) with rubbers in an attempt to obtain materials exhibiting novel performance characteristics. However, as earlier mentioned, the opted time and energy intensive solution- and high temperature melt-blending methods tend to vanquish the limited improvement in the property profile of new blend materials on economic constraints. The blending of polyurethanes with nitrile rubbers has attracted particular attention due to the mutual polar character and the possibility of synergism in the properties of hybrid material. Dimistrievski et al. [20] melt-blended NBR and NR with thermoplastic polyurethane ionomers (anionomer and cationomer) at around 170°C and concluded that the prepared blends exhibit temperature-dependent dynamic mechanical properties. The polyurethane ionomers reinforce the rubber matrix at 25°C; however, at 100°C the reinforcement vanishes due to the softening of polyurethane phase. Furthermore, the charge-dipole interactions between polyurethane ionomers and NBR were concluded from a slight shift in glass transition temperature, an indication of tenuous compatibilization. In another study, the existence of secondary molecular linkages from weak interactive molecular associations between NBR and polyurethane (PU) has been concluded from the dynamic mechanical studies. The dependence of storage modulus on strain amplitude for different PU loaded NBR compounds was investigated. The decrease in reinforcing tendency of PU at high strain amplitude was linked to the breakdown of secondary structures between chains of NBR and PU [18]. Tang et al. [19] reported an existence of some compatibility in thermoplastic PU and NBR phases of dynamically vulcanized blends. The blends were prepared by melt-blending at 160°C. It was reported that the tensile strength of blend vulcanizates was even better than pure thermoplastic PU due to the significant synergistic effect between the blend polymers. Desai et al. [33] investigated solution blending of NBR and solution-synthesized PU. The PU was prepared from hydroxyl terminated

polybutadiene, toluene diisocyanate and 1,1,1-trimethylol propane in NBR solution. The investigated blends were found to behave synergistically with regard to tensile strength and elongation at break. In another study, the improved performance characteristics of NBR and diphenylmethane-4,4'-diisocyanate/polyether based thermoplastic PU blends have been reported for marine applications. The acrylonitrile content of NBR was reported to influence the physical characteristics of blends. It was further reported that the compatibility between NBR and thermoplastic PU was improved with increasing acrylonitrile content of NBR [34]. Roy et al. [21] reported sulfur and peroxide cured blends of carboxylated NBR and PU rubber; prepared via pre-blending, master-batch and preheating techniques. The preheated and peroxide cured blends were found to exhibit improved properties due to the enhanced phase adhesion by inter-chain crosslinking, which was verified by Fourier transform infrared spectroscopy. The blending of ethylene propylene diene rubber (EPDM) with one component polyurethane adhesive was investigated by XU et al. [26]. The crosslinking of EPDM and curing of PU was accomplished at the vulcanization temperature of 170°C. The carbon black (CB) containing blends of EPDM and PU were reported to exhibit improved mechanical and tribological properties. It was concluded that the incorporation of CB and PU adhesive increases the stiffness of EPDM compounds in the rubbery plateau region. The coefficient of friction and specific wear rate was found to depend on blend composites. Hybrid rubber blends of peroxide curable hydrogenated NBR (HNBR) and one component polyurethane adhesive (polyol and blocked polyisocyanate) were reported to exhibit improvements in wear resistance. During vulcanization of HNBR at 170°C, the hot melt PU adhesive is also cured due to the deblocking of block polyisocyanate and its reaction with polyol at the vulcanization temperature [28]. A similar hybrid system was further investigated by incorporating CB in blends of hot melt PU adhesive and HNBR. The added different grades of CB reinforced preferentially the rubber phase [29]. Kotal et al. [22] prepared layered double

hydroxide (LDH) filled NBR/PU blend nanocomposites by solution intercalation process. It was observed that the partial exfoliation of LDH imparted to nano-composites an improved reinforcement and thermal stability owing to polar/ionic interactions among NBR, PU and LDH. J.H. Tan et al. [23] prepared blends of NBR and polyurethane-silica (PU-SiO₂) hybrid network systems. The isocyanate-terminated prepolymer and hydroxyl groups on silica surface were proposed to react during the vulcanization process and resulted in improving the properties of the NBR/PU-SiO₂ blends. The incorporation of up to 20 parts of hygrothermally decomposed polyurethane (HD-PU) per hundred parts in natural rubber (NR), NBR, styrene butadiene rubber (SBR), epoxidized natural rubber (ENR), and carboxylated nitrile rubber (XNBR) was extensively investigated by J. Karger-Kocsis et al. [35-38]. The HD-PUR was found to accelerate the sulfur-based curing of NR, XNBR and SBR. Interestingly, an increase in the degree of curing, stiffness, tensile strength and decrease in elongation at break was observed for SBR. Whereas, for XNBR, an opposite tendency with plasticizing effect from HD-PUR was reported. HD-PUR improves moderately the tensile strength, elongation at break and abrasion loss of NR, however, an inverse trend was observed for NBR. Investigations also showed that the HD-PUR increased resistance to thermo-oxidative aging and did not alter much the function of CB in a conventional or semi-efficient curing of Epoxidized NR. The layered silicates filled NR/PU blend composites were prepared by latex mixing route. The morphological and spectroscopic measurements revealed that the layered silicates are preferentially intercalated by PU in an incompatible NR/PU blend system. Despite incompatibility between the NR and PU phases, the blend composites exhibited excellent mechanical properties [39, 40]. Siengchin et al. [41] prepared ternary composites, based on polyoxymethylene, polyurethane and alumina, by direct melt blending and masterbatch blending techniques. It was found that the ternary composites produced by the masterbatch technique were superior in their mechanical and thermal characteristics as

compared to the direct melt compounded composites. Similar ternary composites were also examined by dielectric spectroscopy in order to identify different relaxation processes and to relate the temperature dependence of relaxation processes to the Arrhenius or Vogel–Fulcher–Tamann equations [42]. Chlorosulfonated polyethylene rubber, epichlorohydrin rubber, polychloroprene rubber, ethylene acrylic rubber, polyacrylic rubber, chlorobutyl rubber, chlorinated polyethylene rubber, ethylene vinyl acetate rubber, XNBR and HNBR were blended with PU rubber via masterbatch and/or preblending and preheating-preblending method to study the influence of blending technique on thermal stability of blend system [43-57]. It was concluded that the preheating-preblending technique improved thermal stability of rubber/polyurethane blends over masterbatch and preblending technique. Blends of grafted silicon and PU rubbers were reported to exhibit improved mechanical properties as compared to the ungrafted silicon rubber/PU blends. The blends of ENR and thermoplastic PU were reported to exhibit superior modulus, hardness, shear viscosity, stress relaxation and heat resistant properties compared to the unmodified NR and thermoplastic PU [58]. Melt blending of maleated natural rubber (MNR), ENR and natural rubber-graft-poly(methyl methacrylate) (NR-g-PMMA) with thermoplastic PU (TPU) has been investigated. It was observed that the MNR/TPU blend exhibit finer grain morphology and superior mechanical properties compared to TPU blends with ENR, unmodified NR and NR-g-PMMA [59]. In order to improve the resistance to thermal degradation, incorporation of antioxidants in dynamic blend vulcanizates based on ENR and TPU have been investigated. Temperature scanning stress relaxation measurements showed that the *N*-(1,3-dimethylbutyl)-*N*-Phenyl-*p*-phenylenediamine (6PPD), amongst the investigated antioxidants, imparted blends with much improved thermal characteristics [60]. The effect of the plasticizer and processing oil (DOP, TDAE oil and paraffinic oil) on the properties of ENR/TPU blends has been investigated [61]. It was concluded that the incorporation of plasticizer and

processing oil caused a decrease in glass transition temperature of TPU and ENR, tension set and loss factor values. The preparation of rice husk ash and conventional silica filled ENR/TPU blend composites has been reported. It was found that blend composites filled with rice husk ash exhibit ultimate tensile properties similar to silica filled vulcanizates [62]. The thermoplastic dynamic vulcanizates composed of ENR and TPU (80 shore A) were reported to be prepared by melt blending method. The rubber phase was crosslinked by peroxide and by conventional (CV), effective (EV) and semi-effective (semi-EV) sulfur curing system. The peroxide cured blend vulcanizates were reported to exhibit comparatively higher modulus, high hardness and shear viscosity. The dynamically CV-cured blends exhibit higher oil resistance and mechanical strength than semi-EV and EV-cured blends [63]. Similar dynamic vulcanizates of ENR and TPU have been reported for superior rheological and mechanical properties as compared to ENR/TPU blends prepared by simple blending [64]. The effect of curing system, accelerator type and epoxy content of NR on the properties of thermoplastic dynamic vulcanizates of natural rubber and TPU was investigated. It was found that the EV curing system provided better tensile properties than Semi-EV and CV. The selection of accelerator was found to hugely influence the ultimate tensile strength of vulcanizates. It was also reported that the higher level of epoxy content of NR resulted in enhanced tensile characteristics of blend vulcanizates [65]. Nasir et al. prepared blends of thermoplastic polyurethane-urea (TPUU) and XNBR by solution blending method. It was concluded that the mechanical properties of the neat and nano-clay reinforced blends improved progressively with increasing quantity of TPUU in XNBR [24, 25].

The blending of a range of polyurethanes with different rubbers has been reported and certain improvements in the mechanical and dynamic-mechanical properties of blends have been claimed. However, the reported blends possess a narrow temperature range of application due to the melting of polyurethane (-urea) phase. Additionally, the time and energy consuming

solution-or high temperature melt-blending methods have mainly been considered to blend either the pre-synthesized thermoplastic polyurethane or the solid polyurethane precursors (polyol and blocked polyisocyanate) or the in-solution synthesized polyurethane with rubbers [18-30].

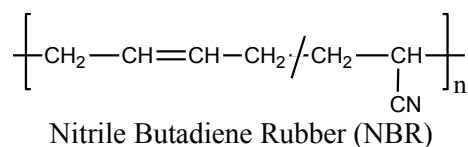
In contrast to the conventional solvent- and melt blending methods, a simple reactive-blending process is suggested and investigated extensively in this research work to blend *in-situ* synthesized polyurethane-urea with rubbers to obtain novel blends offering unprecedented performance benefits.

3 Experimental: Materials, Blending process and Characterization techniques

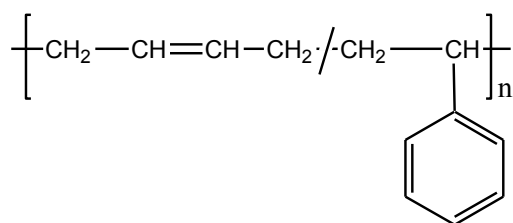
3.1 Materials

The following grades of synthetic rubbers were obtained from LANXESS, Germany:

Acrylonitrile butadiene rubber/NBR (KRYNAC 3345 F) is a copolymer of acrylonitrile and butadiene with acrylonitrile content of 33 wt% and Mooney viscosity (ML (1+4) 100°C) of 45 MU.

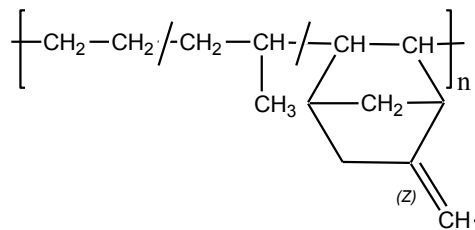


Solution styrene butadiene rubber/sSBR (VSL 4526-0 HM) is a copolymer consisting of styrene and butadiene monomers with styrene content of 26 wt% and Mooney viscosity (ASTM D 1646) of 65 MU.



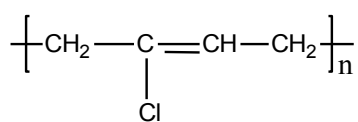
Solution Styrene Butadiene Rubber (sSBR)

Ethylene propylene diene/EPDM (EP G6850) is a terpolymer of ethylene (51 wt%), propylene and 7.7 wt% of ethylidene norbornene monomer with a Mooney viscosity (ML (1+4) 125°C) of 60 MU.



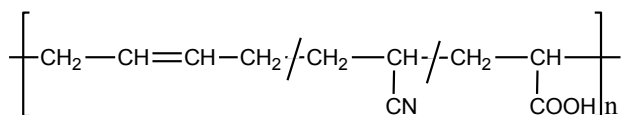
Ethylene Propylene Diene Monomer Rubber (EPDM)

Chloroprene rubber/CR (Bayprene 611) is a sulfur-modified grade. It has a Mooney viscosity (ML (1+4) 100°C) of 35±5 MU and a slight to medium crystallization tendency.



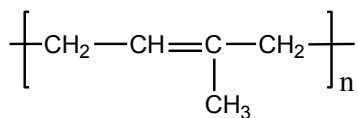
Chloroprene Rubber (CR)

Carboxylated nitrile butadiene rubber/XNBR (X740) has an acrylonitrile content of 26.5±1.5 wt% and a Mooney viscosity (ML (1+4) 100°C) of 38±4.



Carboxylated Nitrile Butadiene Rubber (XNBR)

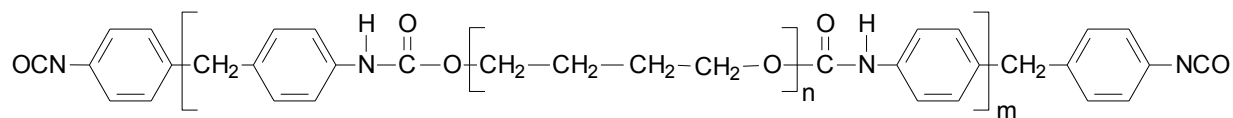
The natural rubber (NR), Standard Malaysian Rubber of grade SMR 10 was provided by the Tun Abdul Razak Research Centre, Hertford, United Kingdom.



Natural Rubber (NR)

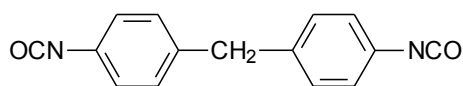
4, 4-diphenylmethane diisocyanate (MDI) and poly(tetramethylene ether) glycol (PTMEG) based isocyanate end-capped prepolymer MT2184 was provided by Covestro Elastomers SAS (previously Baulé SAS), France. The viscosity of MT 2184 was reported to be 0.8 Pa·s at 80°C. A ¹H NMR spectroscopic analysis of the viscous MT2184 reveals a PTMEG, also known as polytetrahydrofuran, based soft segment of prepolymer. The reported isocyanate contents

(8.55wt%) of prepolymer were considered to adjust the stoichiometry with diamines for preparing the premix.



isocyanate-terminated prepolymer chain based on polytetrahydrofuran (PTMEG)

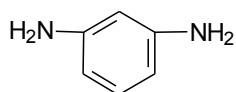
and diphenylmethane-4,4'-diisocyanate (MDI)



MDI molecule

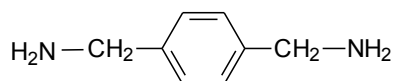
In total, the following four diamine chain extenders were used to obtain polyurethane-urea polymers of different chain structures:

1,3-phenylenediamine (mPD) is over 99% pure with a melting point of about 64°C and was obtained from Sigma-Aldrich Co. LLC, USA. The stoichiometric premix of mPD and MT2184, if reacted completely, should form polyurethane-urea of 32.8 wt% hard segments contents.



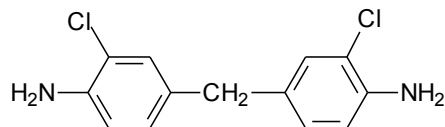
1,3-phenylenediamine (mPD)

1,4-Bis(aminomethyl)benzene (pXD) was acquired in solid form from Tokyo Chemical Industry Co., Ltd, Japan. Its melting point is given to be 60-63°C.



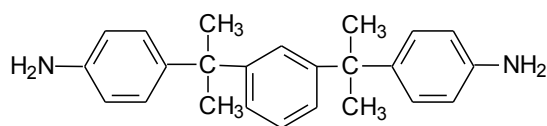
1,4-bis(aminomethyl)benzene (pXD)

4,4'-Methylene-bis(2-chloroaniline) (MBCA) was kindly provided in powder form by Ihara Chemical Industry, Japan. It melts at around 110°C.



4,4'-methylene-bis(2-chloroaniline) (MBCA)

4,4'-(1,3-phenylenediisopropylidene)dianiline (Bisaniline-M, BisAM), is over 99% pure diamine powder with melting point of 116°C and obtained from Mitsui Fine Chemicals, Japan. The flakey/crystalline diamines were grounded to fine powder by mortar and pestle.



4,4'-(1,3-phenylenediisopropylidene)dianiline (BisAM)

The peroxide (Perkadox BC-40K-pd) containing 40% dicumyl peroxide was obtained from Akzo Nobel Polymer Chemicals, The Netherlands. The coagent (Rhenogran TAC-50) is a 50% triallyl cyanurate and was provided by Rhein Chemie, Germany. The reinforcing grade of carbon black/CB (Corax N330) was provided by Orion Engineered Carbons GmbH, Germany. The CB has the nitrogen surface area (BET) of 78m²/g.

3.2 Reactive blending process

In order to achieve objectives aforesaid in section 1.2, the polyurethane-urea is synthesized from the polyaddition reactions of an isocyanate-terminate urethane prepolymer with a diamine chain extender in presence of rubber in an internal mixer at the preset processing conditions. The scheme of the proposed process of reactive blending and the corresponding laboratory equipment are shown in Fig. 3.1 and Fig. 3.2 respectively. The critical processing parameters, i.e. the temperatures of premixing (T_{premix}) and reactive blending (T_{RB}), are obtained from the chemorheological measurements. For that purpose, the prepolymer is expeditiously mixed with a

stoichiometric quantity of diamine at a room temperature to get a viscous premix, which instantly is put to test between parallel plates of a rheometer.

The reactive blending of rubber with *in-situ* synthesized PUU is carried out in an internal mixer at T_{RB} and fixed rotor speed of 70 RPM (mostly). Initially, the rubber is masticated in a preheated internal mixer followed by the pouring of premix, which is obtained by mixing the viscous prepolymer with a powdered diamine at T_{premix} and at an isocyanate index of 1. The isocyanate groups of the prepolymer and the amino groups of the diamine react to generate *in-situ* PUU in the rubber matrix. The obtained blends are structurally characterized by ^1H NMR spectroscopy (preferably) to confirm the *in-situ* polymerization to PUU. Subsequent to the structural characterization, the blends are compounded with curatives (peroxide, sulfur, metallic oxide etc.) on a two-roll mixing mill at about 50°C . Finally, the blends are vulcanized to their optimum cure time by compression moulding in a heated press at 160°C .

The incorporating of additives and auxiliaries typical to rubber technology, like fillers, can readily be realized in the suggested process of reactive blending.

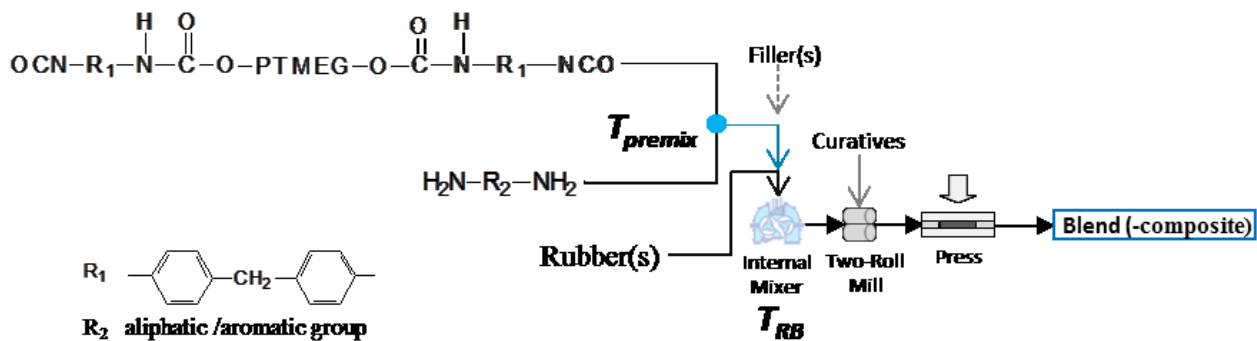


Figure 3.1 Reactive blending process to prepare blend (-composite) based on rubber and *in-situ* synthesized PUU.

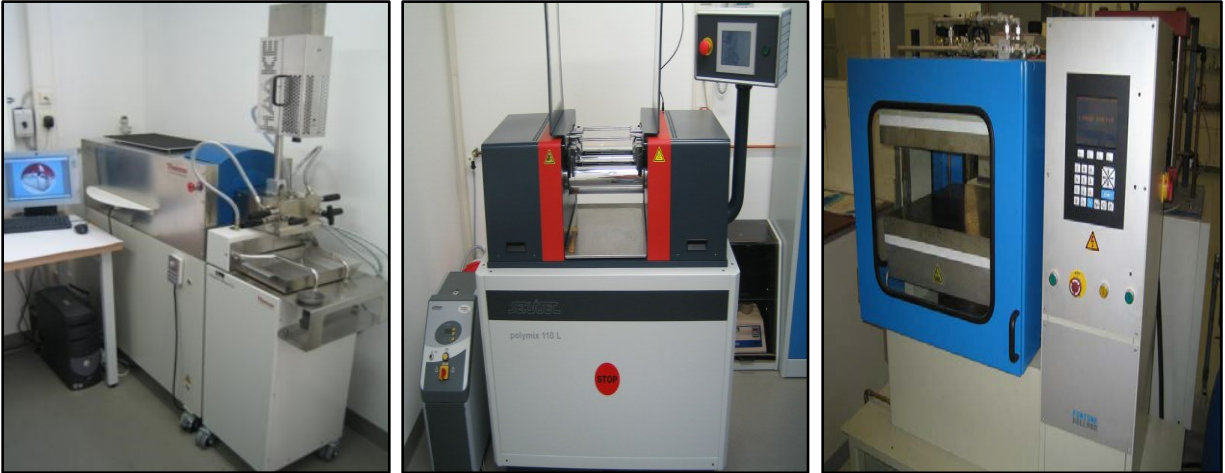


Figure 3.2 Internal mixer (Haake Rheomix 80ml), two roll mixing mill (Polymix 110 L) and compression moulding machine

3.3 Characterization techniques

3.3.1 Chemo-rheological measurements

The temperatures of premixing and reactive blending are obtained from the temperature dependent viscoelastic response of a prepolymer-diamine premix. The rheological measurements are carried out by an ARES-G2 rheometer (TA instruments, USA, see Fig. 3.3) in oscillatory shear mode by using a parallel plate geometry of 25 mm plate diameter with gap distance of 2 mm. The temperature sweep experiment is performed from 25°C to 170°C with a heating rate of 2 K/min, a constant angular frequency of 10 rad/sec and a strain of 1 %. The results of shear elastic (G') and loss (G'') modulus vs. temperature were analyzed to determine the temperatures for the reactive blending process.



Figure 3.3 ARES-G2 Rheometer showing parallel-plate test geometry
[<http://www.tainstruments.com/ares-g2/>]

3.3.2 Proton nuclear magnetic resonance spectroscopy

Proton nuclear magnetic resonance (^1H NMR) spectra are recorded on an Avance III 500 spectrometer (Bruker, Germany, see Fig. 3.3) operating at 500.13 MHz for ^1H . The test samples are prepared by treating about 10 mg of blend in a NMR tube with deuterated dimethylsulfoxide (DMSO-d_6) at 100°C for 30 min. During this time, the tube is ultrasonicated several times, which results in a breakdown of the blend pieces and an improved extraction of the PUU. Finally, insoluble rubber formed a plug on the top of solution without effecting the measurement. The spectra are recorded at room temperature using the solvent as lock and internal standard ($\delta = 2.50$ ppm).

3.3.3 Curing study

The curing behavior of neat rubbers, blends and blend composites are analyzed at 160°C by using a rubber processing analyzer Scarabaeus SIS V50 (Scarabaeus GmbH, Germany, see Fig. 3.4). The optimum cure time is obtained from the cure curves and used to vulcanize compounds with compression moulding machine at 160°C.



Figure 3.4 Rubber process analyzer: moving die rheometer (Scarabaeus SIS V50)

3.3.4 Transmission electron microscopy

The heterophase morphology in blends is investigated by transmission electron microscopy (TEM). Thin sections of the blends are cut by ultramicrotome (Leica UC6/FC6, Leica Microsystems GmbH, Wetzlar, Germany, see Fig. 3.5) at -140°C. The thin sections are stained with OsO₄ and inspected in Libra200 TEM (Carl Zeiss Microscopy GmbH, Oberkochen, Germany) at an acceleration voltage of 200kV.

In particular for NBR/PUU 70/30 blend of section 4.1.4, the interface is visualized by elemental mapping using energy filtered imaging and image-spectroscopy in plasmon loss region (10 eV to 60 eV with 2 eV step and 5 eV energy filtering aperture), as described in [66].



Figure 3.5 Transmission electron microscope (Libra 200 MC) by Carl Zeiss

3.3.5 Scanning electron microscopy with energy dispersive X-ray analysis

For section 4.2, the sample preparation for the 3.3.5 Scanning electron microscopy (SEM) is as following: The smallest side of approximately 3 mm x 3 mm x 10 mm pieces is cut by a diamond knife at -120 °C to achieve a flat surface with dimensions of approx. 2 mm x 2 mm. The specimens are stained for 20 min in OsO₄ vapor at room temperature, let degas for 24 hours in a fume hood, mounted with universal glue on a SEM holder and coated with approx. 20 nm thin amorphous carbon film in Leica SCD 500 coater (Leica Microsystems GmbH, Wetzlar, Germany). The images are acquired in NEON40 SEM (Carl Zeiss Microscopy GmbH, Oberkochen, Germany) (see Fig. 3.6) at operating voltage of 3 kV using back-scattered electron detector to suppress topography contrast and obtain material contrast (the OsO₄-stained NBR is bright, unstained PUU is dark). Since the morphology of the investigated blends is complex and domain sizes stretch from tens of nanometers to tens of micrometers, panorama images composed of 25 x 25 single images are acquired and stitched using Zeiss SmartStitch software.

For the energy dispersive X-ray analysis (EDX) investigation, the blend specimens are cryofractured and sputtercoated with platinum before scanning with ultra plus scanning electron microscope from Zeiss NTS (Oberkochen, Germany). The energy-dispersive X-ray analysis is performed with X-Flasch 5060F detector from Bruker nano GmbH (Berlin, Germany) to perform elemental oxygen mapping in order to distinguish phases of heterogeneous blends.



Figure 3.6 Scanning electron microscope (NEON 40 EsB) by Carl Zeiss

3.3.6 Mechanical testing

The tensile testing of dumbbell specimens is performed by using the tensile testing machine Zwick 1456, Z010, Ulm, Germany (see Fig. 3.7). According to the DIN 53504 standard, a preload of 0.2 N and a cross-head speed of 200 mm/min were the testing parameters. The tear strength is measured according to the test method B explained in ISO 34-1:2004(E) standard. The force with a constant speed of 500 mm/min is applied to propagate the nick in an angle test piece and the maximum force is taken to calculate the tear strength. The test method given in standard ISO 815:1991(E) is considered to determine the compression set of test specimens compressed to

25% of their initial thickness and kept at the temperature of 70°C for 24h. The hardness (Shore A) is measured by impact penetration method (DIN 53505). The results of mechanical testing are expressed as the arithmetic mean values.



Figure 3.7 Universal testing machine (Zwick 1456, Z010) by Zwick/Roell AG

3.3.7 Dynamic mechanical measurements

Dynamic mechanical measurements are performed on 2x10x35 mm specimens in tensile mode by means of a Dynamic Mechanical Thermal Spectrometer (Eplexor 150 N and 2000 N, Gabo Qualimeter, Ahlden, Germany) (see Fig. 3.8).

The temperature sweep test is performed at a frequency of 10 Hz, constant heating rate of 2 K/min and temperature range from -100 °C up to 180 °C. The specimens are subject to a static pre-strain of 1% and oscillated to a dynamic strain of 0.5%. The results are shown as the tensile storage modulus (E') and loss modulus (E'') and the loss factor ($\tan \delta$) vs. temperature profiles.

The amplitude sweep test is conducted in tensile mode at 25 °C. The dynamic strain sweep is done from ca. 0.01% to 30% of the strain amplitude on a 2x10x35 mm specimen subjected to a static prestrain of 60%.

Flexometer test: The heat build-up test was performed according to the DIN 53533 standard. The cylindrical specimens, having diameter of 18mm and height of 25mm, were preconditioned at 50°C for 30 min. The preconditioned specimens were put to test in compression mode with 1 MPa preload and at a dynamic compressive strain of 4.45 mm and frequency of 30 Hz. The temperatures on the surface (during the test) and at the core of specimen (at the end of test) are measured and presented.



Figure 3.8 Dynamic Mechanical Thermal Spectrometer (Eplexor 2000 N) by GABO Instruments

3.3.8 Wide angle X-ray scattering

Wide angle X-Ray Scattering (WAXS) measurements are performed by means of a 2-circle diffractometer XRD 3003 Θ/Θ (GE Sensing & Inspection Technologies GmbH, Seifert-FPM, Freiberg/Sa., Germany) (see Fig. 3.9) using Cu $K\alpha$ radiation in the region from $2\theta = 1$ to 40° in steps of 0.05° .



Figure 3.9 X-ray Diffractometer (XRD 3003 T/T) by GE Sensing & Inspection Technologies

3.3.9 Raman spectroscopy

Raman spectroscopy is performed with a laser wavelength of 785 nm using the RAMAN Imaging Microscope System alpha 300R (WITec GmbH, Ulm, Germany) (see Fig. 3.10). 5-40 mW is the laser power and the samples with an objective having a 20x magnification are measured. The integration time is 0.5 s for a single spectrum, which is accumulated 200 times. The area for the Raman Imaging measurements is 500 x 500 μm with a measurement point distance of 5 μm . 10.000 spectra with an integration time of 0.5 s for every spectrum are measured.



Figure 3.10 Raman Imaging Microscope (alpha 300R) by WITec GmbH
(<http://www.witec.de>)

4 Results and Discussion

4.1 Reactive blending of NBR and *in-situ* synthesized PUU

The generalized reactive blending process, given in section 3.2, has to be adapted to blend the nitrile butadiene rubber with the *in-situ* synthesized polyurethane-urea (see Fig. 4.1). The temperatures of premixing, T_{premix} , and reactive blending, T_{RB} , are obtained from the chemorheological test of a premix composed of MDI/PTMEG prepolymer and 1,3-Phenylenediamine (mPD). The formulation of compounds is given in Table 4.1.

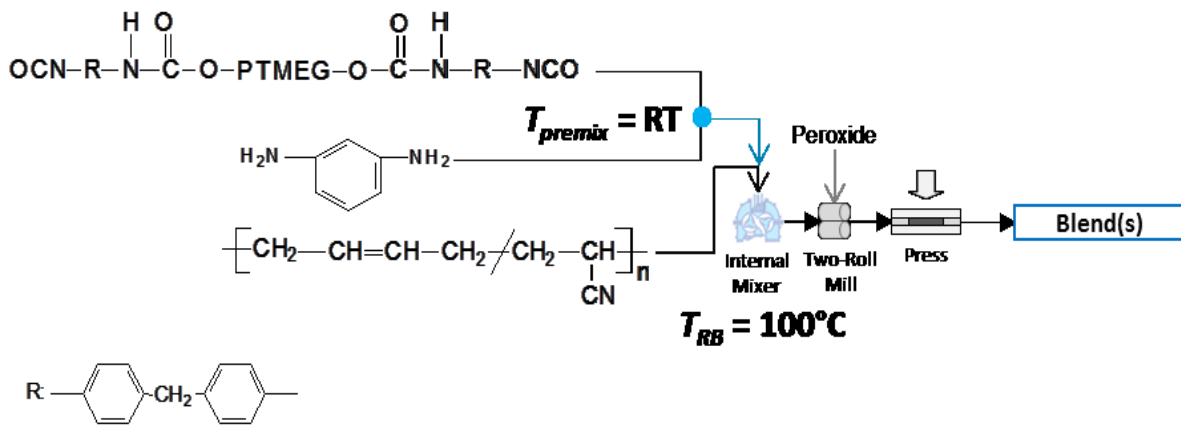


Figure 4.1 Reactive blending process to prepare NBR/PUU blends. The temperatures of premixing and reactive blending are obtained from the chemorheological investigation of the premix.

Table 4.1 Formulations and designations of compounds are given. Quantities of curatives are in parts per hundred parts of blend.

Ingredients	NBR	NBR/PUU 90/10	NBR/PUU 80/20	NBR/PUU 70/30	NBR/PUU 60/40	NBR/PUU 50/50
Nitrile butadiene rubber	100	90	80	70	60	50
premix of prepolymer and mPD NCO:NH ₂ (1:1)	-	10	20	30	40	50
Peroxide (Perkadox BC-40K-pd)	3	3	3	3	3	3
Coagent (Rhenogran TAC-50)	2	2	2	2	2	2

4.1.1 Chemo-rheological investigation

The permissible temperature range of premixing a prepolymer with a diamine and the reactive blending temperature are obtained from chemo-rheological measurements. The shear storage (G') and loss modulus (G'') versus temperature profiles of a premix (MDI/PTMEG prepolymer admixed with mPD) are shown in Fig 4.2. At low temperatures, the viscous character of the premix prevails ($G'' > G'$) due to the absence of polymerization reactions and causes a gradual decrease in the viscoelastic response up until the onset temperature (T_o) of 45 °C. The shear storage and loss modulus show a steep rise beyond T_o , which indicates the initiation of polyaddition reactions and the generation of isocyanate and amine end-capped oligomers along with the extension of isocyanate-terminated prepolymer chains.

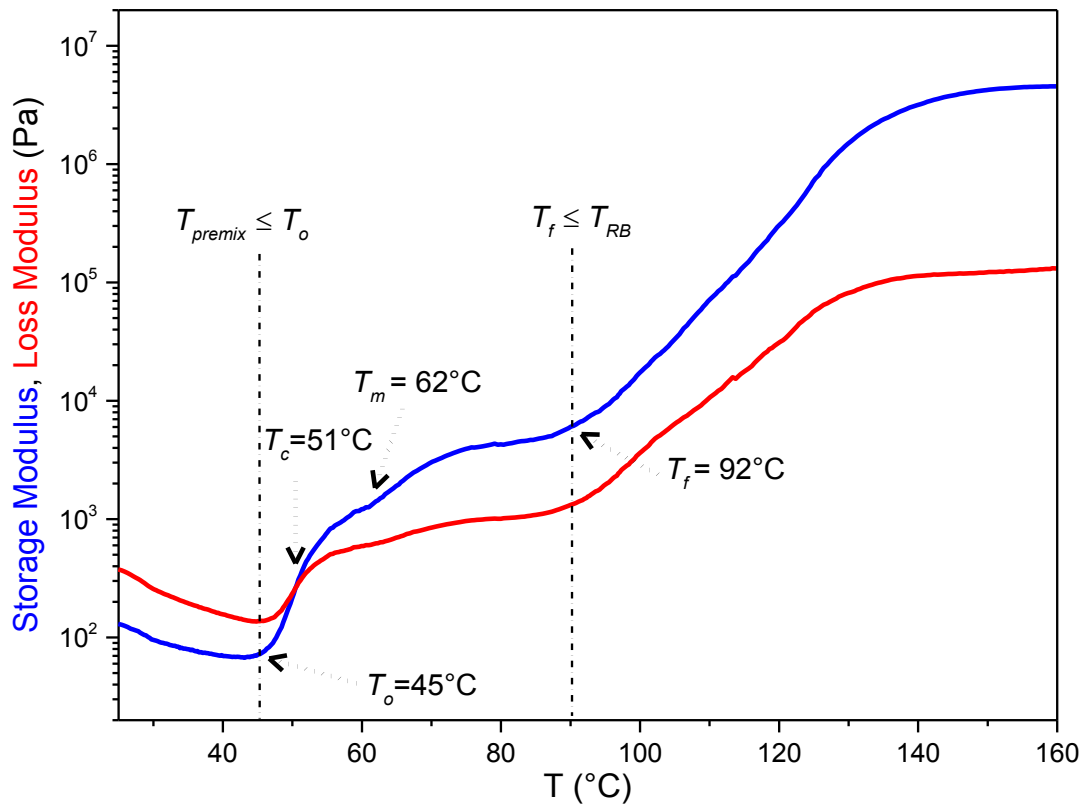


Figure 4.2 Storage modulus/ G' and loss modulus/ G'' versus temperature curves of a premix composed of PTMEG/MDI prepolymer and mPD chain extender

The crossover of the viscoelastic moduli ($G' = G''$) at the crossover temperature of $T_c = 51$ °C is considered a sol-gel transition temperature and corresponds to a critical reaction rate for an abrupt increase in the average molecular weight of the reaction mixture [67-73]. Over the crossover point, the elastic character dominates and the elastic modulus (G') grows faster than that of the loss modulus (G''). Interestingly, the propagation of polymerization (development of viscoelastic response) tends to slow down beyond the crossover temperature (T_c) due to less reactive amino groups of the generated oligomeric amine molecules. This relates to the fact that both the primary amino groups ($-NH_2$) are present on the same aromatic ring of mPD molecule and the reactivity of the second amino group is compromised once the first amino group reacts to generate an oligomeric amine molecule [31].

A slight kink at around 62°C reflects melting of undissolved mPD in prepolymer and is designated as the melting temperature (T_m).

Further on, there is a phase separation of hard segments whereat the viscoelastic response stabilizes until the inflection point temperature (T_f) of 92°C. The inflection point temperature (T_f) corresponds to the inception of complex reaction sequences between isocyanate and amino groups of oligomeric, prepolymeric and partially extended prepolymeric chains in a complex reaction mixture. Finally, G' and G'' achieve a plateau value, indicating the termination of the polymerization and the solidification of formed polyurethane-urea polymer.

In order to avoid any premature gelation and to successfully realize the reactive blending procedure in an internal mixer, the temperature of premixing a prepolymer with diamine (T_{premix}) should be less than the onset temperature (T_o) and is taken to be the room temperature (RT). The temperature of reactive blending (T_{RB}) should be higher than the inflection point temperature (T_f) to ensure high conversion of amino groups and is taken to be 100 °C.

4.1.2 Torque-time response of the reactive blending procedure

The torque vs. time curves from the internal mixer provides a direct indication of the *in-situ* polymerization of PUU during the reactive blending procedure with NBR. In Fig 4.3, the torque profiles are distinguished into three zones: The loading and mastication of NBR towards a steady-state torque value is shown in Zone I. The level of this steady-state torque decreases gradually with the load factor of neat NBR for different blend compositions. Zone II reflects pouring of premix into the mixing chamber containing NBR. The torque rises and stabilizes immediately, indicating a fast propagation of polymerization to generate PUU in NBR. This abrupt rise in torque reflects high reactivity of isocyanates towards amino functional groups.

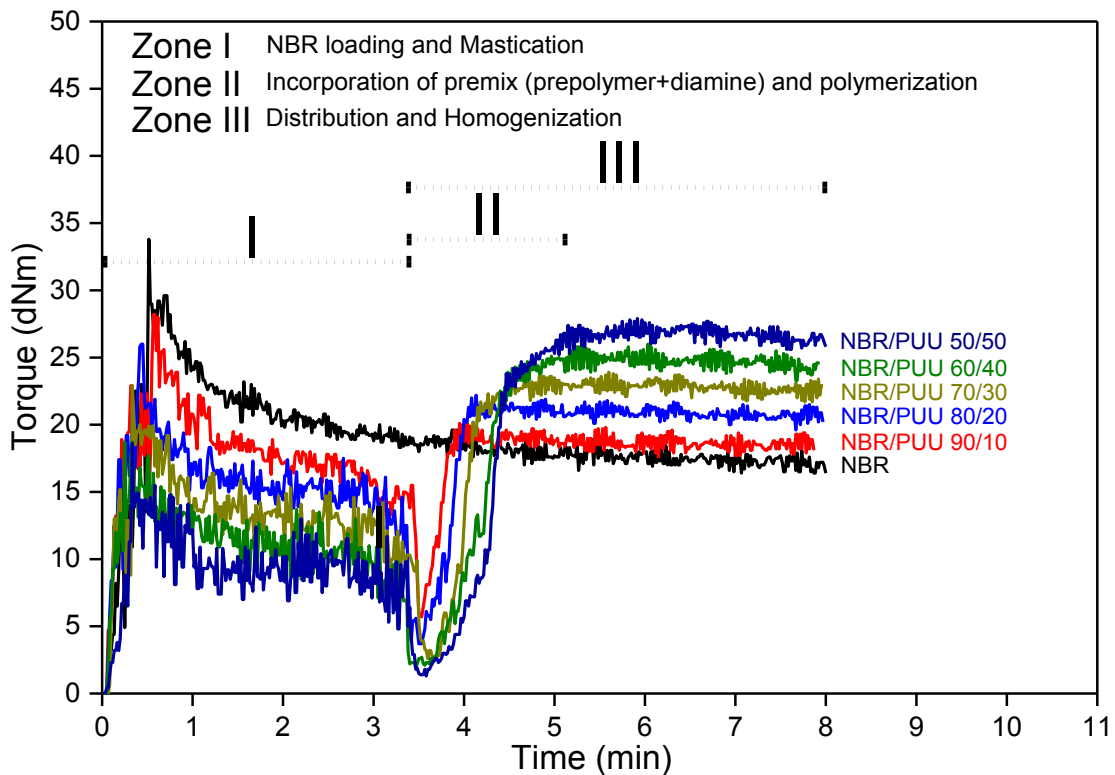


Figure 4.3 Torque versus time curves of NBR and NBR/PUU blends reflect (I) the mastication of NBR, (II) the incorporation of premix and *in-situ* generation of PUU, and (III) the distribution of premix/*in-situ* generated PUU in rubber matrix, homogenization of blend components and steady level of final torque

Zone III indicates disintegration and distribution of the premix and *in-situ* generated polyurethane-urea in NBR, and homogenization of the blend components. The level of final steady state torque rises gradually due to the presence of stiff PUU phase in NBR/PUU blends and reflects blend compositions. The overall reaction scheme to the *in-situ* synthesized PUU is shown in Fig. 4.4.

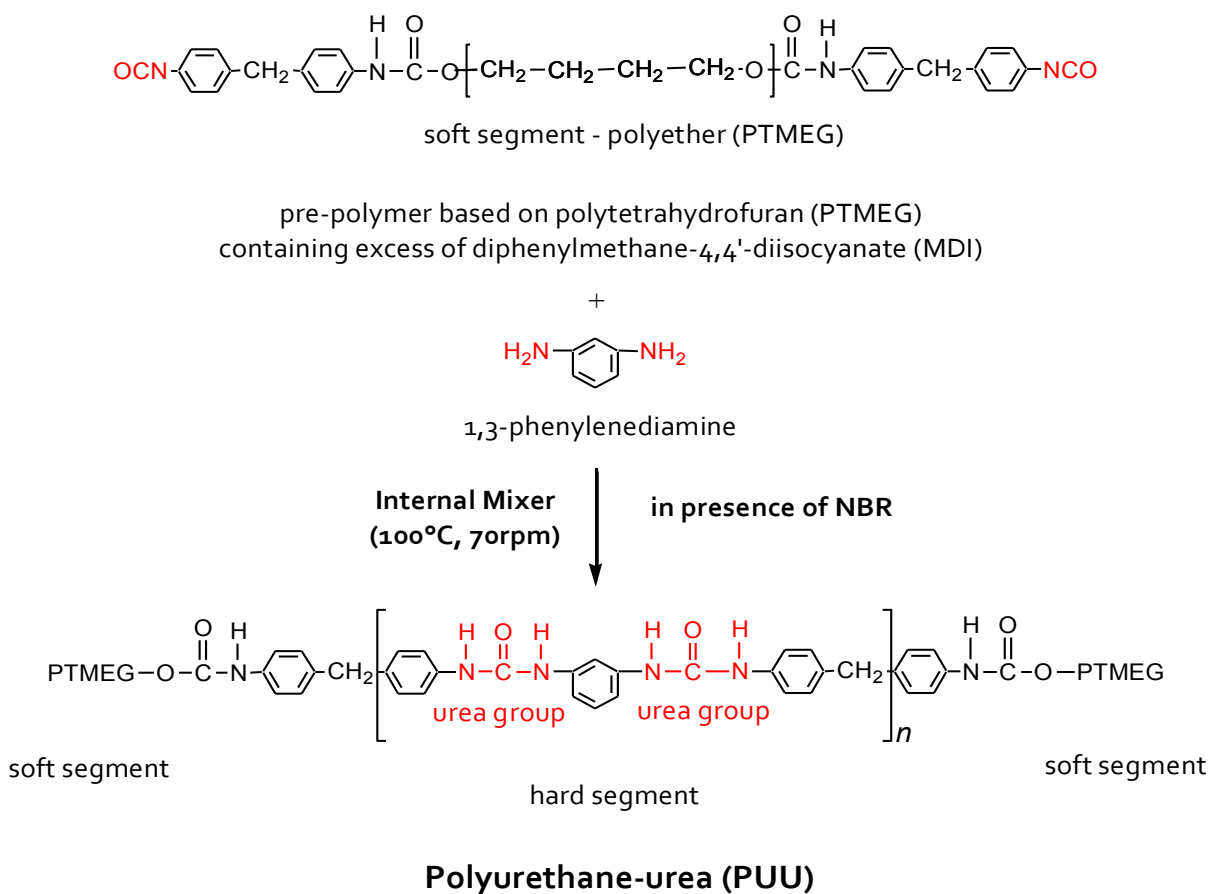


Figure 4.4 Overall reaction to the *in-situ* generated polyurethane-urea in presence of NBR in an internal mixer at 100°C and 70 rpm, $n = 3.8$ (determined from ^1H NMR spectroscopy).

4.1.3 Structural characterization of *in-situ* PUU

The *in-situ* synthesized PUU is extracted from the blends by DMSO- d_6 at 100°C and the obtained solution is directly characterized by ^1H NMR spectroscopy. Even though a small amount of NBR was also dissolved, there is no signal overlap, which hampers the evaluation of the urea group formation. The ^1H NMR spectrum (Fig. 4.5) depicts the region of urethane, urea and aromatic

proton signals of the extract from NBR/PUU 70/30 and is exemplarily for all extracted PUUs. The structural units observed in this spectral region are characteristic for the formed hard segments. The NH signal at 9.45 ppm results from the urethane groups formed by reaction of MDI with the hydroxyl end groups of the PTMEG soft segment. The urea NH signals appear in the 8.7 – 8.3 ppm region.

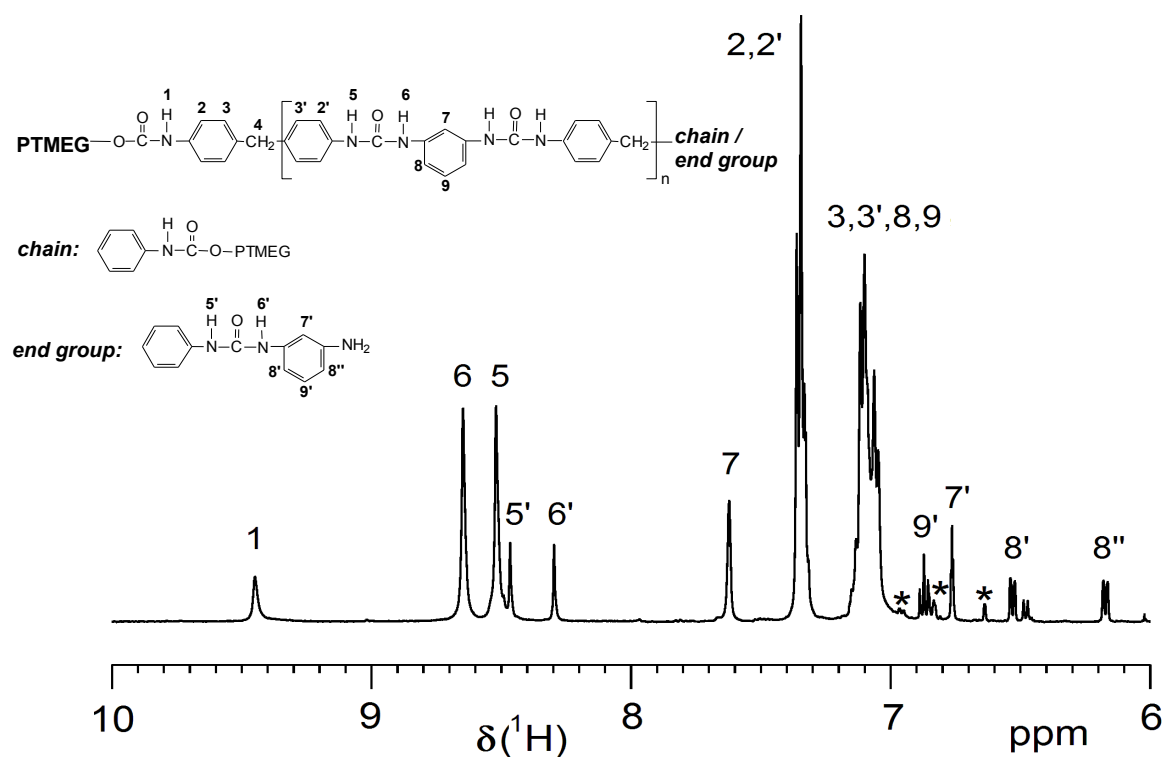


Figure 4.5 ¹H NMR spectrum (region) of NBR/PUU 70/30 blend (solvent: DMSO-d₆) with formula of the PPU hard segment for signal assignment. PTMEG denotes the polytetrahydrofuran based soft segment.

* marks the NBR signals

The non-symmetric substitution of the urea group results in two signals of same intensity both for the hard segment repeating unit (H₅ at 8.52 ppm and H₆ at 8.65 ppm) and for end groups resulting from one-side reacted 1,3-aminobenzene (H_{5'} at 8.47 ppm and H_{6'} at 8.30 ppm). This end group also results in aromatic proton signals (H₇ – H₉) in the 6.9 – 6.1 ppm region whereas the aromatic backbone signals are low-field shifted and partially overlap for 4,4'-methylene diphenyl (H₂ - H_{3'})

and 1,3-phenylene units ($H_7 - H_9$). In consequence of amino end groups some of the hard segments are not incorporated between soft segments but terminate PUU chains.

The conversion of amino groups was calculated from the urea NH signals integrals (I) of $H_{6'}$ and H_6 . For all PUUs the conversion of amino groups was found to be 87 ± 3 % as calculated from $\text{conversion} = 1 - I_{H_{6'}} / (I_{H_6} + 2 I_{H_{6'}})$. This amino group conversion is less, probably due to steric hindrance or reduced reactivity of the second amino group. Nevertheless, this is a good conversion, taking into account problems in adjusting exact stoichiometric ratio of amino and isocyanate groups. The number of repeating units in the hard segment n , is determined by the reactive NCO content in the prepolymer. With the reasonable assumption that each polyurethane-urea hard segment starts and terminates with a urethane group (see formula in Fig. 4.5), a number average of $n = 3.8 (\pm 0.2)$ can be calculated from urethane and urea NH signal integrals.

4.1.4 Energy-filtered transmission electron microscopy

TEM micrographs are shown in Fig. 4.6 to present the dispersed elliptical-shaped PUU domains in NBR matrix and to perform the interfacial characterization of the exemplarily selected NBR/PUU 70/30 blend. In bright field image (Fig. 4.6(a)), the darker continuous area corresponds to the NBR stained with OsO_4 , the brighter disperse areas correspond to PUU. Fig. 4.6(b) depicts elemental distribution of carbon where a 30 nm thin interphase layer is visible as dark borderline along the interface between NBR and PUU. In order to observe the presence of an interphase, image spectroscopy in the plasmon loss region was performed. Amplitude (Fig. 4.6(c)), position (Fig. 4.6(d)) and width (Fig. 4.6(e)) of the plasmon peak in each pixel of the image was evaluated. The amplitude depends on specimen composition and local specimen thickness, thus even though it shows a contrast, it cannot be evaluated easily alone. The width of the plasmon peak cannot be interpreted directly, but provides a hint to the existence of the

interphase. The position of the plasmon peak is related to the chemical composition. Line scans in Fig 4.6(d) clearly give proof of the existence of an interphase. The overall gradient in the image is caused by the drift of TEM's high tension during the acquisition of the image series but still the interphase region is clearly observable.

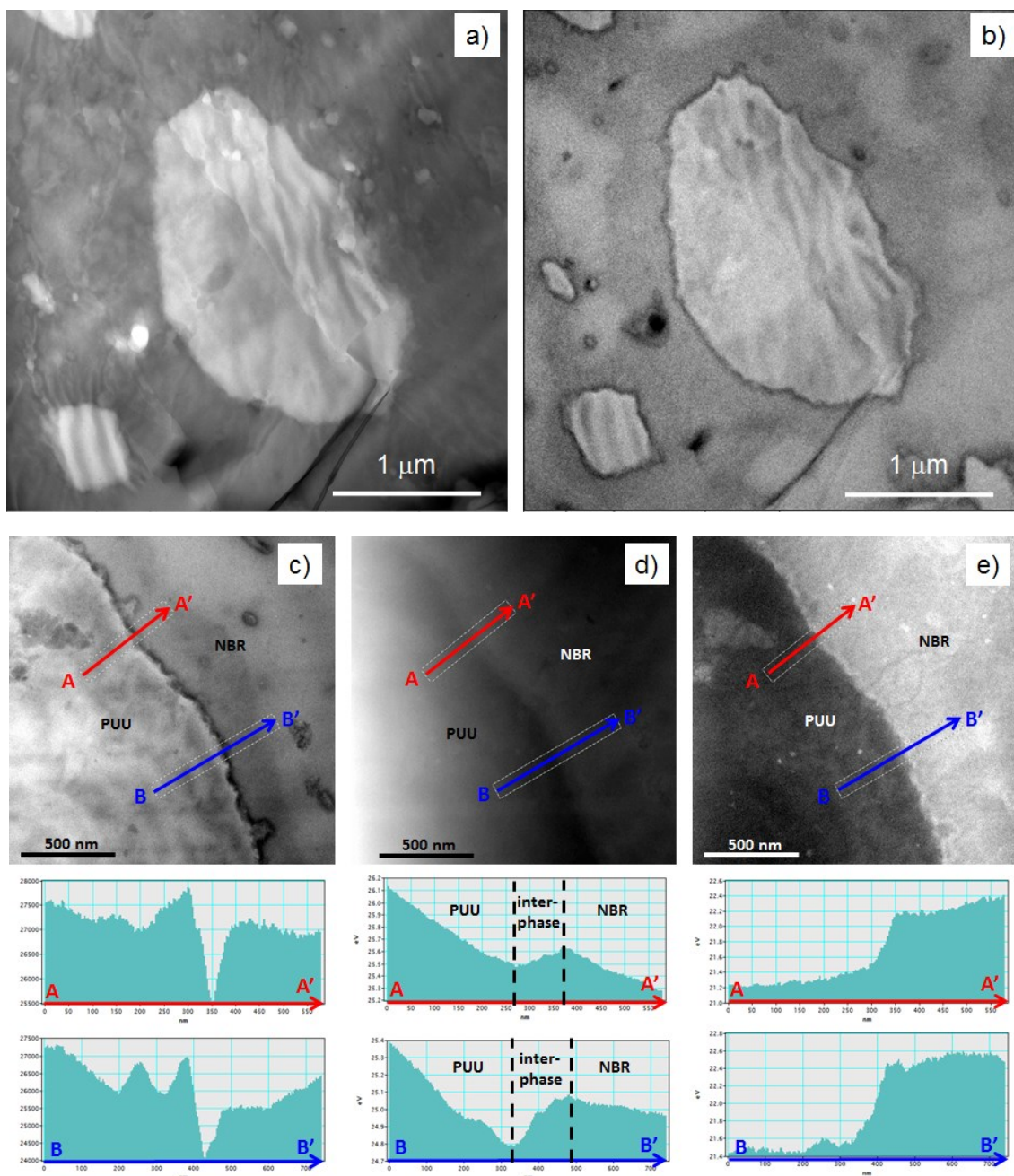


Figure 4.6 TEM images of the NBR/PUU 70/30 blend. (a) Bright field image. (b) Carbon map. Note the thin dark borderline between the NBR and PUU phases, (c), (d), (e) amplitude, position and width of plasmon peak, respectively of the boundary region between the NBR

4.1.5 SEM-EDX analysis

The strong interfacial adhesion between the phases of PUU and NBR is verified by the scanning electron microscopy along with the energy dispersive X-ray spectroscopic investigation of the NBR/PUU blends. A SEM micrograph of the cryo-fractured surface of a 70/30 blend specimen is exemplarily shown in Fig. 4.7. The oxygen-rich nano- to micro-sized domains of *in-situ* synthesized PUU can be seen dispersed in dark NBR matrix. The absence of interfacial separations (gaps) along the irregular interfacial boundary indicates a strong adhesion between PUU and NBR. This attribution is related to the mutual interpenetration, intermingling and interlocking of polymer chains, which occurs during the *in-situ* polymerization of PUU in NBR. The process of compatibilization i.e. the mutual diffusion of polymer chain and the formation of entangled interfacial region is the key to the significant improvements in mechanical and dynamic-mechanical properties of the blend compositions as will be discussed from here onwards.

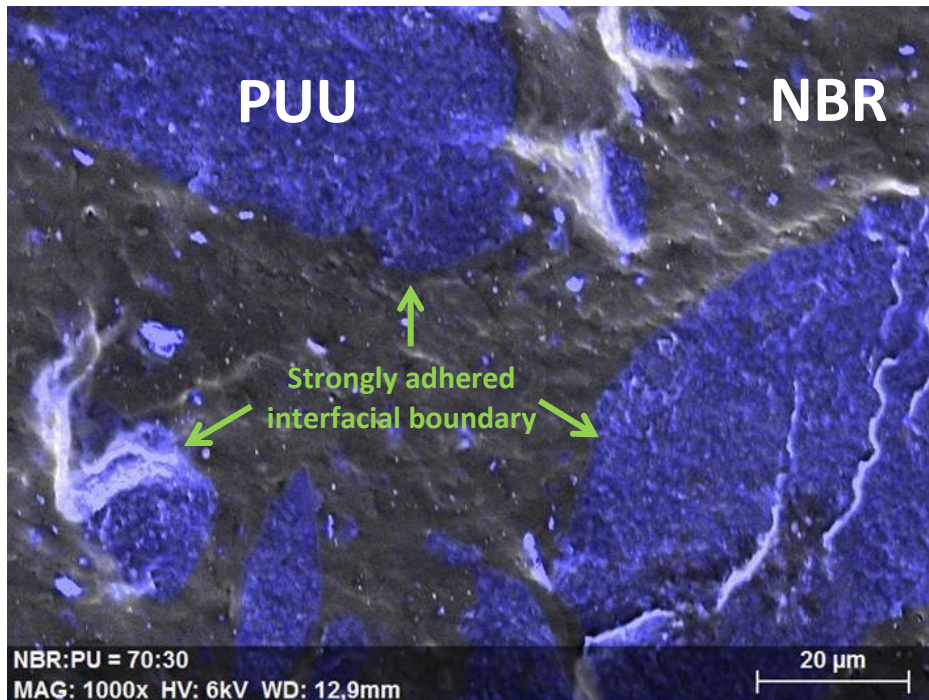


Figure 4.7 SEM-EDX micrograph of NBR/PUU 70/30 blend

4.1.6 Curing behavior

The cure curves, given in figure 4.8, show a gradual rise in the minimum (M_L) and maximum torque (M_H) values with increasing PUU to NBR ratio in compounds. The steady increase in minimum and maximum torque is attributed to the strong reinforcing tendency of *in-situ* synthesized PUU phase in blends. The existence of interphase is revealed in section 4.1.4 and its repercussions are observed during the vulcameter test.

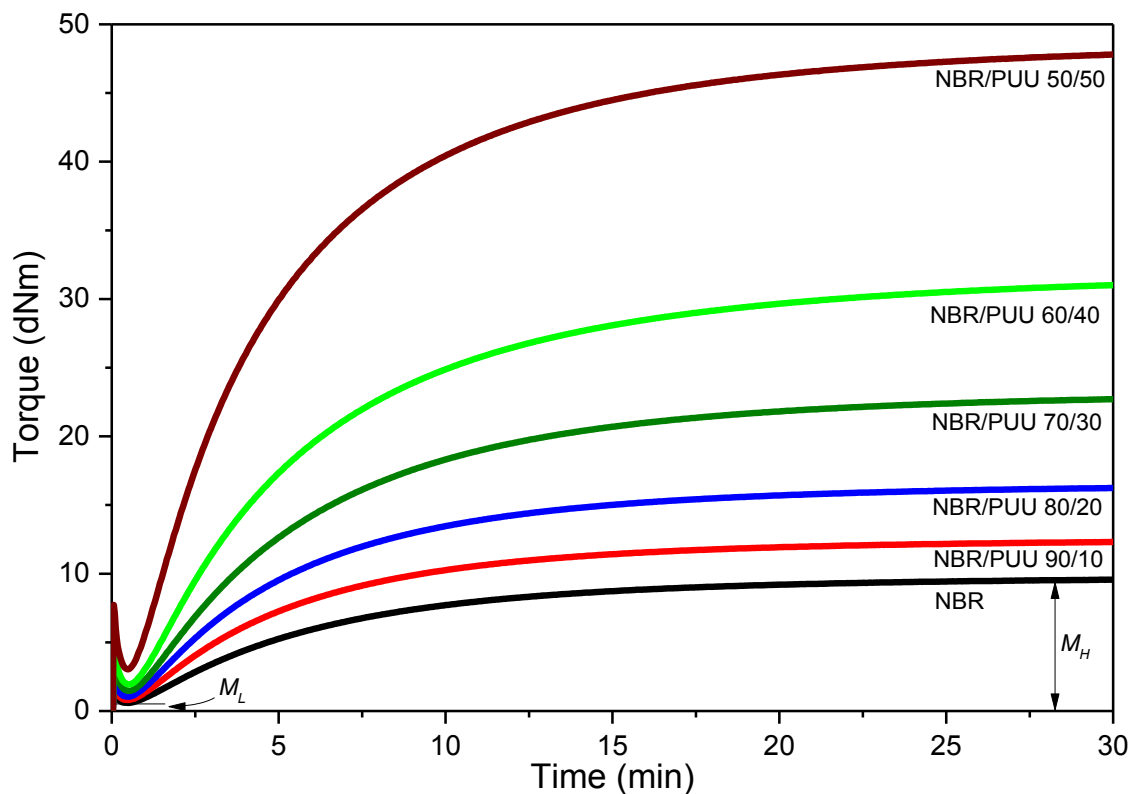


Figure 4.8 Cure curves of NBR/PUU blends in comparison with neat NBR

The *in-situ* synthesized PUU resists shearing deformation during the rheometer testing of blends and leads to a gradual rise in the minimum torque (M_L) value with increase in stiff PUU to soft NBR weight ratio in blends. The dispersed PUU domains act as physical crosslinks in NBR matrix. Higher loading produces more PUU domains and physical crosslinks in blends. The peroxide crosslinking of a physically crosslinked NBR matrix brings a consistent rise in

maximum torque (M_H) value with increasing PUU weight fraction in NBR/PUU blends. Additionally, the interfacial radical co-vulcanization of rubber and polyurethane-urea chains is conceived, which also contributes to torque development. It has been reported that the methylene group of MDI unit of urethane/urea moieties can undergo radical formation and participate in a chemical crosslinking process through hydrogen abstraction [74, 75]. Importantly, it is clear that the PUU domains retain stiffness at the vulcanization temperature of 160°C.

4.1.7 Mechanical properties

Fig 4.9 presents a comparison of stress-strain curves of all the compounds. The tensile response of compounds is reinforced steadily with increasing PUU to NBR weight ratio. It appears that the deformation of compounds under tensile loads relates to the extent of torque developed (M_H - M_L) during the cure test.

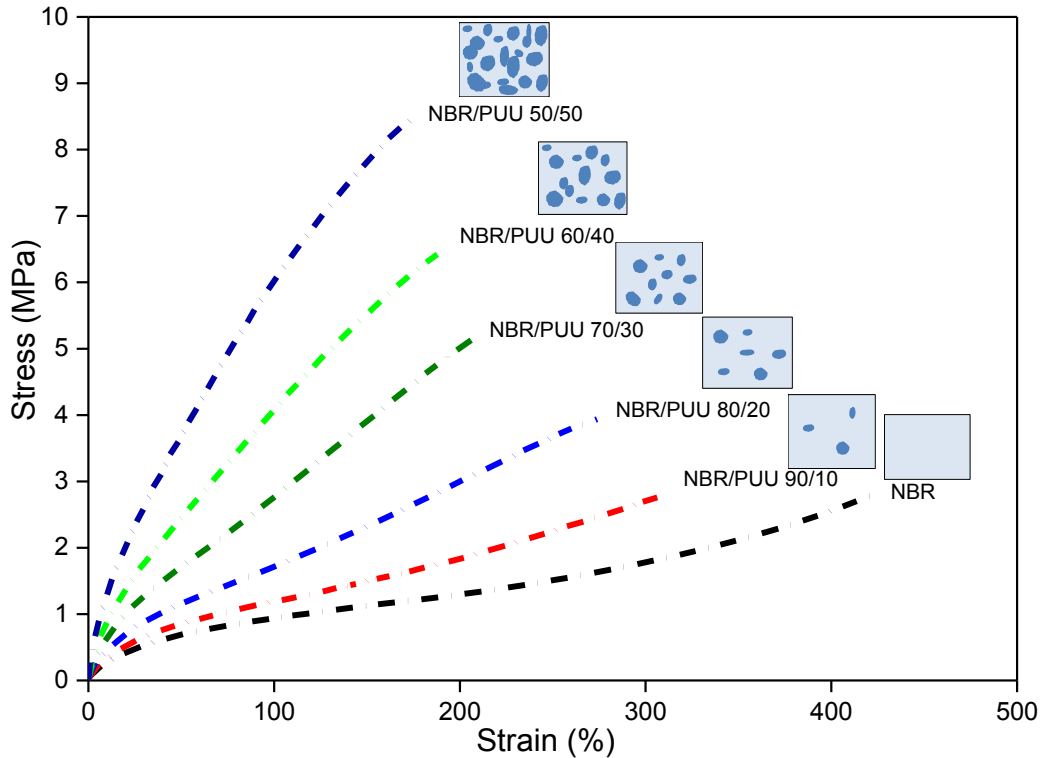


Figure 4.9 Stress-strain curves of neat NBR and its blends with *in-situ* synthesized PUU. The corresponding morphological sketches of the heterophase blends are also shown.

The existence of an interphase causes an effective stress transfer between the blend components and, consequently, the tensile response improves steadily towards higher PUU to NBR ratio in the compounds. The tensile modulus and ultimate strength improve steadily, however, with a compromise on ultimate elongation at break on increasing PUU to NBR ratio in blends. Noticeably, the load-bearing capacity of compounds varies from a sigmoidal rubbery behavior towards a brittle fracture behavior on replacing elastic NBR with the stiff PUU.

Table 4.2 shows that the tear strength improves with blend ratio as a consequence to a higher hindrance offered by the stiff PUU domains towards propagation of tearing paths. The hardness increases due to the presence of stiff PUU phase in blends. Interestingly, the compression set values are better for blends as compared to the neat NBR. This refers to the fact that the stiff PUU domains are spatially deflected, without being pressed, in a continuous rubber matrix during the compression set test. The compression set value decreases on lowering NBR weight fraction in blends; this is due to a less contribution towards compression set from the rubber portion of blends.

4.1.8 Dynamic-mechanical analysis

The influence of incorporating the *in-situ* synthesized PUU on the tensile storage modulus (E') and loss factor ($\tan \delta$) of NBR is shown as a function of temperature in Fig. 4.10 (a) and (b) respectively. The peak of the $\tan \delta$ vs temperature curve is taken as the glass-transition temperature, which appears at around $T_{g,NBR} = -12.8^\circ\text{C}$ for NBR in all compounds (see Fig 4.10(a)). The soft segments of PUU exhibit a broad glass transition relaxation peak at $T_{g,ss} = -52^\circ\text{C}$ in all the blends. The appearance of two distinct and unshifted glass transitions temperatures shows immiscibility between components of heterogeneous blends. However, the blend components are compatibilized during the process of reactive blending, as is explained in

section 4.1.4 and 4.1.5. The broad relaxation peak of the soft segments reflects a restricted mobility of the soft chain segments trapped in lengthy and rigid hard segments. The ability of urethane/urea moieties of hard segments to establish hydrogen bonding with ether groups of SS facilitates this mixing of soft and hard segments. It is important to mention here that the PUU domains retain stiffness and don't get soften up to 180°C, which is due to the strong bidentate hydrogen bondings among hard segments.

Table 4.2 Mechanical properties of compounds with and without *in-situ* synthesized PUU

	NBR	NBR/PUU 90/10	NBR/PU U 80/20	NBR/PUU 70/30	NBR/PUU 60/40	NBR/PUU 50/50
Young's Modulus (MPa)	2.4	3.0	4.4	6.7	8.3	14.4
Modulus at 10% (MPa)	0.3	0.3	0.4	0.6	0.9	1.3
Modulus at 50% (MPa)	0.7	0.8	1.2	1.6	2.4	3.7
Modulus at 100% (MPa)	1.0	1.2	1.7	2.5	4.1	6.0
Tensile Strength (MPa)	2.8	2.7	3.6	4.7	6.5	8.4
Elongation at Break (%)	411	293	248	214	190	173
Tear Strength (kN/m)	5.9	7.0	9.3	10.5	13.6	17.3
Hardness (Shore A)	45	51	57	65	71	77
Compression Set (%)	17.9	18.4	17.0	15.6	14.4	15.6

At $T_{g,NBR}$, a steady decrease in $\tan \delta$ peak height indicates an improved elastic response from the blends. The inset of Fig 4.10(b) presents the magnified region of $\tan \delta$ plot, which shows a gradual lowering of the loss factor values with increasing PUU to NBR ratio in blends. This indicates a lesser energy dissipation in blends as compared to NBR. The stability of E' and $\tan \delta$

values at two different temperatures shows a temperature stable viscoelastic behavior of the blends (see table 4.3). The blends develop a stable rubbery plateau region due to the temperature-stable stiffness of PUU domains in blends. This is ascribed to the fact that the secondary interactions of hydrogen bonding are very strong in hard segment domains of the PUU phase in blends.

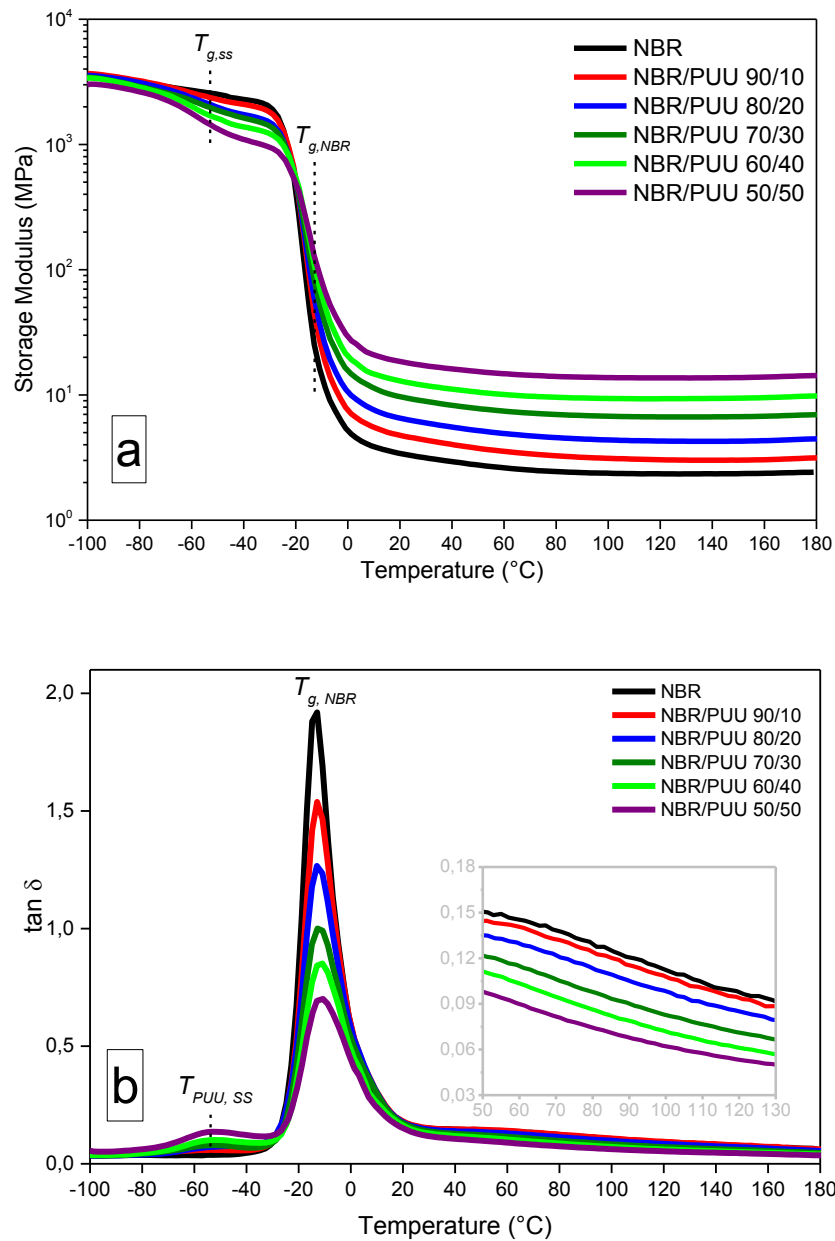


Figure 4.10 Dynamic temperature sweep measurements reflect a concentration-dependent improvement in a) storage modulus/ E' and b) loss factor/ $\tan \delta$ of NBR/PUU blends

The possible hydrogen bonding interactions within the PUU phase are shown in Fig. 4. 11. The urethane groups develop mono-dentate, whereas the urea groups develop bi-dentate hydrogen bonds. The bi-dentate H-bonds are very strong and dissociate close to the decomposition temperature of the polymer [76-79]. The hard segment domains remain associated by strong bi-dentate hydrogen bonding till very high temperatures. As a consequence, the stiffness and the reinforcing capability of the *in-situ* PUU phase remains intact, even at high temperatures.

Table 4.3 Dynamic mechanical characteristics of NBR and NBR/PUU blends as obtained from the storage modulus/ $\tan \delta$ vs temperature curves

	$T_{g, NBR}$	$T_{g, SS}$	E' at 60°C	$\tan \delta$ at 60°C	E' at 120°C	$\tan \delta$ at 120°C
NBR	-12.8	-	2.49	0.145	2.21	0.098
NBR/PUU 90/10	-12.8	-53.5	3.48	0.141	3.09	0.093
NBR/PUU 80/20	-12.6	-52.6	4.79	0.130	4.19	0.084
NBR/PUU 70/30	-12.6	-52.7	7.17	0.115	6.69	0.070
NBR/PUU 60/40	-11.9	-52.8	9.84	0.104	9.34	0.062
NBR/PUU 50/50	-11.8	-52.8	14.49	0.090	13.96	0.053

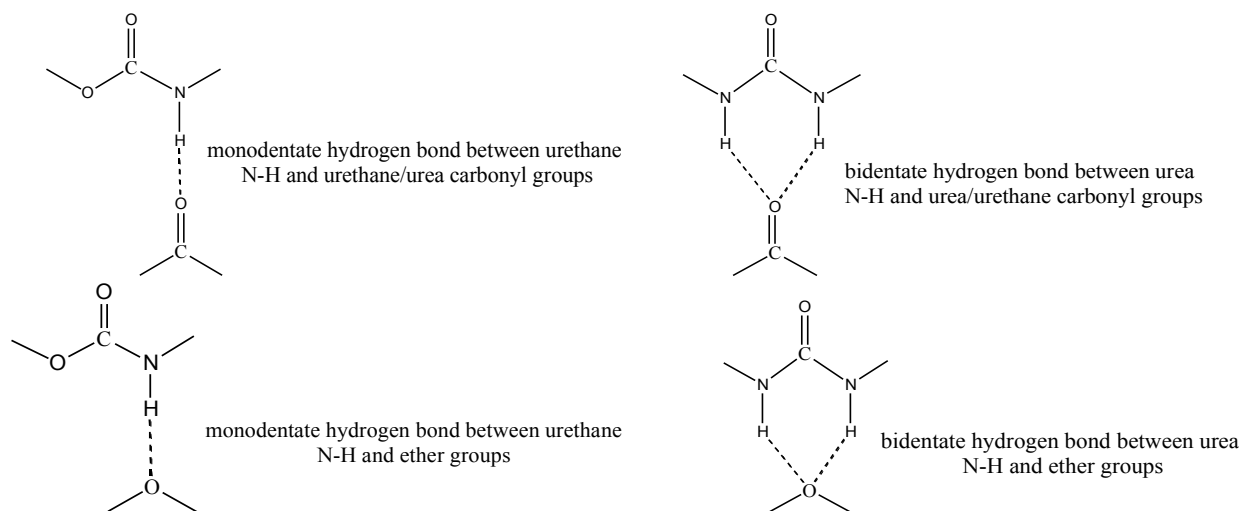


Figure 4.11 Hydrogen bonding interactions (mono- and bi-dentate) amongst segments of PUU phase in blends [84].

4.1.9 Wide angle X-ray scattering

In order to visualize segmental arrangements within the PUU phase, X-ray diffraction patterns as a function of Bragg angle (2θ) are obtained (see Fig. 4.12) for all the compounds. NBR shows a broad amorphous scattering hump at the diffraction angle (2θ) of 18.7° . The scattering patterns of blends also exhibit an amorphous halo; an indication of random segregation of hard segments and disorderly structured hard domains within the PUU phase. A weak reflection at $2\theta=21.3^\circ$ shows poor ordering of hard segments within hard domains.

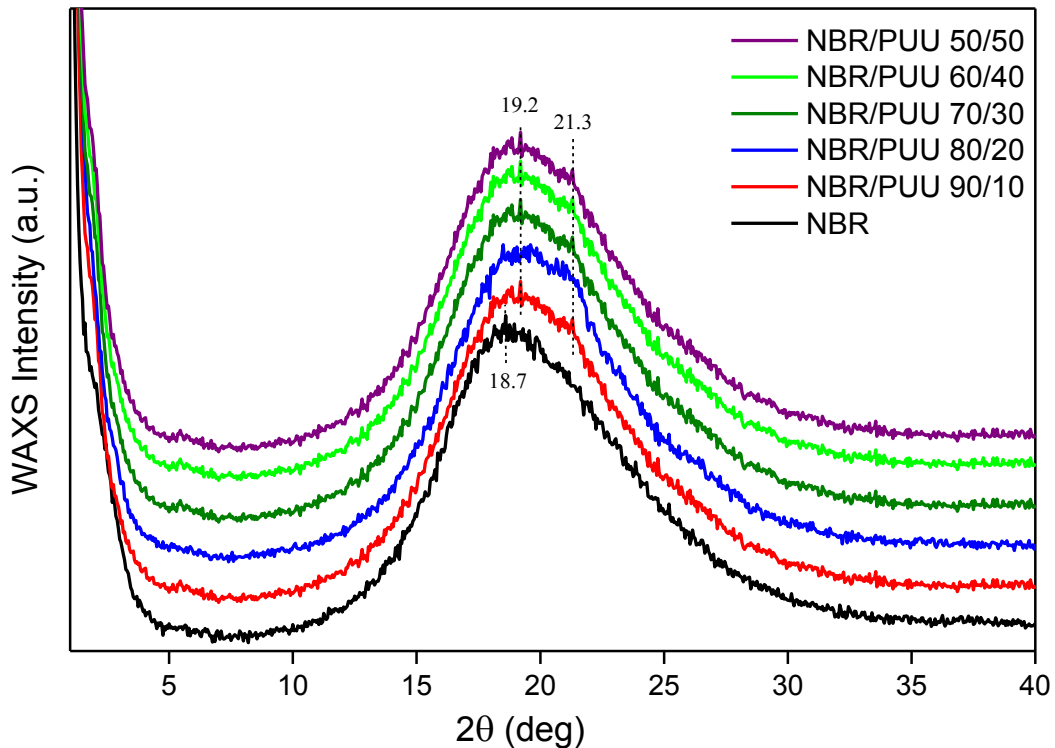


Figure 4.12 X-Ray scattering scans of NBR/PUU blends in comparison with neat NBR.

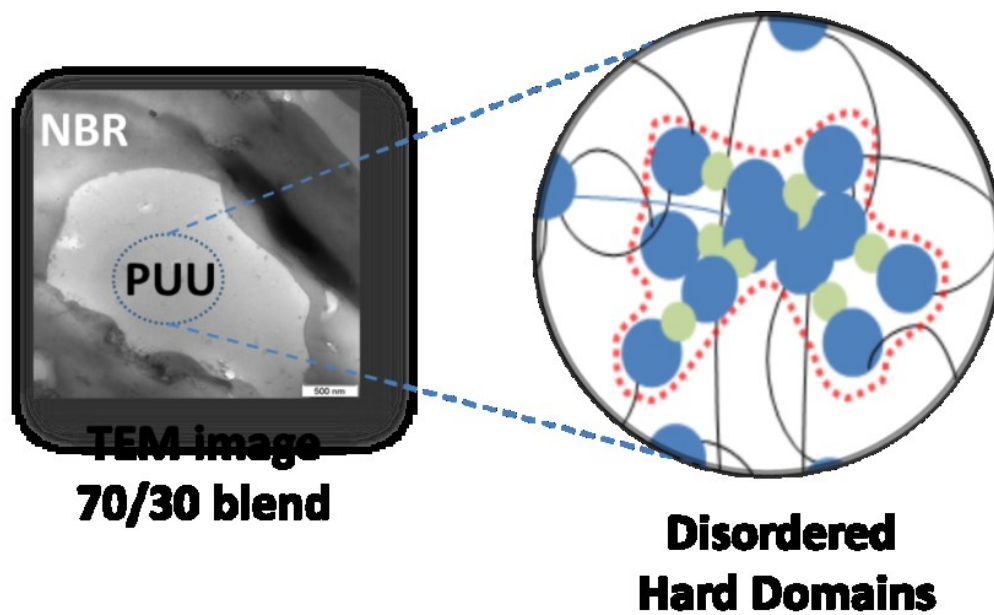


Figure 4.13 An exemplary TEM image (scale bar 500nm) of NBR/PUU 70/30 blend with the graphical representation of disorderly structured hard segment domains of *in-situ* synthesized PUU.

The ordered segregation of hard segments is hindered due to the restricted spatial movements of polyurethane-urea chains and the limited conformation of the rigid and lengthy HS containing intrinsically kinked MDI [32] and mPD units. The WAXS curves show a slight shift of amorphous halo from $2\theta=18.7^\circ$ for NBR to 19.2° for blends due to a collective X-ray scattering from the amorphous NBR matrix and the disorderly structured PUU phase (see graphical sketch in Fig. 4.13).

4.2 Role of diamine structure

The influence of structurally different diamines on the reactive blending procedure, the structural and morphological aspect of *in-situ* synthesized PUU and the performance characteristics of NBR/PUU 70/30 blends are thoroughly investigated in this study. Four structurally different diamines are selected, namely 1,3-phenylenediamine (mPD), 4,4'-(m-phenylenediisopropylidene)dianiline (BisAM), 1,4-Bis(aminomethyl)benzene (pXD) and 4,4'-Methylene-bis(2-chloroaniline) (MBCA). The structures of diamines are shown in section 3.1. The prepolymer is the same as used in section 4.1 and is based on 4, 4'-diphenylmethane diisocyanate (MDI) and poly(tetramethylene ether) glycol (PTMEG). The formulations of compounds are given in Table 4.4.

Table 4.4 Composition of compounds along with the stoichiometric quantities of prepolymer and diamine*

Ingredients	Blend-DA***				NBR
	Blend-mPD	Blend-pXD	Blend-MBCA	Blend-BisAM	
NBR	70	70	70	70	100
Premix**	30	30	30	30	
(PP/DA) NCO : NH ₂ 1:1	(27.05 / 2.95)	(26.28 / 3.62)	(23.64 / 6.36)	(22.27 / 7.73)	-

*Each blend is mixed with 3 and 2 parts of peroxide (Perkadox BC-40K-pd) and coagent (Rhenogran TAC 50) respectively per hundred parts of blend.

**PP/DA premix: PP stands for the prepolymer and DA stands for the type of diamine (mPD, pXD, MBCA or BisAM). Subsequent to the *in-situ* polymerization, PP/DA premix is written as PUU-DA.

*** Blend-DA represents Blend-mPD, -pXD, -MBCA and -BisAM compounds based on NBR and PUU-DA.

4.2.1 Chemo-rheological investigation

Stoichiometric quantities of the prepolymer and powdered diamine are mixed at room temperature for a homogenous premix to investigate the development of viscoelastic moduli (shear storage and loss modulus) in a linear temperature ramp experiment using a parallel plate rheometer. The viscoelastic response in this shear experiment, shown from Figure 4.14 to 4.17, is unique for each diamine because of the different solubility, reactivity, phase separation and structural aspects of the prepolymer/diamine based complex reaction mixture.

In general, the storage (G') and loss modulus (G'') decrease to a minimum value for all the premixes due to the absence of polyaddition reactions between isocyanate and amino groups of prepolymer and diamine respectively. The viscosity of prepolymer decreases, the solubility of diamine in prepolymer and the reactivity between reactive (amino, isocyanate) groups increases as the temperature rises. The initiation of addition reactions befalls at the onset temperature (T_o). Beyond T_o , both the storage and loss moduli rise by compensating the thermal effects of temperature ramp and the heat of exothermic polyaddition reactions. T_o limits the temperature to prepare a premix of prepolymer and diamine to avoid premature gelation. The crossover of viscoelastic moduli at the crossover temperature (T_c) is taken as the sol-gel transition point, whereat the reaction mixture crosslinks into a gel-like structure. The kink at T_m (melting temperature) represents melting of an undissolved diamine mass fraction. In PP/pXD and PP/mPD, the inflection point temperature at T_f is considered to be induced by the phase separation (beyond T_c) within the complex reaction mixture. The inflection point at the T_f reflects also a complex sequence of reactions between the amino and isocyanate groups of oligomers, prepolymer and partially extended prepolymer chains.

In specific, the PP/MBCA premix exhibits the simplest viscoelastic response (see Fig 4.14). The curves of storage and loss modulus do not exhibit the melting and high temperature inflection point temperature. The absence of T_m relates to the polarity of MBCA molecules i.e. the substituted chlorine atoms on the MBCA molecule enhance polarity and the solubility of MBCA molecules in prepolymer, due to which the melting temperature is not observed [80].

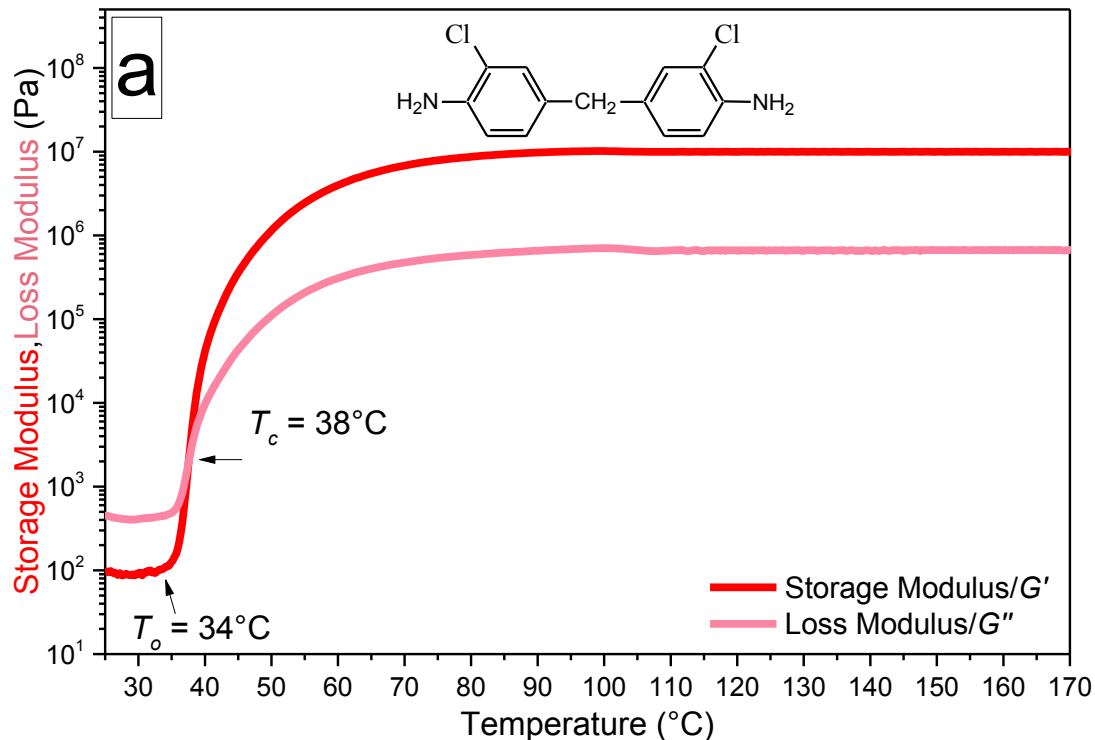


Figure 4.14 Temperature-dependent viscoelastic response (storage modulus/ G' and loss modulus/ G'') of PP/MBCA premix

The absence of T_f refers to the nonoccurrence of phase separation within the reaction mixture. This relates to the fact that the produced hard segments (based on MDI and MBCA) do not phase separate, however, do associate via hydrogen bonding. The mobility of chains, containing bulky MBCA molecules, is highly restricted, which seems to hinder the phase separation of hard segments. The segmental associations via hydrogen bonding do not seem to hinder the propagation of polymerization for the PP/MBCA premix. The rapid development of viscoelastic moduli shows a similar reactivity of the monomeric and oligomeric amine molecules towards the isocyanate-terminated molecules.

Fig. 4.15 shows that the viscoelastic moduli curves of the PP/pXD premix do not exhibit the melting temperature (T_m), which reflects complete solubility of the aliphatic pXD in the prepolymer. Beyond the crossover temperature (T_c), the propagation of polymerization reactions

is hindered by the phase separation of the flexible hard segments into hard domains and induces a high temperature inflection point at T_f .

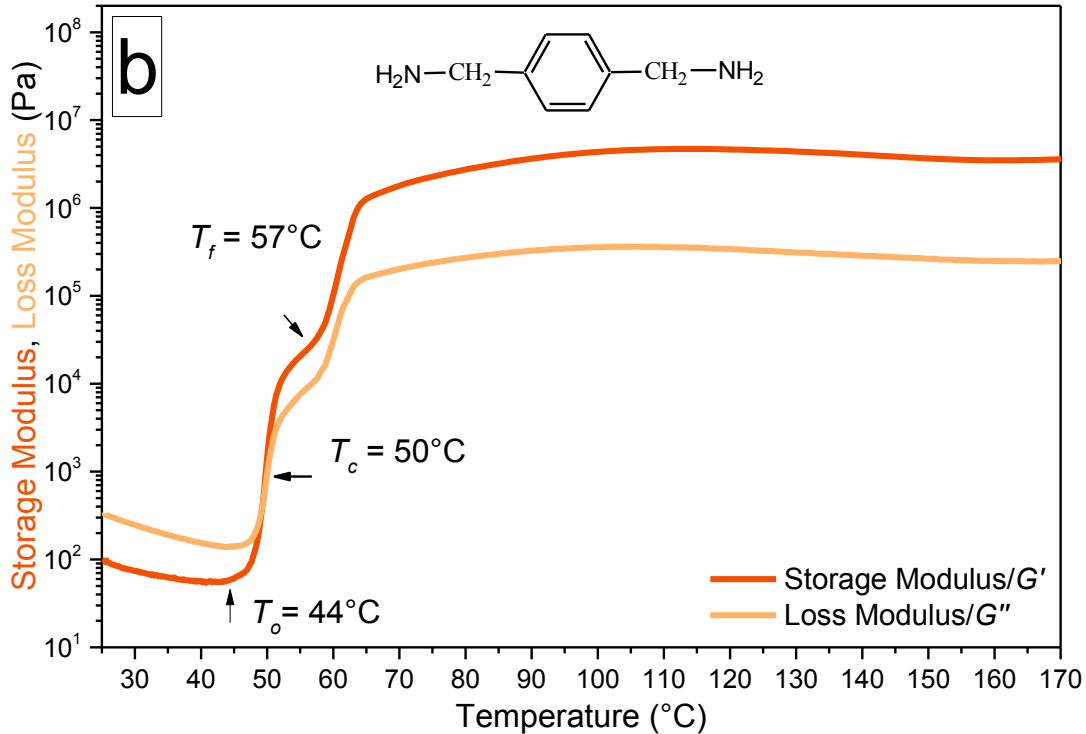


Figure 4.15 Temperature-dependent viscoelastic response (storage modulus/ G' and loss modulus/ G'') of PP/pXD premix

It appears from the Fig 4.16 that the incomplete solubility of mPD in the prepolymer entails the melting temperature (T_m) for the PP/mPD premix [81]. Importantly, the development of viscoelastic moduli tends to slow down beyond the crossover temperature (T_c) due to the less reactive amino groups of the generated oligomeric amine molecules. This relates to the fact that both the primary amino groups ($-\text{NH}_2$) are present on the same aromatic ring of the mPD molecule and the reactivity of second amino group is compromised once the first amino group has reacted to the isocyanate group [31]. Similar to the PP/pXD, the hard segments appear to phase separate into hard domains and the viscoelastic moduli shows steady values up until the inflection point temperature (T_f) of 92 $^{\circ}\text{C}$.

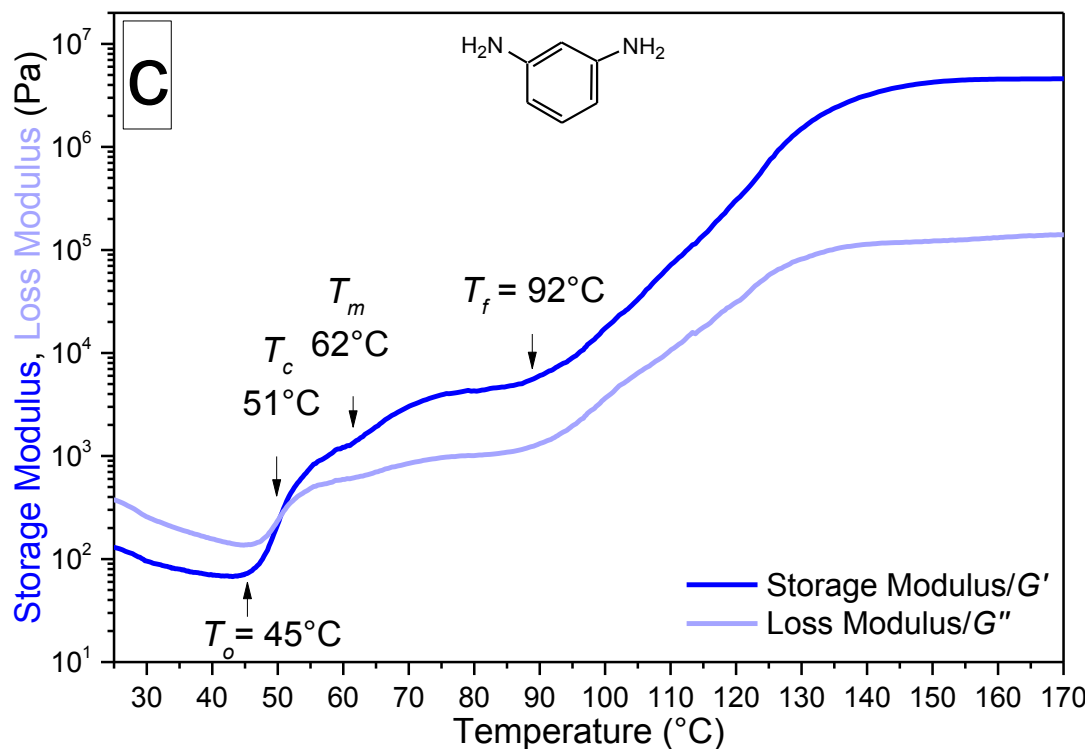


Figure 4.16 Development of viscoelastic response (storage modulus/ G' and loss modulus/ G'') during temperature ramp test of PP/mPD premix

The curves of the viscoelastic moduli of the PP/BisAM premix show a pronounced delay in the onset temperature ($T_o = 63^\circ\text{C}$) due to the low solubility of bulky BisAM in the prepolymer (see Fig 4.17). The curves show a prominent drop at the melting temperature (T_m) due to a large stoichiometric quantity of the BisAM in the prepolymer (see table 4.5). The moduli curves reflect a softening temperature (T_{soft}) at 157°C , which reflects dissociation of weak H-bond interactions developed between the hard segments to soften the polymerized PUU-BisAM. The softening of PUU-BisAM is an indication of the limited chain mobility and conformational flexibility of the clumsy hard-segments and the barrier of BisAM isopropylidene groups to develop stronger inter-hard-segmental H-bond associations amongst loosely packed PUU-BisAM chains. It becomes obvious that the weak inter-hard-segmental H-bond associations can survive up to 123°C in the polymerized PUU-BisAM. The pXD, mPD and MBCA do not exhibit softening temperature

(T_{soft}), which reflects the strength of bidentate hydrogen bonding among the hard segments of the polymerized polyurethane-urea.

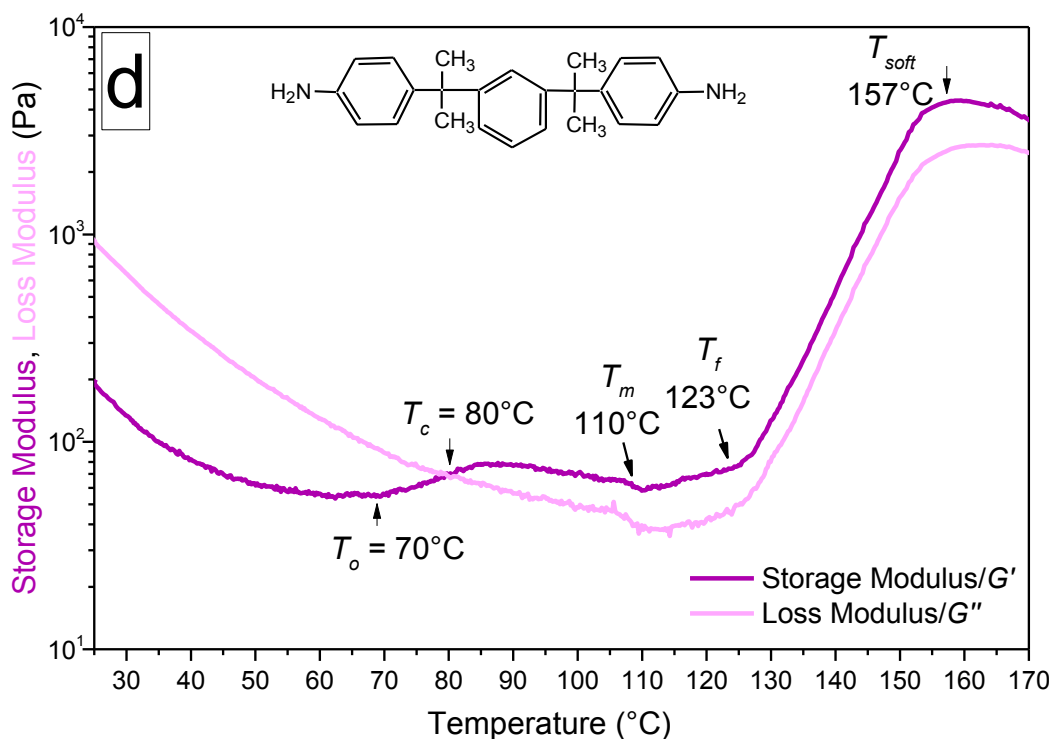


Figure 4.17 Development of viscoelastic response (storage modulus/ G' and loss modulus/ G'') during temperature ramp test of PP/BisAM premix

Table 4.5 Characteristic temperatures obtained from the chemo-rheological investigation of PP/mPD, PP/pXD, PP/MBCA and PP/BisAM premixes

Temperature ($^{\circ}\text{C}$)	Prepolymer-diamine Premix			
	PP/MBCA	PP/pXD	PP/mPD	PP/BisAM
T_o	34	44	45	70
T_c	38	50	51	80
T_m	-	-	62	110
T_f	-	57	92	123
T_{soft}	-	-	-	157
T_{premix}	≤ 34	≤ 44	≤ 45	≤ 70
T_{RB}	≥ 38	≥ 57	≥ 92	≥ 123

The temperatures of premixing (T_{premix}) and reactive blending (T_{RB}) are obtained from the chemo-rheological analysis. It is shown in table 4.5 that the chemo-rheology of PP/BisAM premix provides the highest value of the inflection point temperature (T_f), which is considered as the

temperature of reactive blending to prepare all the four blends. The temperature of reactive blending (T_{RB}) is taken to be 125°C. All the premixes were prepared at the room temperature (RT) because the minimum value of onset temperature to avoid premature gelation is 34°C.

4.2.2 Reactive blending and torque-time profiles

It is important to mention here that the chemo-rheological measurements serve as a directive to select the temperatures for the reactive blending process. However, one should have in mind that the propagation of polymerization and the dynamics of polyurethane-urea chains are different between parallel plates of rheometer and in the mixing chamber of the internal mixer.

The blending process is adapted to blend NBR with the *in-situ* synthesized PUU, obtained from the premix of MDI/PTMEG prepolymer with mPD, pXD, MBCA and BisAM chain extenders (see Fig. 4.18). The T_{premix} and T_{RB} are RT and 125 °C respectively. The *in-situ* polymerization of polyurethane-urea is reflected in the torque-time response of the reactive blending procedure in the used internal mixer.

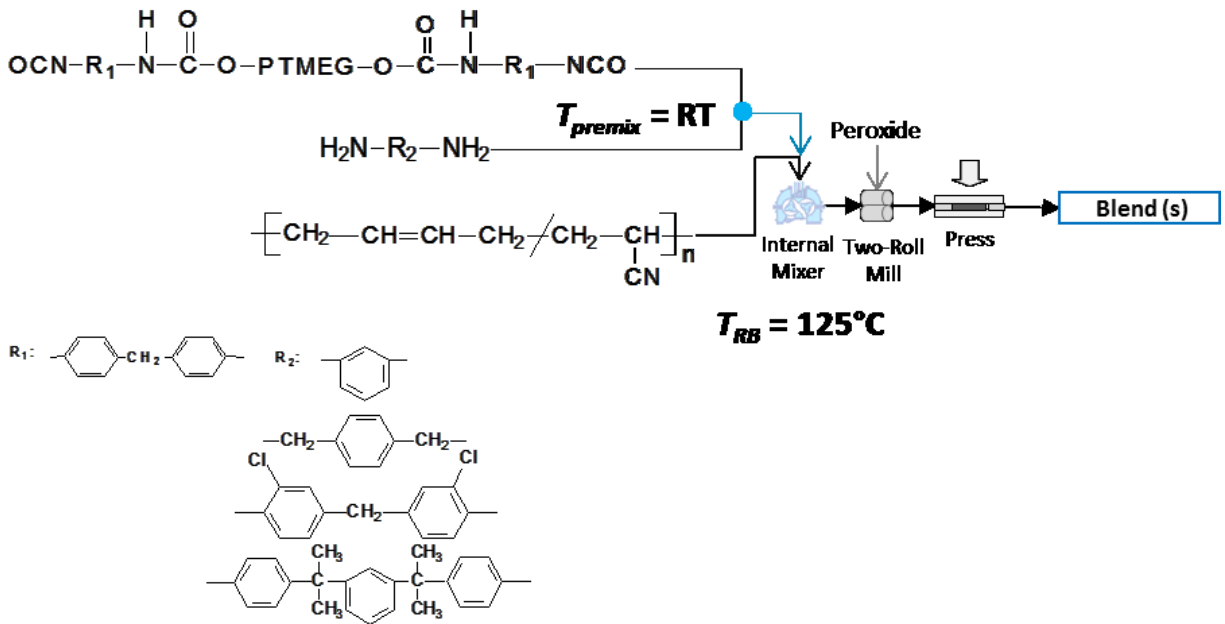
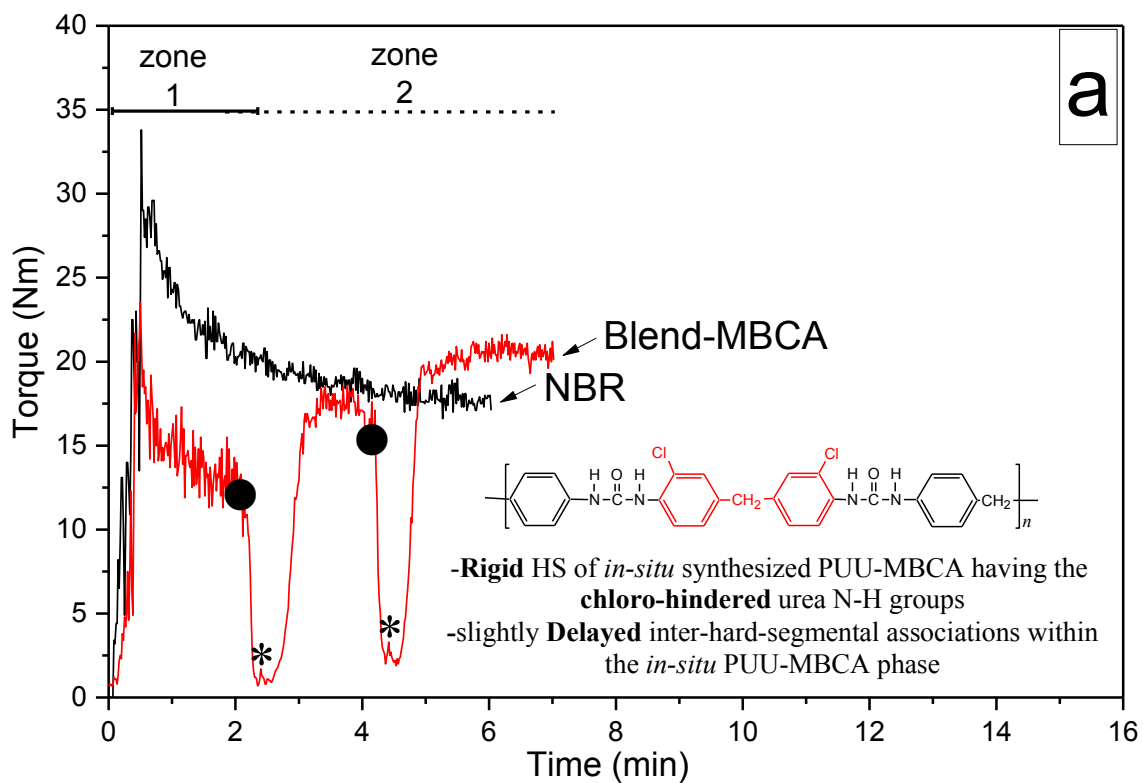
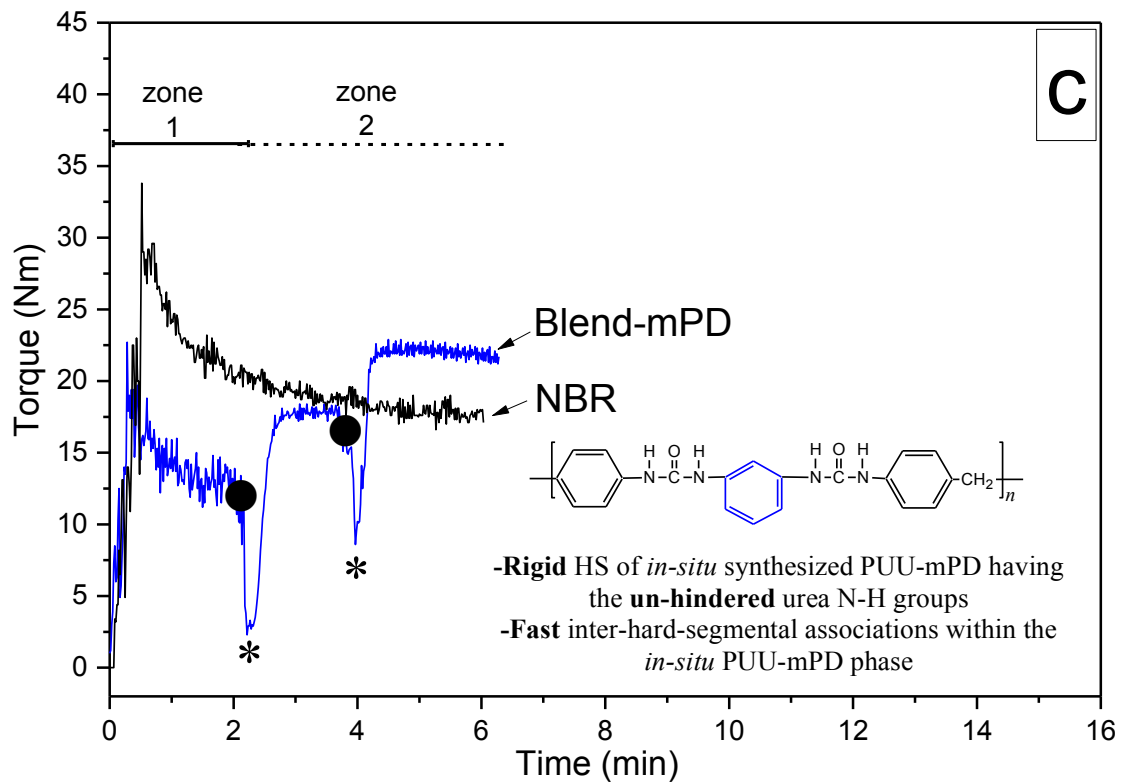
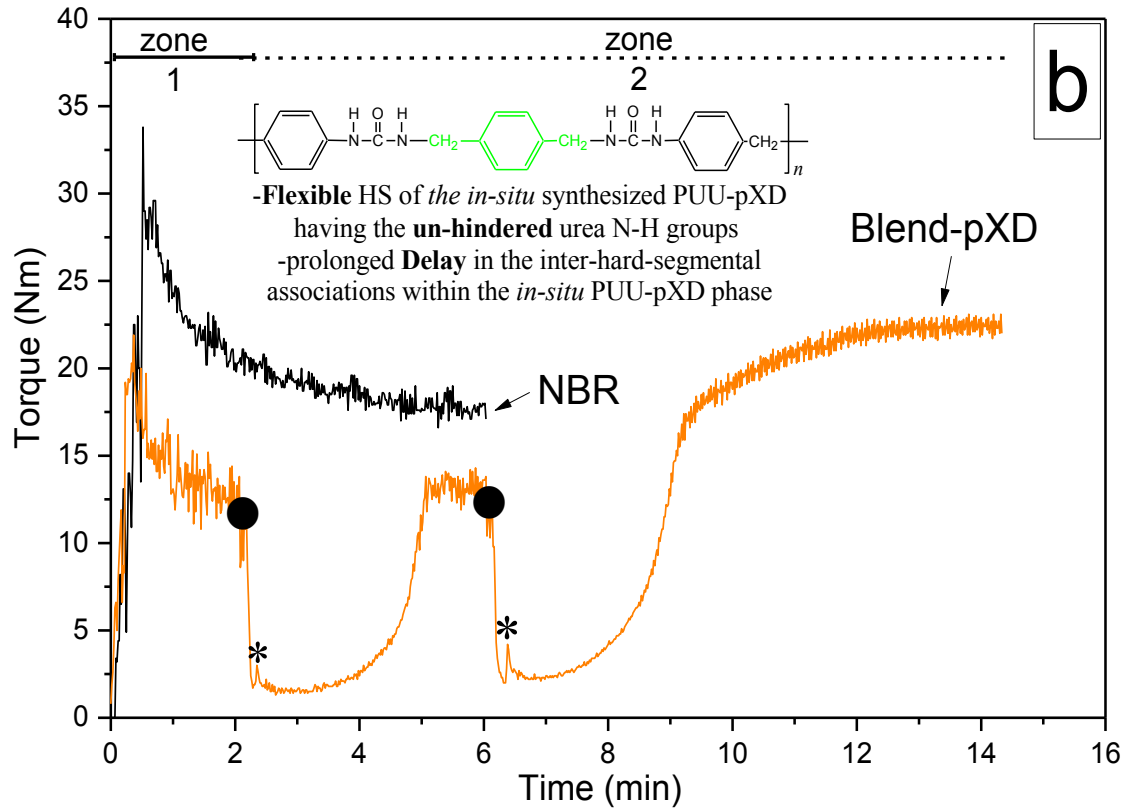


Figure 4.18 Process of reactive blending to prepare blends from NBR and premixes of MDI/PTMEG prepolymer with mPD, pXD, MBCA and BisAM

Fig. 4.19 shows the torque-time curves of the mixing cycle, which is distinguished into two zones. Zone 1 reflects the charging and pressing of NBR by ram into the mixing chamber and the mastication of the rubber thereon. Zone 2 reflects the lifting of ram, pouring of premix into the mixing chamber containing NBR at 125 °C, *in-situ* polymerization to PUU and dumping of NBR or NBR/PUU blends out of the mixing chamber.





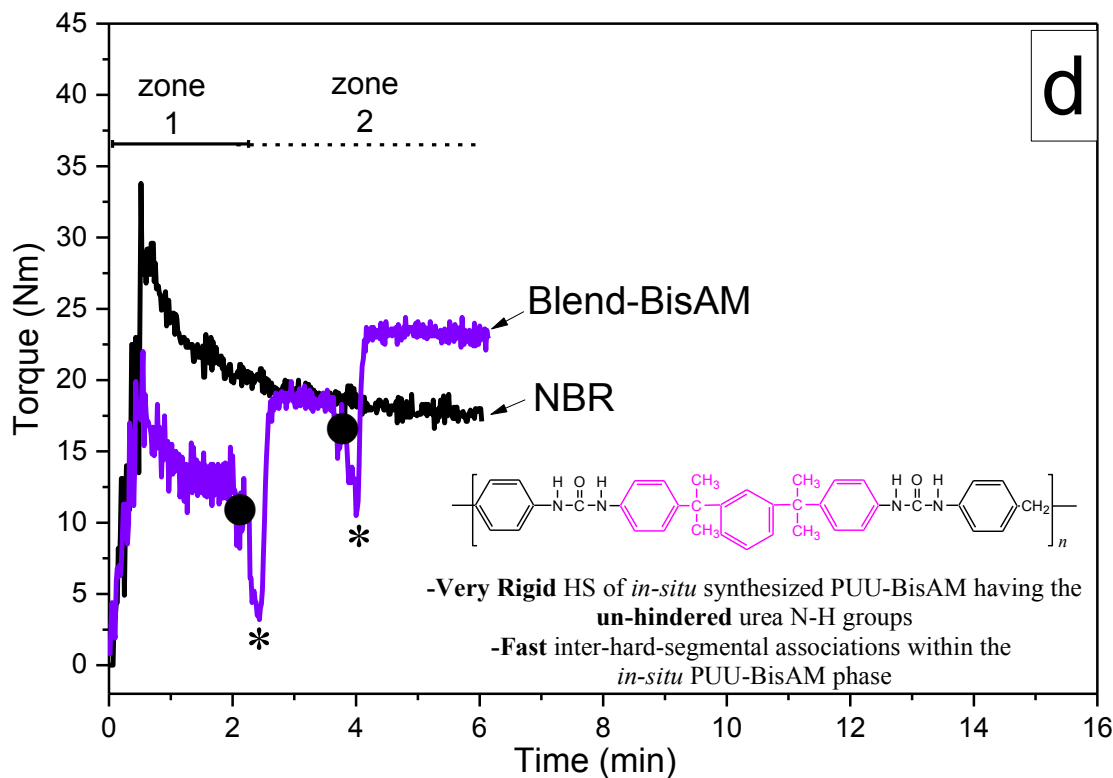


Figure 4.19 Torque vs time profiles of a) Blend-MBCA, b) Blend-pXD, c) Blend-BisAM, d) Blend-mPD. The solid dot (●) and the asterisk (*) indicate pouring of premix and occurrence of polyaddition reactions respectively. The chemical structure and the characteristic features of the *in-situ* generated HS of PUU-mPD, -MBCA, -pXD and -BisAM, as apprehended from the respective torque-time profiles, are also shown. The value of n is given in ^1H NMR section.

The torque-time profile of NBR is shown as a reference, to prepare blends of NBR with four different kinds of *in-situ* synthesized PUU, the two-step pouring of premix is indicated by the solid dots (●) in Fig 4.18. The torque rises after the pouring of premix and is allowed to attain a steady-state value. The pouring of PP/mPD and PP/BisAM premixes (see Fig 4.19 (c) & (d)) leads to an abrupt rise in torque towards its stable level, whereas the PP/MBCA and PP/pXD premixes (see Fig 4.19 (a) & (b)) bring about an abrupt rise and an immediate drop in the torque value. The torque rises due to the *in-situ* polymerization of polyurethane-urea and is indicated symbolically by an asterisk (*). The rising torque is an indication of increasing shearing forces to maintain a preset shearing rate during the blending procedure.

The fast acquisition of a stable torque level during blending of NBR with the *in-situ* synthesized PUU-BisAM and -mPD indicates the rapid associations amongst polyurethane-urea chains. The strength of these interactive associations will be discussed in subsequent sections.

Interestingly, the *in-situ* synthesized PUU-MBCA and -pXD behave initially as a polymer melt. In PUU-MBCA, the associations of chain segments are delayed due to the steric hindrance of the chloro-substituent in ortho position to the urea N-H group of the hard segments. In PUU-pXD, the aliphatic diamine produces a flexible urea linkage and the inter hard-segment association via hydrogen bonding is excessively impeded. On the addition of PUU-MBCA and -pXD premixes; the torque rises owing to polymerization of polyurethane-urea phase, drops immediately owing to flabbiness of PUU phase and rises once again when the polyurethane-urea phase acquire strength due to inter-chain association via mono/bidentate hydrogen bonding. The observations regarding each *in-situ* synthesized polyurethane-urea are summarized in their respective Fig. 4.19.

The unhindered amino group reacts faster with isocyanate group as compared to the hindered one however the reactivity of aliphatic, aromatic and the hindered diamines is normalized on performing the polymerization at a high temperature of 125 °C. Subsequent to polymerization reactions, structural aspects of the *in-situ* generated hard segments play a vital role in imparting strength to the PUU domains. It is established from the torque profiles that the inter-segmental hydrogen bonds can form and survive under strong shearing conditions of the thermo-mechanical blending conditions in an internal mixer.

4.2.3 Structural characterization by ^1H NMR

The *in-situ* synthesized PUU was solvent extracted from the not vulcanized blend materials and analyzed by ^1H NMR spectroscopy. Fig. 4.20 depicts the signal region of aromatic and

urethane/urea protons for the four PUUs investigated. The expected PUU structure could be proved for all blends. The signal of the urethane group resulting from the reaction of PTMEG with MDI appears for all samples at 9.27 ppm (H1). The chemical shifts of the two protons of the urea group (H5 and H6) are heavily dependent on the structure of the diamine. Thus, the ortho-chlorine atom in MBCA results in a significant low-field shift (9.17 ppm) compared to substituents without ortho-substitution resulting from mPD, BisAM, or MDI (8.1 – 8.6 ppm). For the only aliphatic-aromatic urea group of PUU-pXD the urea proton of the aliphatic site (H6) results in a signal at 6.4 ppm (Fig. 4.20d). Focusing on the diamine conversion the signals of end groups resulting from incomplete conversion of the diamines (inserts in Fig. 4.20a-d) are of interest. Based on the integral intensities of appropriate main chain and end group signals of PUU-mPD (H6 and H6'), -BisAM (H5,6 and H7'), -MBCA (H6 and H9''), and -pXD (H7 and H7') the conversion of amino groups was calculated (see Table 4.6). The lowest conversion (84%) was found for MBCA. This diamine has a NMR purity of only 95% and probably impurities result in a lowered conversion. Moreover, the rather intensive signal at 8.49 ppm resulting from reaction of MDI with an amine group of hydrolyzed MDI points to moisture in the reaction system. Generally, a small amount of amine groups resulting from hydrolysis of isocyanate groups is indicated for all samples by two doublets at 6.48 and 6.83 ppm. Isocyanate hydrolysis as main side reaction influences the stoichiometry of the system and could also a reason for lowered amine conversion.

Finally, the number average length of the hard segments, n , is calculated from the signal intensities of urethane and urea protons based on the reasonable assumption that each PUU hard segment starts and terminates with a urethane group according the structure given in Figure 4.21. Because the prepolymer contains an excess of MDI, the content of urethane groups resulting from the reaction of MDI with two PTMEG chains should be low. They cannot be distinguished in the

NMR spectrum from urethane groups next to hard segments but would lower the calculated value of n .

The *in-situ* synthesized PUUs are solvent extracted from the blends with dimethylacetamide (DMAc) and analyzed by GPC to determine their number average (M_n) and weight average (M_w) molar mass. The molar masses of PUUs are higher than the prepolymer, which accentuate the efficacy of the opted reactive blending process. The high value of the polydispersity index indicates a broad distribution of PUU's molar mass (see Table 4.6). The possible reasons might be the presence of free MDI molecules in prepolymer leading to the formation of oligomers of broad size range and the presence of inter-hard-segmental H-bond interactive associations during the blending process, which tend to restrict mobility of the reactive end-groups.

High conversion leads to a high molar mass, as is the case with PUU-pXD and -BisAM. The inter-chain associations are delayed in PUU-pXD (see Fig. 4.19) and are weak in PUU-BisAM ensuring high conversions and molar masses. Comparatively, the low conversion of mPD is ascribed to the rapid polymerization and strong inter-chain associations during the *in-situ* polymerization process, which hinders high conversion of amino groups. The low conversion of MBCA is due to its relatively low percent purity as is described earlier in this section.

Table 4.6 Summary of GPC and ^1H NMR analysis

Sample	M_n (g/mol)	M_w (g/mol)	Dispersity Index	Conversion (%)	n
Prepolymer	2,735	3,528	1.29	-	-
PUU-mPD	18,000	122,000	6.78	88±3	3.3
PUU-MBCA	21,000	134,000	6.38	84±3	2.2
PUU-pXD	24,000	156,000	6.50	95±3	2.2
PUU-BisAM	24,000	162,000	6.75	96±3	3.1

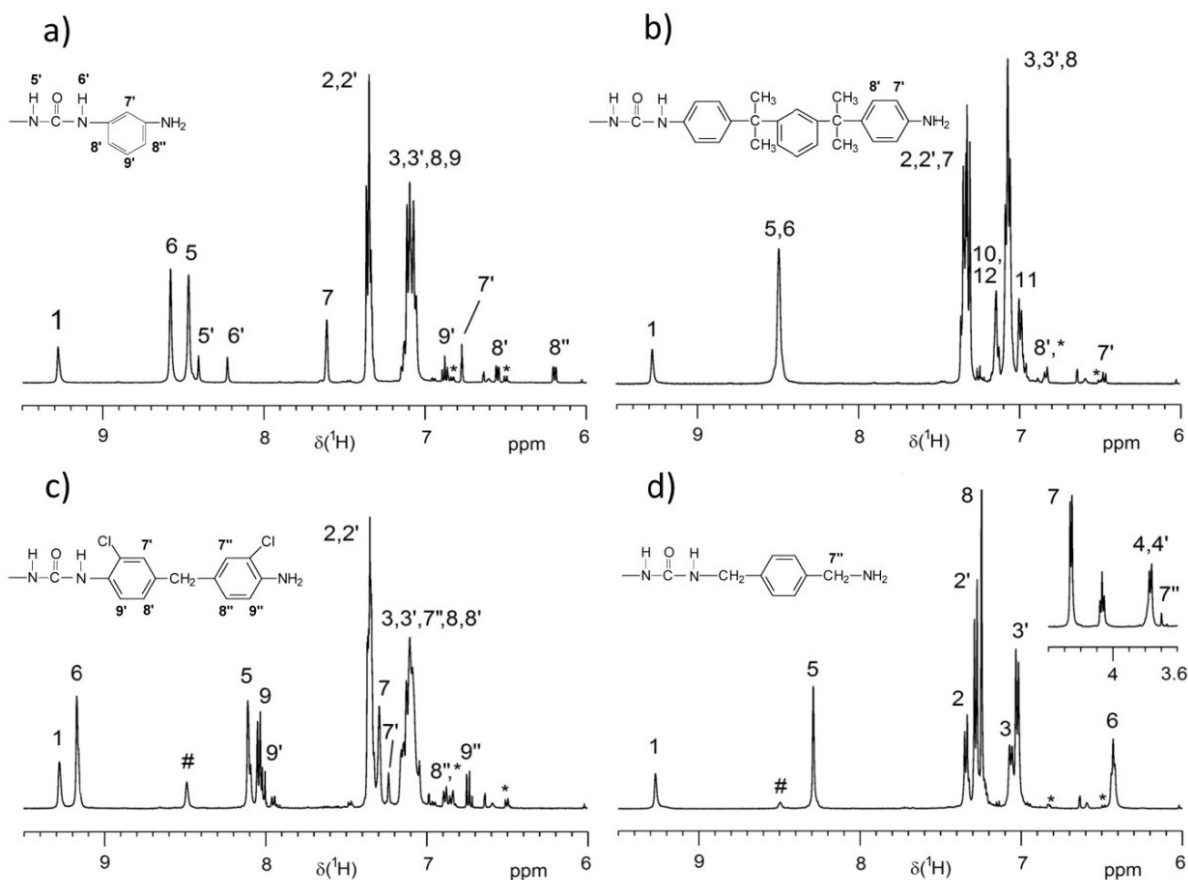
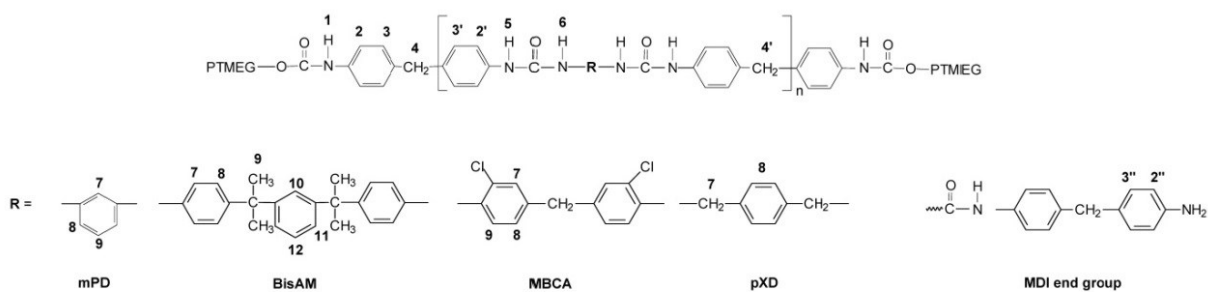


Figure 4.20 ^1H NMR spectra (regions) of the PUUs extracted from a) Blend-mPD, b) Blend-BisAM, c) Blend-MBCA, and d) Blend-pXD. The top formula depicts the general PUU structure with different structures R depending on the used diamine. The formulas of the diamine-based end groups are given next to the spectrum. Hydrolysis of MDI results in the MDI end group (* marks 2'' (~6.5 ppm) and 3'' (~6.82 ppm)) which can react with MDI to form a MDI-NH-CO-NH-MDI urea bond (# marks the NH proton, overlapped in a) and b)). Solvent: DMSO- d_6 at 60°C.

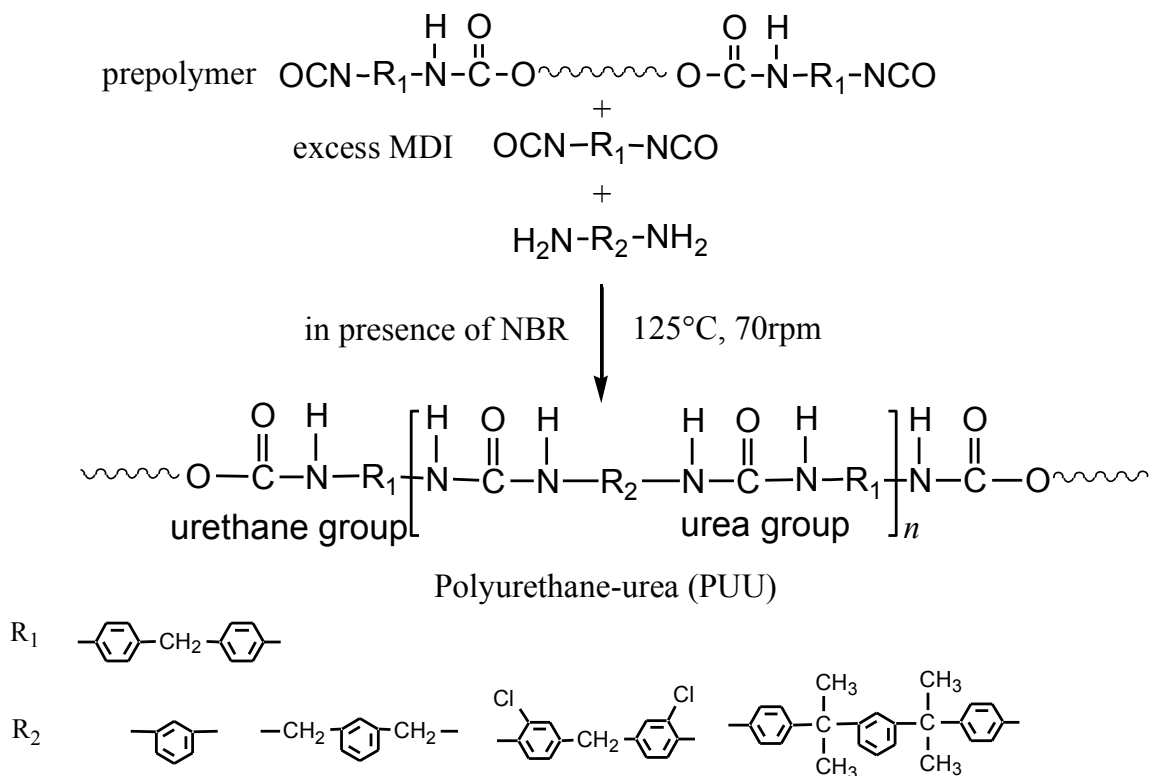


Figure 4.21 Overall reaction to the *in-situ* synthesized PUUs in presence of NBR in an internal mixer. The value of n is given in table 4.6.

4.2.4 Curing study

Fig. 4.23 shows that the blending of NBR with the *in-situ* synthesized polyurethane-ureas, namely PUU-mPD, -pXD and -MBCA brings about a noticeable improvement in the torque development (M_H - M_L) during the cure test. All the blends show a high value of minimum torque (M_L), which reflects a decrease in processing ease. This is due to the fact that the shearing deformation of the rubber matrix is hindered by the dispersed polyurethane-urea domains (embedded in the rubber matrix) during the rheological testing. This also shows strong interfacial associations between the dispersed PUU and the continuous NBR phases. The maximum torque (M_H) developed by the Blend-mPD, -pXD and -MBCA is significantly higher than that of neat NBR due to the fact that the PUU-mPD, -pXD and -MBCA retain their stiffness at the test temperature of 160°C. The dispersed domains of PUU-mPD,-pXD and -MBCA retain stiffness

owing to the strong hydrogen bonding interactions amongst hard segments of the poly-urethane-urea phase.

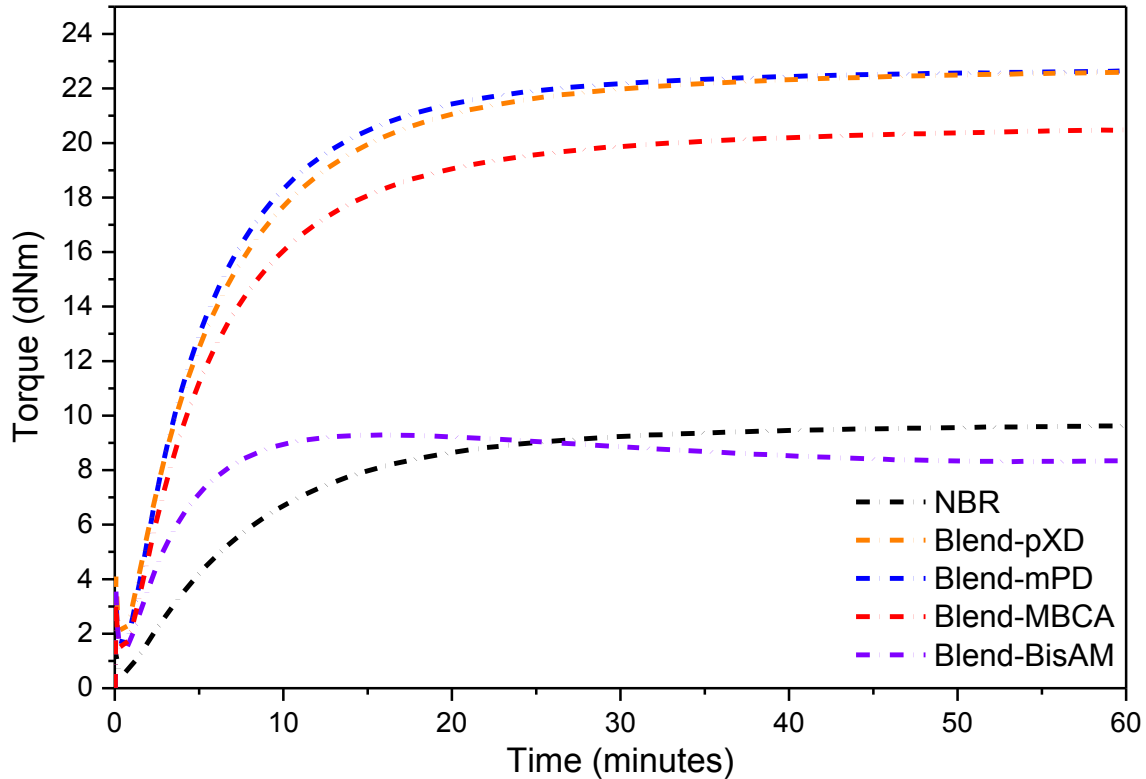


Figure 4.22 Cure curves of NBR and its blends with four different kinds of polyurethane-ureas Blend-BisAM shows a unique curing behavior. At the beginning of the vulcameter test, its torque rises due to the stiffness of PUU-BisAM phase. However, the PUU-BisAM phase softens over time to give the lowest value of M_H . This is due to the fact that the thermal effects overcome weak hydrogen bonding interactions amongst the hard segments of the polyurethane-urea phase and cause softening of the PUU-BisAM phase to reverse its contribution to torque development. The curing behavior of Blend-BisAM compound indicates that the curatives do not migrate to any of the PUU phase of four blends and crosslink only the NBR matrix.

4.2.5 Morphology of hetero-phase blend-vulcanizates

The two phase morphology of the heterogeneous blends is investigated by the scanning electron microscopy (SEM). The SEM micrographs of the cryo-cut surface of each blend are shown in Fig. 4.22. In the same figure, the corresponding histogram plot and the SEM image of the cryo-fractured surface are shown as an overlay for each blend specimen.

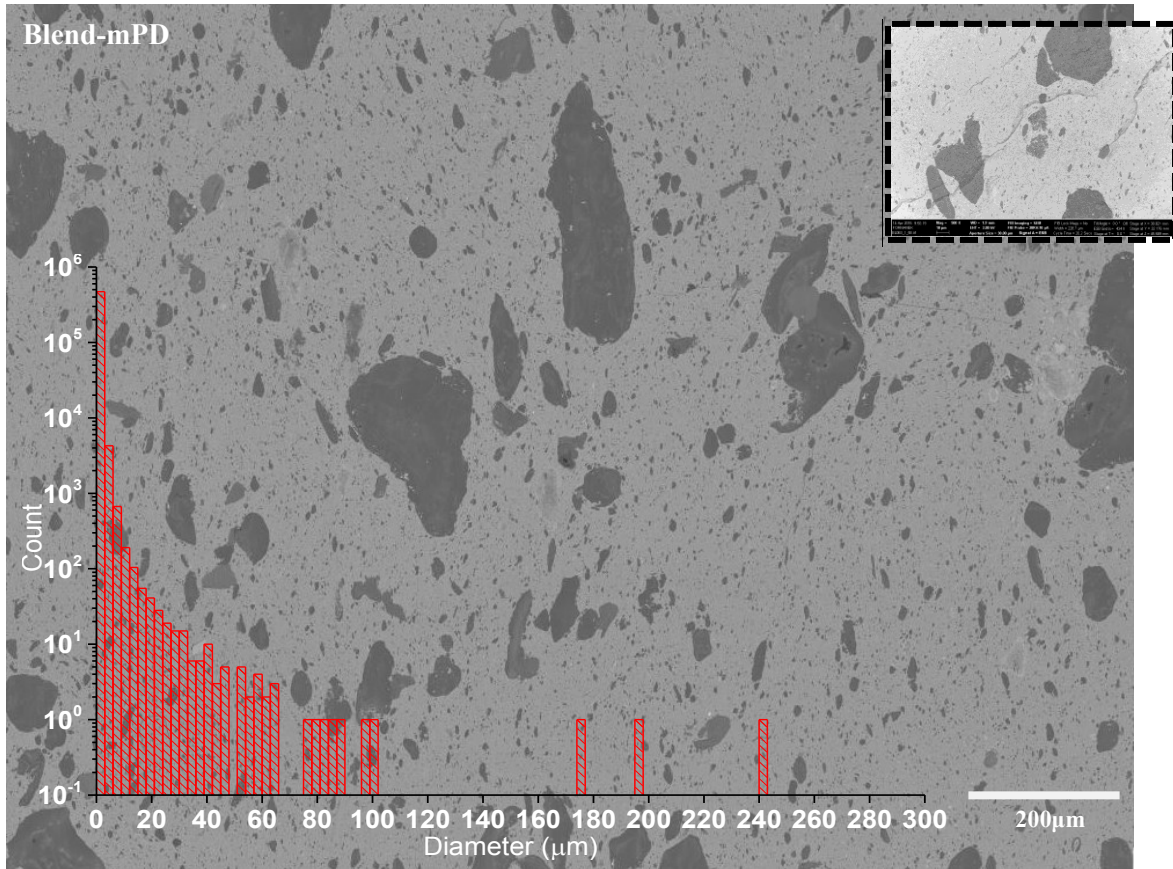
Microscopic investigations of the cryo-cut surfaces identify PUU domains (dark) as a thoroughly dispersed phase in continuous NBR matrix (bright). It is observed that the fine domains of PUU-MBCA, laminar and fibrillar domains of PUU-BisAM, irregular-shaped domains of PUU-pXD and somewhat ellipsoidal domains of PUU-mPD are dispersed in NBR matrix. The corresponding histogram plot shows that the well dispersed PUU-BisAM and PUU-MBCA domains exhibit a maximum domain size of 170 μm and 40 μm respectively. The histogram plots for the Blend-mPD and -pXD specimens show that the PUU-mPD and PUU-pXD domains are up to 240 μm in mean diameter.

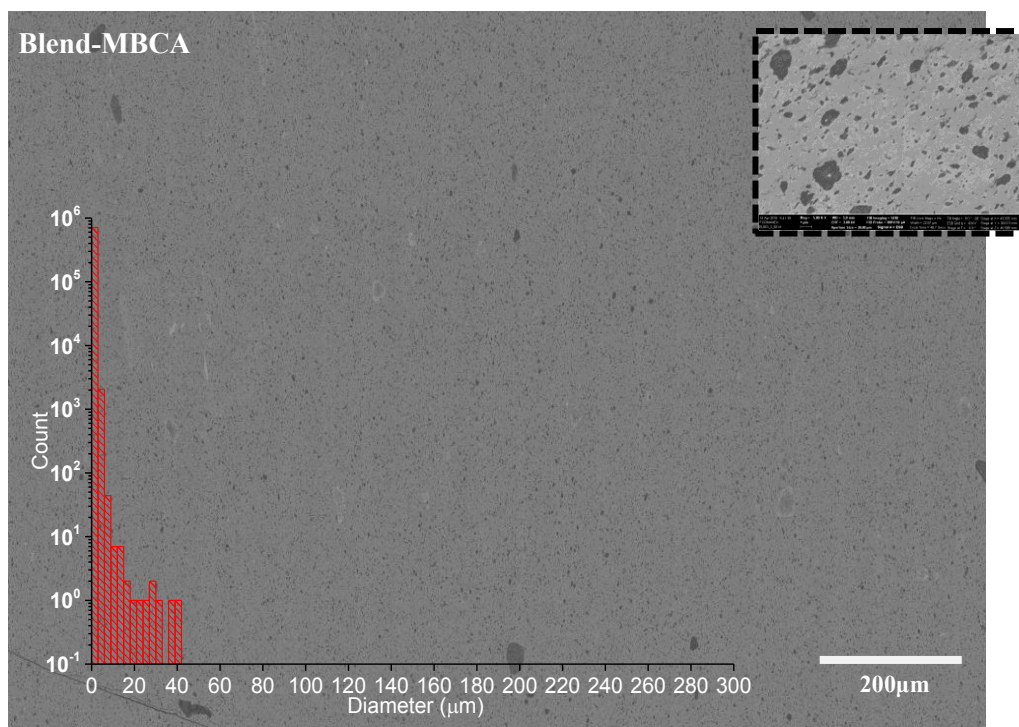
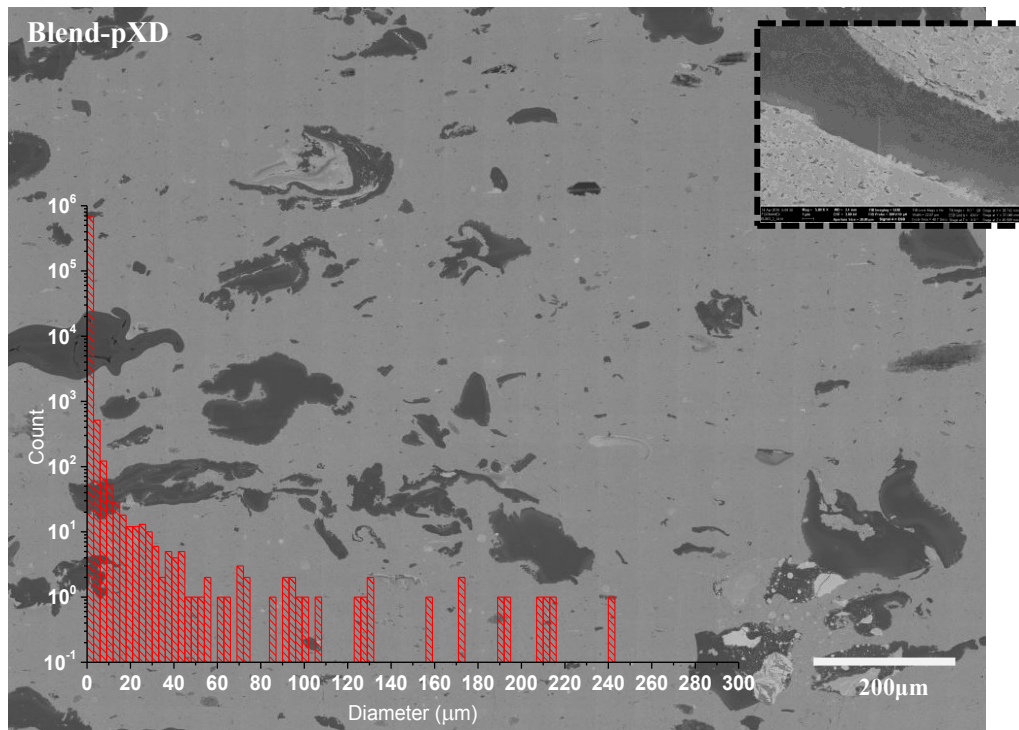
The fibrillar structure of PUU-BisAM domains shows that, owing to the weak hydrogen bonding interactions amongst chains, the PUU-BisAM domains elongate during shearing action in the internal mixer and during plug-like deformational flow of cavity filling in the compression moulding process [82, 83].

The circular-cum-elliptical PUU-mPD domains quickly attain stiffness through strong hydrogen bonding interactions among polymer chains and appear from fine to coarse sizes.

The well-dispersed PUU-MBCA domains develop a fine grain morphology, which characterizes an improved compatibility between the blend components. The two chlorine atoms on MBCA molecules seems to bring polarity of PUU-MBCA close to NBR, which results in the PUU-MBCA domains of much smaller size as compared to the PUU-BisAM and -pXD and -mPD.

The corresponding histograms show that the PUU-MBCA domains are up to 40 μm in mean diameter, whereas the PUU-pXD, -BisAM and -mPD domains span up to hundreds of micrometers in mean diameter.





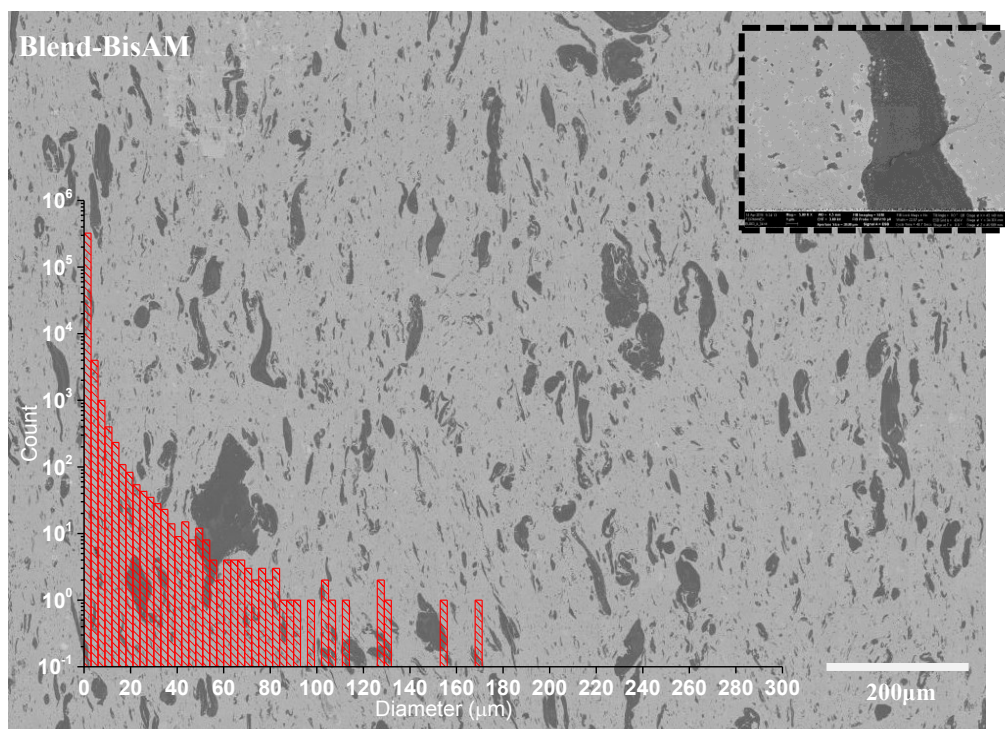


Figure 4.23 SEM images of the cryo-ultramicrotomed (smooth) and OsO_4 stained surfaces of blends (NBR is bright, PUU is dark) containing PUU-mPD, -pXD, -MBCA and -BisAM. The histogram of domain size distributions and the image of cryofractured surface are also shown as an overlay in the corresponding image. (The resolution of the images was reduced for publication. The original resolution is approx. 22 000 x 16 000 pixels ~ 350 megapixels for cryo-ultramicrotomed surfaces).

4.2.6 Stress-strain curves

Tensile testing of all the compounds is performed at RT and the results are shown in Fig. 4.24. Compared to NBR, the highly improved stress-strain response of the blend vulcanizates is an indication of compatibility and effective stress transfer between the elastic NBR and stiff PUU phases.

The specimens of Blend-mPD and -pXD appear to be relatively brittle and break at low strains. This is referred to the presence of coarse domains of PUU-mPD and -pXD in rubber matrix, which are rather inhomogeneously distributed and cause failure of the test specimens at low strain values. The ultimate tensile characteristics of the Blend-MBCA are better than those of Blend-pXD and -mPD. This is ascribed to the homogeneous distribution of fine PUU-MBCA

domains to ensure a uniform transfer of applied stress across the cross-section of the test specimen.

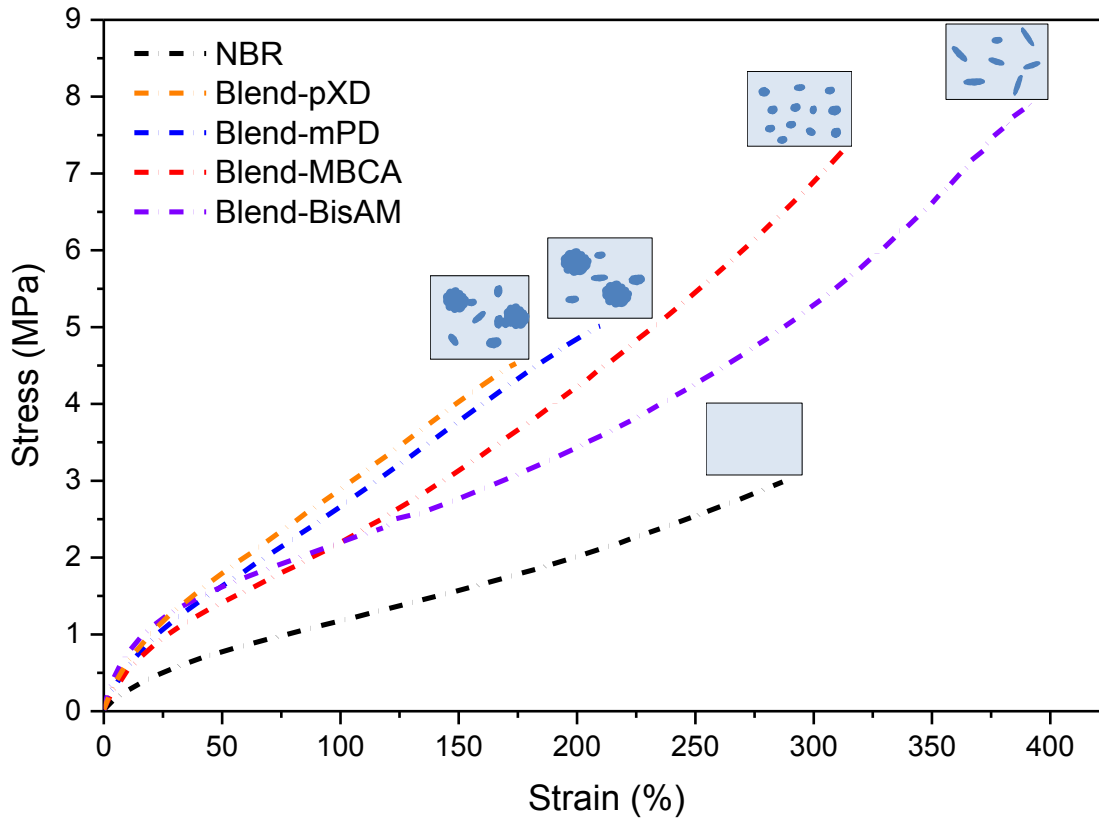


Figure 4.24 Stress-strain curves of NBR, Blend-mPD, Blend-pXD, Blend-MBCA and Blend-BisAM. The morphology of blends is graphically depicted.

Blend-BisAM exhibits the highest ultimate tensile characteristics amongst all the blends, which relates to the fact that the tensile testing is performed at RT whereat the PUU-BisAM domains retain their stiffness and the reinforcing tendency. The fiber-like PUU-BisAM domains brings in an overall improvement in the stress-strain response of the NBR in contrast to the fine PUU-MBCA domains and the inhomogeneously dispersed coarse PUU-pXD and -mPD domains.

4.2.7 Dynamic-mechanical behavior

Fig. 4.25 presents the curves of dynamic temperature sweep measurements performed at a constant frequency of 10Hz and in the temperature range from -100 to +180°C. The peak position

in a $\tan \delta$ curve is taken as the glass transition temperature of a blend component. Blend-pXD, -mPD and -MBCA exhibit two glass transitions; a relaxation peak at low temperature is the soft segments glass transition temperature ($T_{g,ss}$) and a relaxation at -18°C corresponds to the rubber glass transition temperature ($T_{g,NBR}$). Amongst all the compounds, the Blend-BisAM does not exhibit a low temperature relaxation peak, which indicates a high soft and hard segments mixing within the polyurethane-urea phase. This manifestation is ascribed to a negligible structural relaxation of the soft segments, which are entangled by the rigid hard segments of PUU-BisAM chains. The position of $T_{g,ss}$ can be related to the extent of segmental mixing in PUU phase. The higher is the $T_{g,ss}$, the higher is the soft/hard segmental mixing in PUU phase of blends. Accordingly, the phase mixing is the highest in PUU-BisAM, followed by PUU-MBCA, PUU-mPD and PUU-pXD.

Based on $T_{g,ss}$, the *in-situ* PUUs can also be placed in a decreasing order of soft/hard segmental separations and chain flexibility (inset in Fig 4.25(a)).

The *in-situ* synthesized PUU is reinforcing the NBR, as is evident from a lower $\tan \delta$ peak height at $T_{g,NBR}$ for the blends. The storage modulus curves of the Blend-pXD, -mPD and -MBCA (except Blend-BisAM) are stable and much elevated than that of NBR beyond the $T_{g,NBR}$. All the blends behave viscoelastically; however, the Blend-BisAM exhibits some plasticity too and deform permanently (inset in Fig 4.25(b)). This is due to the reason that the PUU-BisAM phase gets soften and deform plastically at temperatures beyond the $T_{g,NBR}$. The softening of PUU-BisAM domains induces plastic deformation and the Blend-BisAM specimen ends up bending permanently. The specimens of NBR/PUU-mPD, -pXD and -MBCA, after the test, do not deform, whereas PUU-BisAM undergoes a non-recoverable bending/deformation.

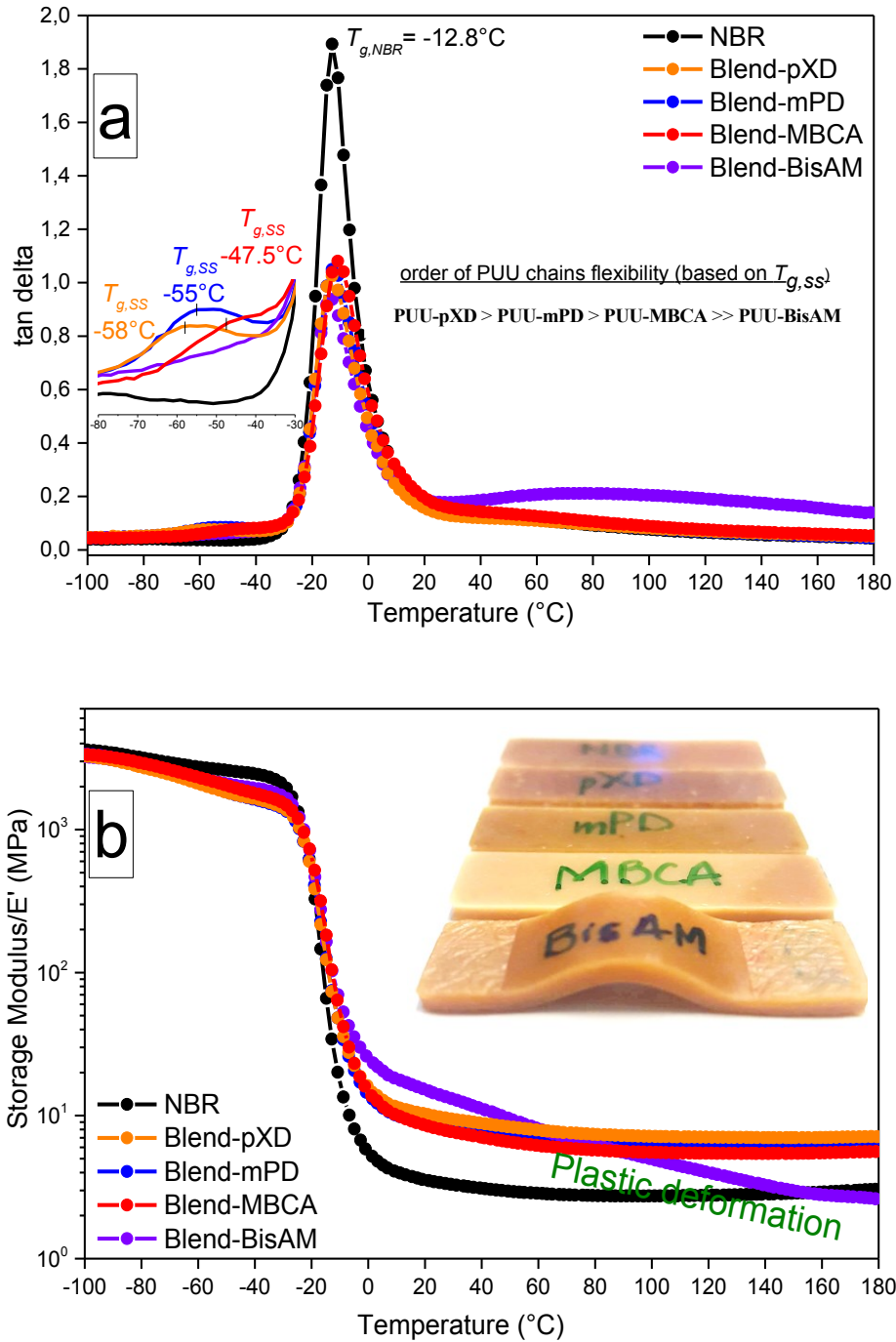


Figure 4.25 **a)** $\tan \delta$ versus temperature curves along with the glass transition region of soft segments (SS) and the order of structurally different PUUs with respect to chain flexibility, **b)** Storage modulus (E') vs temperature curves along with the photo of specimens after temperature sweep test

4.2.8 Wide angle X-ray scattering

X-ray scattering scans of compounds as a function of Bragg angle (2θ) are shown in Fig. 4.26.

The amorphous NBR produces a scattering hump at a diffraction angle (2θ) of 18.7° . The

scattering patterns of the blends, showing a broad maximum at around 19.3° , suggest an existence of disordered segregation of hard segments in PUU phase. For all the blends, the amorphous halo is broader, owing to the collective scattering from an amorphous NBR and the disorderly structured hard segments of PUU phases. Only a few weak reflections of the moderately ordered hard segments can be identified at $2\theta = 16.4^\circ$ and 20.6° for PUU-MBCA, 21.2° for PUU-mPD and 21.0° for PUU-pXD in their corresponding X-ray scans. On the whole, the scattering patterns seem similar and show disordered arrangements of the hard segment in domains. The absence of ordered arrangements within the *in-situ* synthesized PUUs is attributed to multiple factors including the acquisition of inter-chain associations and stiffness by the PUU domains under the vigorous thermo-mechanical conditions of reactive blending, the limited chain mobility due to the lengthy hard segments and the possible associations of urethane/urea moieties of hard segments with the ether groups of soft segments via hydrogen bonding as described in section 4.1.8.

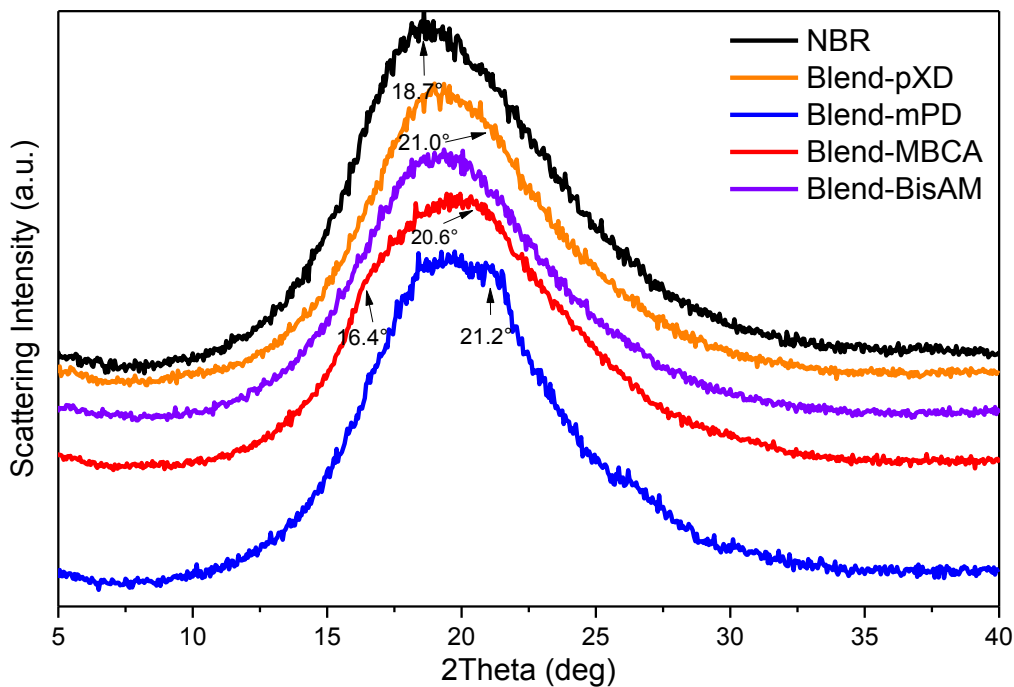


Figure 4.26 Wide-angle X-ray scattering scans of Blend-mPD, -pXD, -MBCA and -BisAM in comparison with NBR

4.3 Blends of polar/non-polar rubbers and *in-situ* PUU

In this study, the *in-situ* synthesized polyurethane-urea is reactively blended with natural rubber (NR) and the synthetic rubbers, XNBR, sSBR, CR, EPDM. The rubber matrix of the prepared blends is crosslinked by either the sulfur, metallic oxides or peroxide based curatives. The improvements in properties of the blends rely on a strong interfacial adhesion between the blend components so that the blends acquire, otherwise unattainable, property profile [84]. Therefore, the interfacial adhesion and the performance characteristics of the Rubber/PUU blends are characterized.

The formulations of the rubber specific recipes are given in Table 4.7.

Table 4.7 Recipe ingredients of compounds in parts per hundred parts (in weight) of rubber (phr)

Ingredients	Rubbers					Rubber/PUU blends				
	NR	sSBR	XNBR	CR	EPDM	NR/PUU	sSBR/PUU	XNBR/PUU	CR/PUU	EPDM/PUU
Rubber	100	100	100	100	100	70	70	70	70	70
Premix of prepolymer and mPD	-	-	-	-	-	30	30	30	30	30
ZnO	3	3	3	5	-	2.1	2.1	2.1	3.5	-
Stearic Acid	2	2	2	-	-	1.4	1.4	1.4	-	-
DPG	2	2	2	-	-	1.4	1.4	1.4	-	-
CBS	1.5	1.5	1.5	-	-	1.1	1.1	1.1	-	-
Sulfur	1.5	1.5	1.5	-	-	1.1	1.1	1.1	-	-
MgO	-	-	-	4	-	-	-	-	2.8	-
Peroxide	-	-	-	-	3	-	-	-	-	2.1
Coagent	-	-	-	-	2	-	-	-	-	1.4

The proposed reactive blending process, shown in Fig. 4.1, is opted to prepare five different kinds of blends. The blending was performed in an internal mixer at the reactive blending temperature of 100 °C and a fixed rotor speed of 80 rpm. Neat rubbers and the prepared Rubber/PUU blends were compounded with curatives on a two roll mill at 50 °C and at a friction ratio of 1.5. The EPDM rubber was crosslinked with peroxide, the CR with oxides (ZnO and MgO) and the NR, XNBR and sSBR with sulfur based curatives.

4.3.1 Curing behavior

The curing curves of the Rubber/PUU blends are compared with their respective neat rubbers in Fig. 4.27. The *in-situ* synthesized polyurethane-urea phase does not disturb, but does reinforce, the curing response of all the polar and nonpolar rubbers. Table 4.8 shows that the minimum (M_L) and maximum (M_H) torques are always higher for blends than the neat rubbers except for the NR/PUU blend; for which the value of M_L is comparable to neat NR. The natural rubber is sensitive to time and temperature of reactive blending as compared to the synthetic rubbers [85]. NR is compounded with curatives on a two roll mill at 50 °C. However, the NR/PUU blend is prepared in an internal mixer at 100 °C before being compounding with curatives on a two roll mill. The *in-situ* synthesized polyurethane-urea phase imparts strength to NR matrix; however, the polyisoprene chains scission due to the high shear forces from the internal mixer seems to balance the reinforcing effect of *in-situ* synthesized PUU [86].

The value of the developed torque ($M_H - M_L$) is higher for each blend than that for the corresponding neat rubber. All the compounds develop a plateau cure; except for the NR system (see Fig. 4.27 (b)). For the NR system, the cure curve reaches to a maximum value and, thereon, exhibits reversion. This is typical for the sulfur-cured natural rubber due to the non-oxidative aging on shearing at high temperature which gives lesser crosslinks on over-curing [87-88].

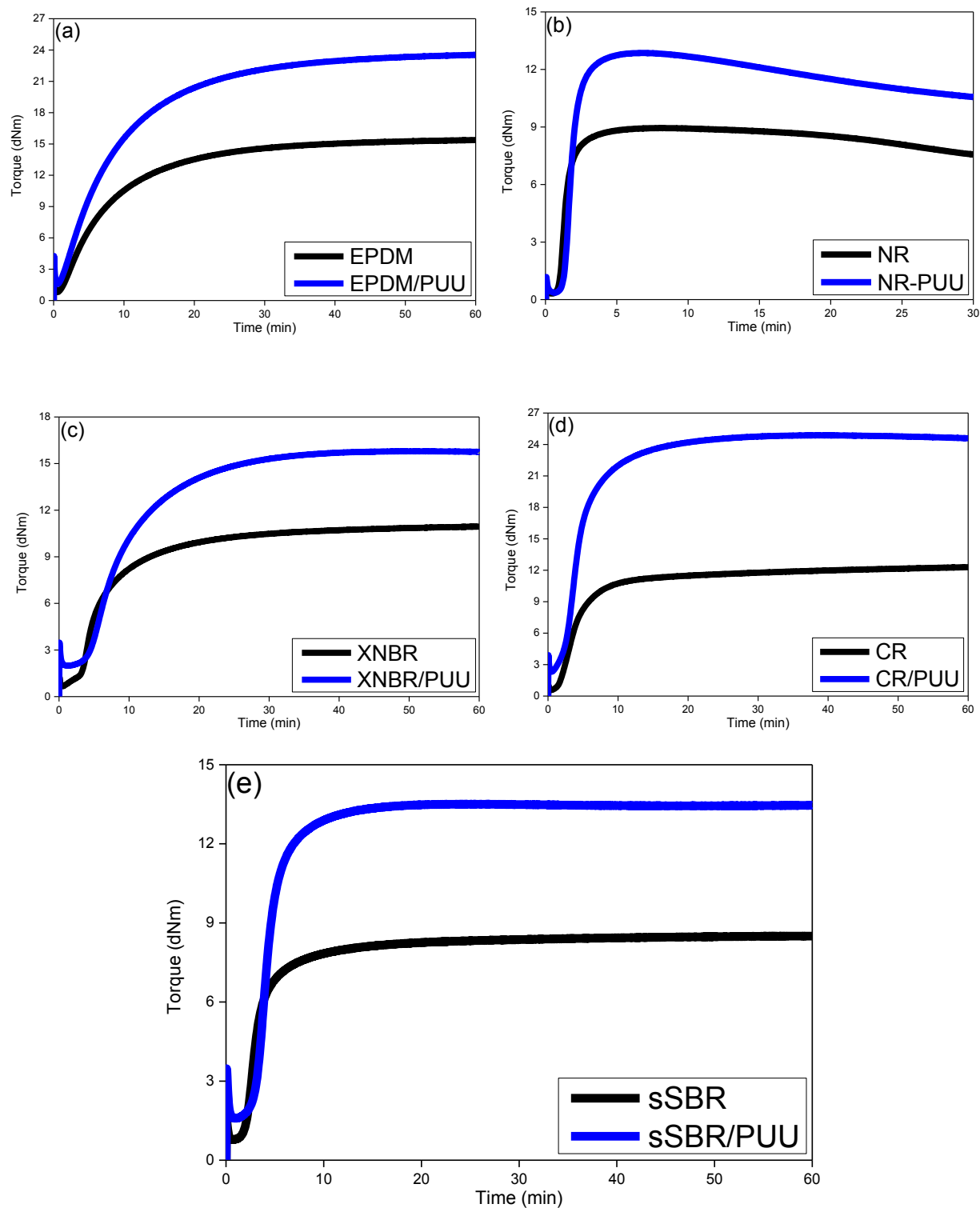


Figure 4.27 Cure curves of neat rubbers and their blends with *in-situ* synthesized PUU. **a)** EPDM and EPDM/PUU, **b)** NR and NR/PUU, **c)** XNBR and XNBR/PUU, **d)** CR and CR/PUU, **e)** sSBR and sSBR/PUU.

Table 4.8 Cure characteristics of compounds as obtained from their respective cure curves

Sample	Minimum Torque/ M_L (dNm)	Maximum Torque/ M_H (dNm)	Torque Developed (M_H-M_L) (dNm)
NR	0.32	8.95	8.63
NR/PUU blend	0.36	12.86	12.5
XNBR	0.67	10.94	10.27
XNBR/PUU blend	1.98	15.79	13.81
sSBR	0.78	8.50	7.72
sSBR/PUU blend	1.59	13.51	11.92
CR	0.58	12.29	11.71
CR/PUU blend	2.32	24.87	22.55
EPDM	0.81	15.38	14.57
EPDM/PUU blend	1.59	23.55	21.96

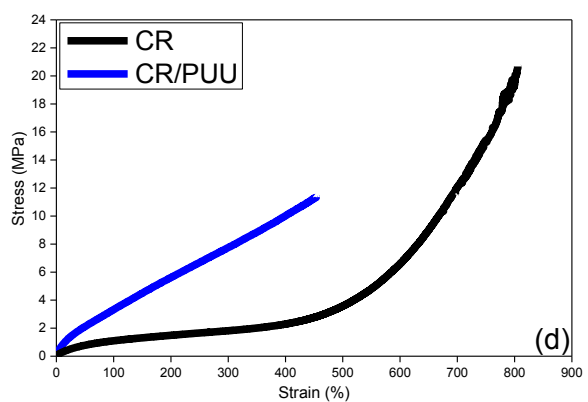
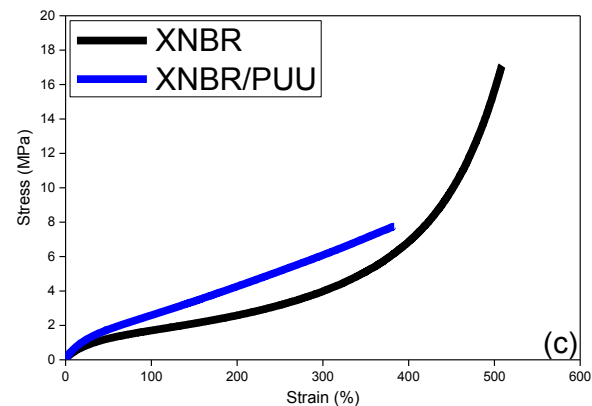
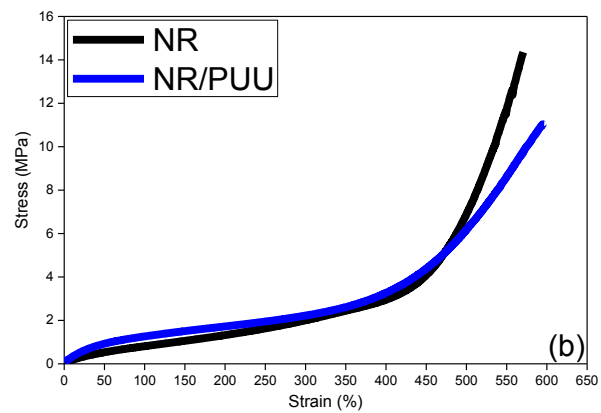
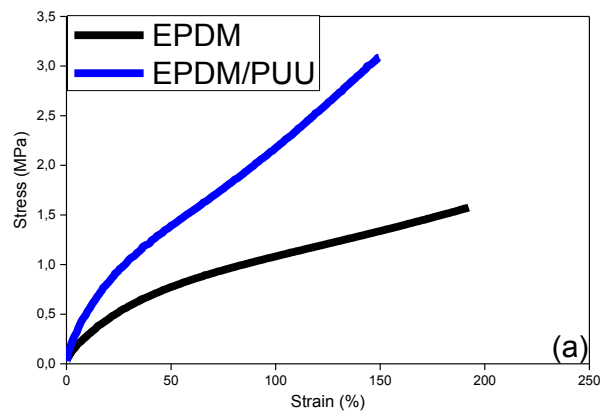
4.3.2 Tensile testing

The *in-situ* synthesized PUU reinforces the stress-strain response of all the five rubbers in low-strain region, as is shown in Fig. 4.28. At low strain levels, the blends require more stress than the corresponding neat rubbers for a same value of percent strain (see Table 4.9). This shows an effective stress transfer across the interface between the discrete PUU and continuous NBR phases. This further implies that the heterophase blend components are compatibilized (good interfacial adhesion) irrespective of the type and polarity of rubber matrix.

Fig. 4.28(b), (c) and (d) show that the neat CR, NR and XNBR test specimens exhibit an upturn of applied stress at large percent strain and possess higher tensile strength as compared to their corresponding blends. In NR, the stress-upturn occurs at about 450% strain due to the strain-induced crystallization [89-91]. This strain facilitated crystallization is hindered by PUU domains as can be seen from a sluggish upturn of tensile profile. Another probable reason is a less rubber fraction, and therefore, less strain-induced crystallizable phase in NR/PUU blend.

In XNBR, the ultimate tensile properties rely on the formation of ionic clusters, wherein the backbone carboxyl groups are ionically linked by zinc oxide molecules [92-97]. In the blends, the *in-situ* synthesized PUU seems to hinder the formation of ionic clusters or the concentration of carboxyl groups decreases due to a possible reaction with isocyanate groups during the process of *in-situ* synthesis of PUU [98].

Similar to NR, the CR also develops strain induced crystallization upon deformation, wherein the crystallites acts as reinforcing entities to give high ultimate tensile properties compared to the CR/PUU blend [99-102].



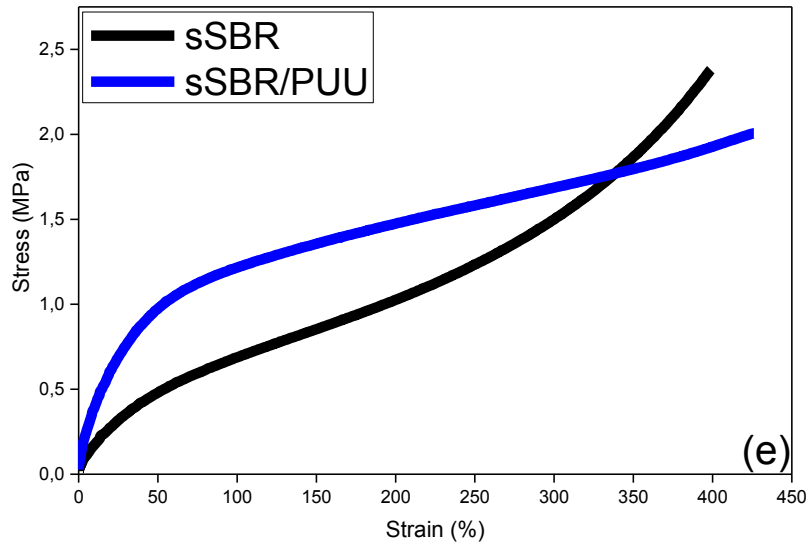


Figure 4.28 Stress-strain curves of compounds. **a)** EPDM and EPDM/PUU, **b)** NR and NR/PUU, **c)** XNBR and XNBR/PUU, **d)** CR and CR/PUU, **e)** sSBR and sSBR/PUU.

Fig. 4.28(a) and (e) show that the sSBR and EPDM are weak compared to XNBR, NR and CR. The neat sSBR shows a slight stress-upturn at high strain due to the strain hardening, giving a higher tensile strength than the corresponding blend [103]. In the sSBR/PUU blend, the entangled interfacial regions around PUU domains may be suffering a failure prior to the rubber matrix.

The stress-strain response of the neat EPDM is highly reinforced by the *in-situ* synthesized PUU and is shifted upwards by a large amount. The large improvement in tensile behavior may be attributed, in addition to interfacial compatibilization, to the interfacial peroxide co-vulcanization of EPDM and PUU phases (also discussed in section 4.1.6).

We may conclude from the stress-strain curves that the failure occurs across the cross-section of the test specimens of EPDM/PUU, XNBR/PUU and CR/PUU. On the contrary, the interfacial failure occurs prior to the failure of rubber matrix in NR/PUU and sSBR/PUU specimens.

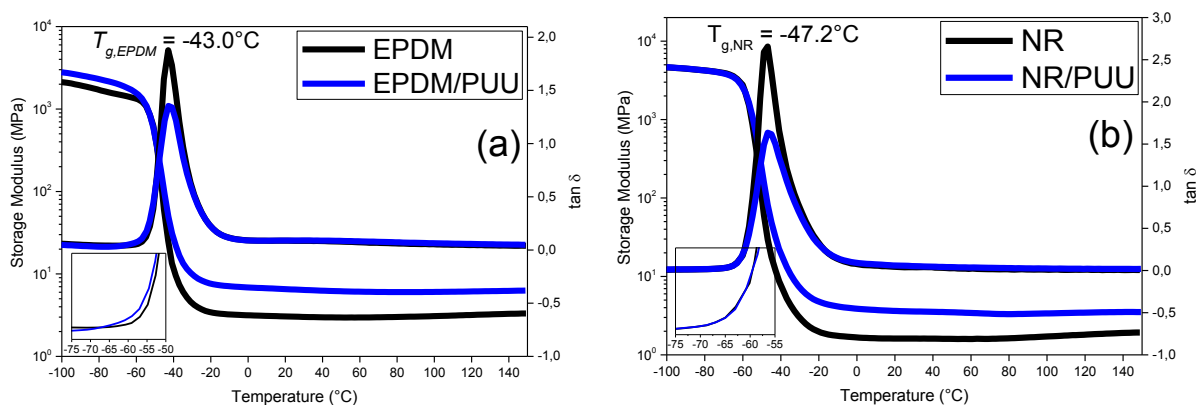
Table 4.9 Tensile characteristics of neat rubbers and their blends with *in-situ* PUU, The modulus values represent stresses at X% deformation.

	NR	NR/ PUU blend	sSBR	sSBR/ PUU blend	XNBR	XNBR/ PUU Blend	CR	CR/ PUU blend	EPD M	EPDM/ PUU blend
Young's Modulus (MPa)	1.33 ± 0.17	3.30 ± 0.15	1.63 ± 0.01	3.89 ± 0.44	4.79 ± 0.12	6.81 ± 0.53	2.72 ± 0.10	8.75 ± 0.25	2.43 ± 0.17	5.12 ± 0.10
10% Modulus (MPa)	0.18 ± 0.00	0.32 ± 0.01	0.17 ± 0.00	0.38 ± 0.01	0.47 ± 0.01	0.68 ± 0.04	0.28 ± 0.02	0.79 ± 0.03	0.28 ± 0.01	0.52 ± 0.00
50% Modulus (MPa)	0.54 ± 0.01	0.92 ± 0.02	0.48 ± 0.00	0.96 ± 0.01	1.24 ± 0.00	1.79 ± 0.04	0.78 ± 0.01	2.11 ± 0.00	0.77 ± 0.01	1.39 ± 0.10
100% Modulus (MPa)	0.83 ± 0.01	1.26 ± 0.01	0.69 ± 0.01	1.2 ± 0.01	1.71 ± 0.01	2.63 ± 0.05	1.10 ± 0.02	3.31 ± 0.03	1.08 ± 0.01	2.16 ± 0.02
200% Modulus (MPa)	1.35 ± 0.02	1.71 ± 0.01	1.03 ± 0.01	1.47 ± 0.00	2.61 ± 0.04	4.34 ± 0.10	1.49 ± 0.03	5.59 ± 0.03	1.60 ± 0.00	-
Tensile Strength (MPa)	14.43 ± 1.20	11.04 ± 0.09	2.48 ± 0.28	2.00 ± 0.03	20.64 ± 5.01	7.08 ± 0.08	20.68 ± 2.10	11.72 ± 0.54	1.65 ± 0.10	3.16 ± 0.10
Elongation at Break (%)	570 ± 8	595 ± 4	403 ± 16	425 ± 10	525 ± 24	373 ± 14	805.12 ± 18	470 ± 23	205 ± 18	154 ± 7

4.3.3 Dynamic mechanical analysis

The plots of storage modulus (E') and loss factor ($\tan \delta$) as a function of temperature for all the compounds are shown in Fig. 4.29. It appears that the dynamic mechanical measurements of CR/PUU, sSBR/PUU and XNBR/PUU reflect two glass transition relaxation peaks in their respective $\tan \delta$ plots (see Fig. 4.29(c)-(d)). The low temperature relaxation peak at approximately -50 °C corresponds to the soft segment glass transition temperature ($T_{g,ss}$). The high temperature relaxations at -26.5 °C, -3.4 °C and -0.9 °C correspond to the glass transition temperatures of CR, sSBR and XNBR respectively. XNBR is quite unique in its dynamic response because it exhibits a third relaxation peak at around 80 °C corresponding to the thermal dissociation of multiplets formed by the association of the carboxylic groups with divalent ZnO

[93, 95, 104]. These multiplets are ionic aggregates acting as crosslinks and have a considerable impact on the rubbery plateau region of XNBR. With the incorporation of *in-situ* synthesized PUU, the glass transition of XNBR is shifted downwards to -3.5°C . This shows a decrease in the concentration of ionic crosslinks/aggregates (act as crosslinks) owing to a probable reaction between the isocyanate groups of the prepolymer and the carboxylic groups of XNBR. It may also be referred to secondary interactions (hydrogen bonding) between the carboxylic groups of XNBR and the urethane-urea moieties of the vicinal PUU domains, which reduce the amount of carboxylic group available for the ionic aggregates. Fig. 4.29(a) and (b) demonstrate that the EPDM/PUU and NR/PUU blends exhibit a single glass transition temperature corresponding to the rubber phase, this is because of the overlapping relaxation regions of the rubber matrix and the soft segments of PUU phase. Blends exhibit an extremely high and stable rubbery plateau modulus as compared to the corresponding neat rubber, which indicates high strength of these thermostable blends. In addition, the overlapping $\tan \delta$ plots in the rubbery plateau region indicate a nearly equal energy dissipation character of EPDM, NR, CR and sSBR and their blends with *in-situ* synthesized PUU. Interestingly, the blending of *in-situ* synthesized PUU with XNBR lowers the dissipation level of the applied energy and causes less heat buildup in XNBR/PUU blend.



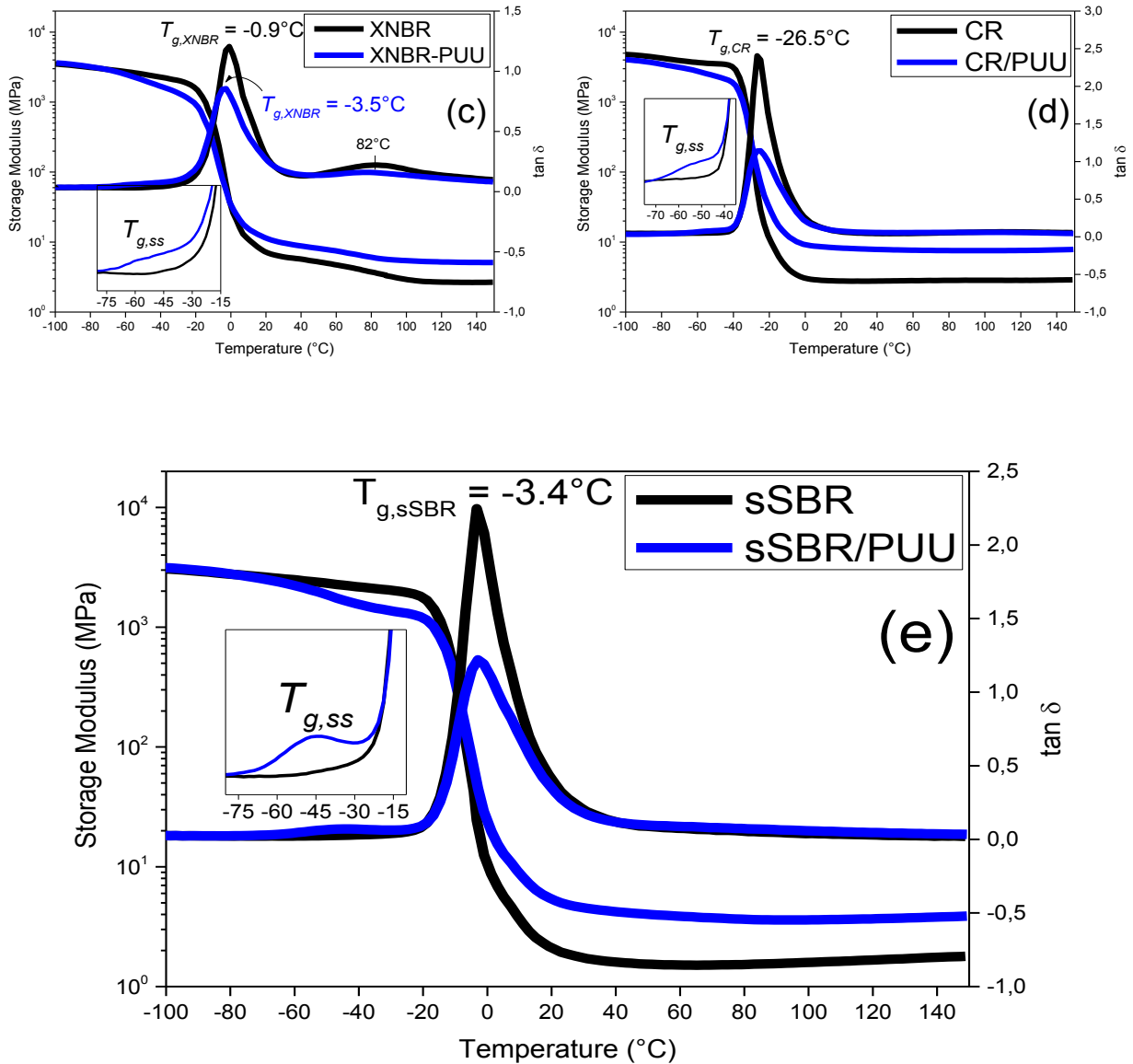


Figure 4.29 Temperature dependence of $\tan \delta$ and storage modulus. **a).** EPDM and EPDM/PUU, **b).** NR and NR/PUU, **c).** XNBR and XNBR/PUU, **d).** CR and CR/PUU, **e).** sSBR and sSBR/PUU.

The loss in $\tan \delta$ peak height and gain in storage modulus depict reinforcement imparted to each rubber by the *in-situ* PUU phase (see table 4.10). This also supports the fact that the PUU domains develop good interfacial adhesion with all the polar and nonpolar rubbers.

Table 4.10 Dynamic-mechanical characteristics of compounds as obtained from their respective temperature sweep test.

Sample	T_g of rubber (°C)	$\tan \delta$ peak height at T_g of rubber	E' at 25°C (MPa)
NR	-47	2.7	1.7
NR/PUU blend	-46	1.6	3.6
XNBR	-1	1.2	6.5
XNBR/PUU blend	-4	0.9	10.2
sSBR	-3	2.3	1.9
sSBR/PUU blend	-3	1.2	4.8
CR	-27	2.4	2.8
CR/PUU blend	-27	1.1	8.0
EPDM	-43	1.9	3.1
EPDM/PUU blend	-43	1.4	6.4

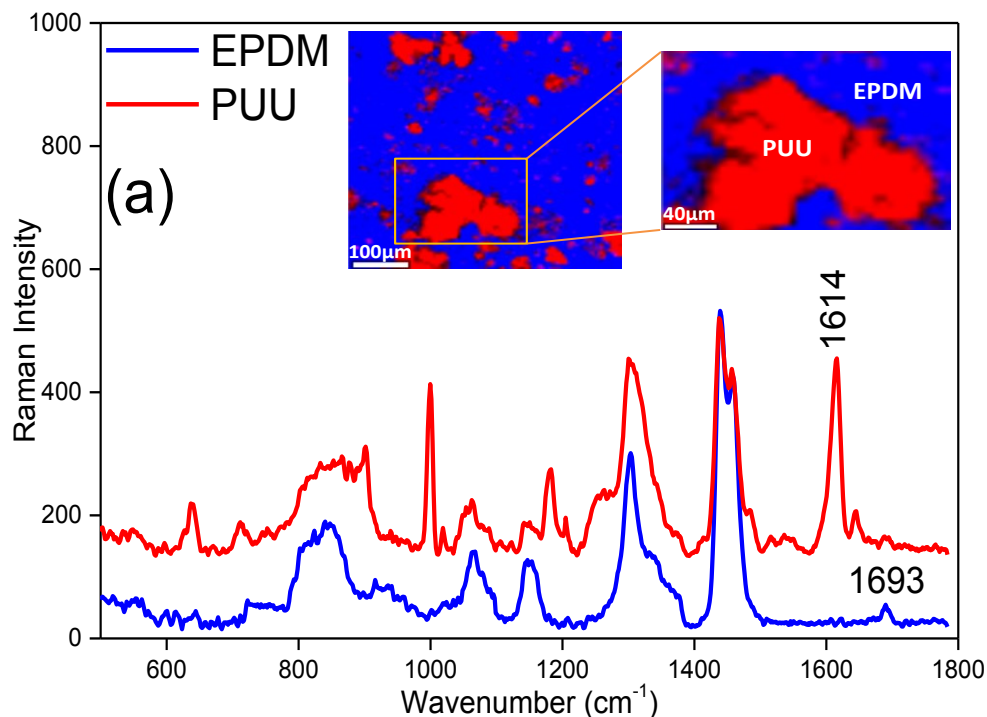
4.3.4 Structural characterization by Raman spectroscopy

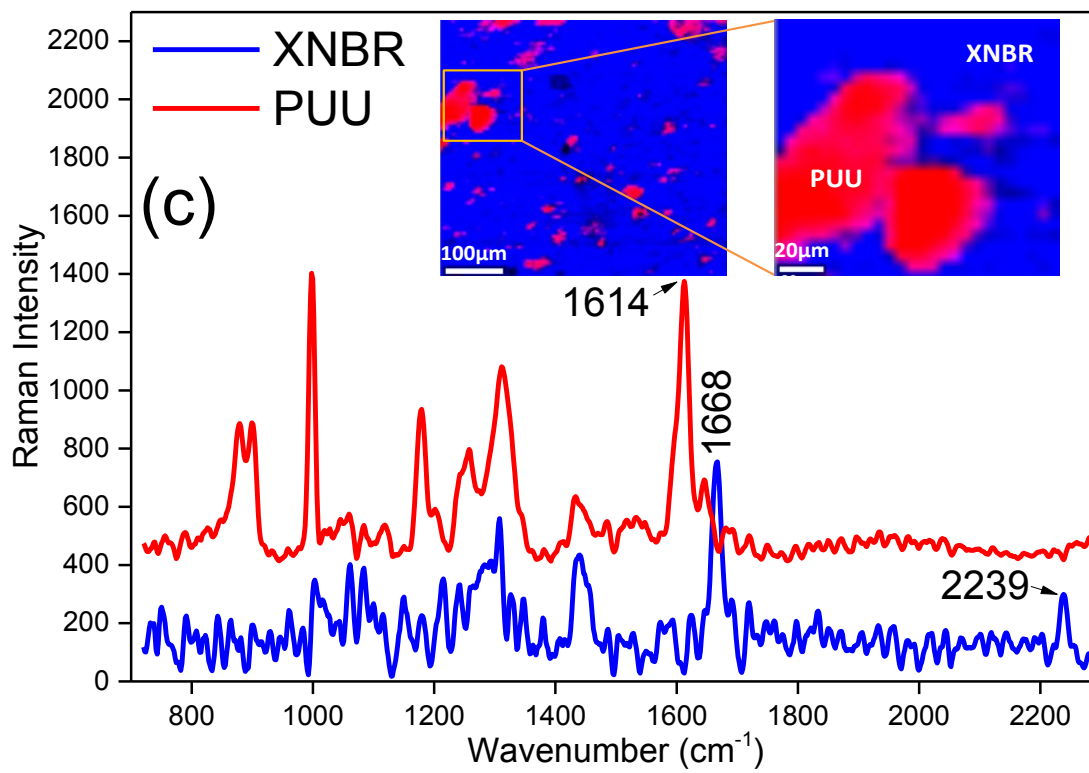
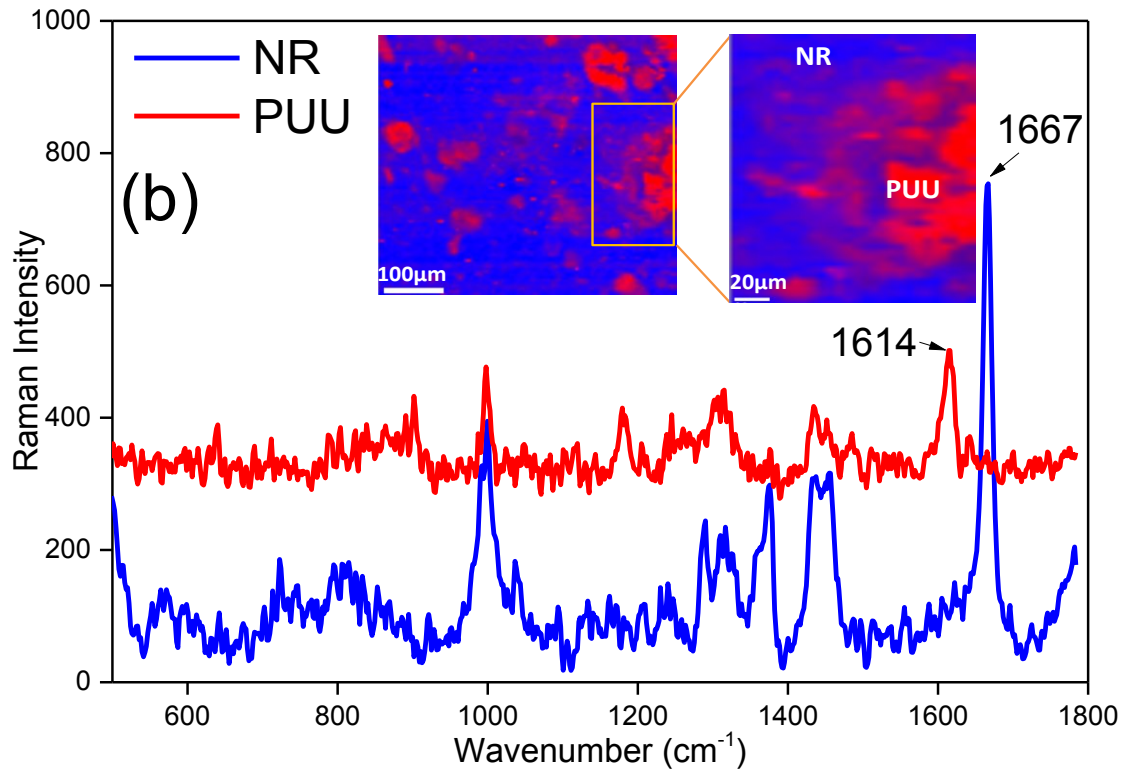
The chemistry of the *in-situ* synthesized PUU is the same as is presented in section 4.1.3. Therefore, the Raman spectroscopy is opted for the structural identification, along with the complementary surface distribution, of the blend phases. The Raman spectra and the corresponding chemical Raman images of each blend are given in Fig. 4.30(a)-(e). The *in-situ* synthesized PUU and rubber phases are shown in red and blue color, respectively, in Raman images.

Raman images show that the irregular microdomains of PUU are dispersed in continuous rubber matrix. The dispersed PUU domains are identified from a strong spectral band at 1614 cm^{-1} corresponding to the aromatic $C=C$ stretching vibration. Fig. 4.30 (a) identifies EPDM matrix by

a distinct $C=C$ stretch at 1693 cm^{-1} corresponding to the side Ethylidene norbornene (ENB) group. The intensity of this peak is low due to only 5 wt% of ENB contents in EPDM. The rubber spectra from Fig. 4.30 (b) to Fig. 4.30 (d) show a distinct stretching vibration of the aliphatic $C=C$ group at 1667 cm^{-1} , 1661 cm^{-1} , 1641 cm^{-1} and 1668 cm^{-1} to support the structural identification of NR, CR, sSBR and XNBR matrices respectively in Raman images. In addition, the stretching vibration corresponding to the acrylonitrile group ($C\equiv N$) at 2239 cm^{-1} is characteristic to the XNBR matrix (see Fig. 4.30 (c)).

Auxiliary, the absence of asymmetric stretching vibration of isocyanate group ($N=C=O$) at around 2250 cm^{-1} in the PUU spectrum of Fig. 4.30 (c) supports a successful *in-situ* polymerization of polyurethane-urea and is exemplary for all rubber/PUU blends.





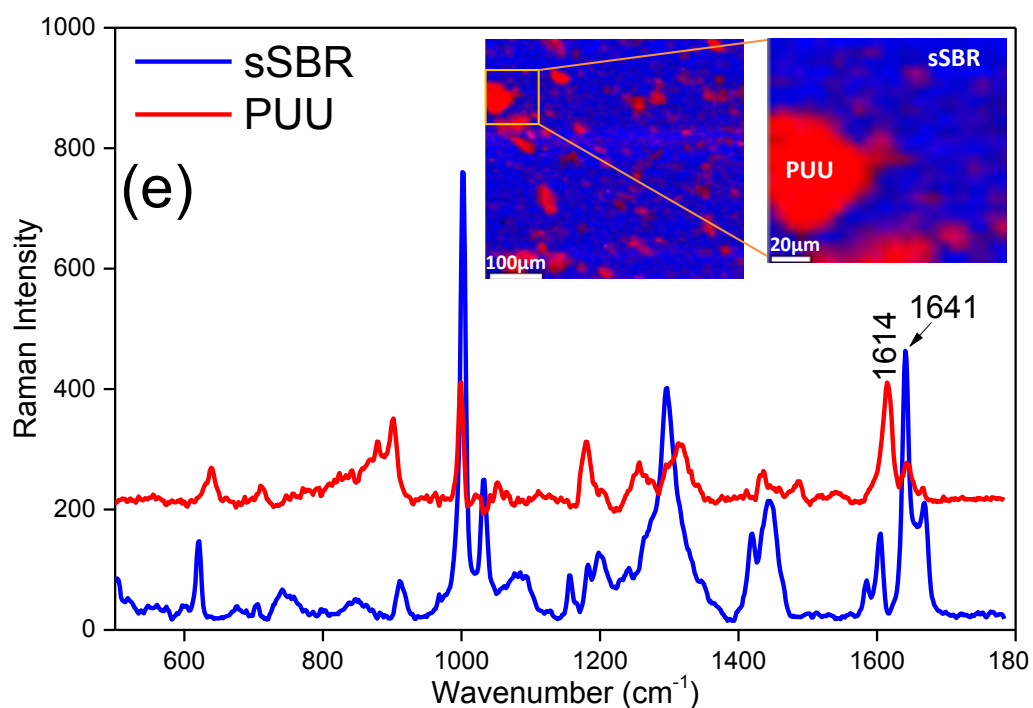
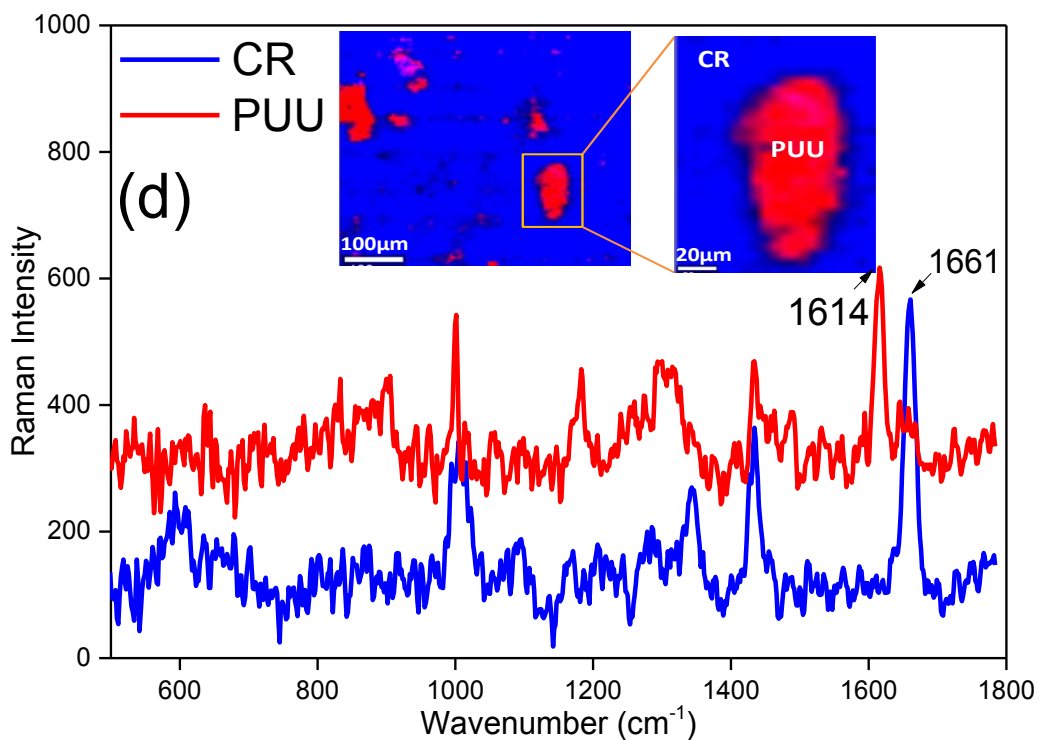
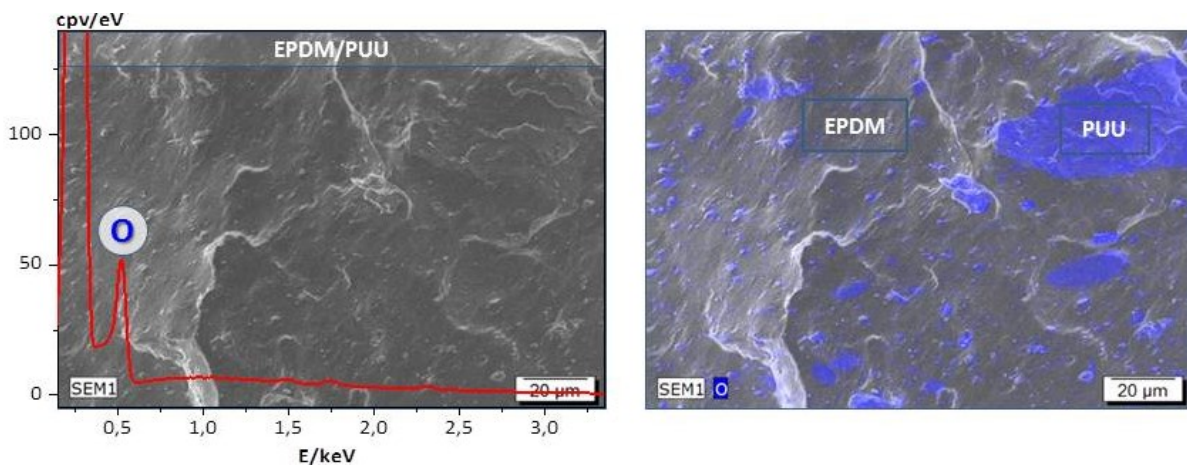
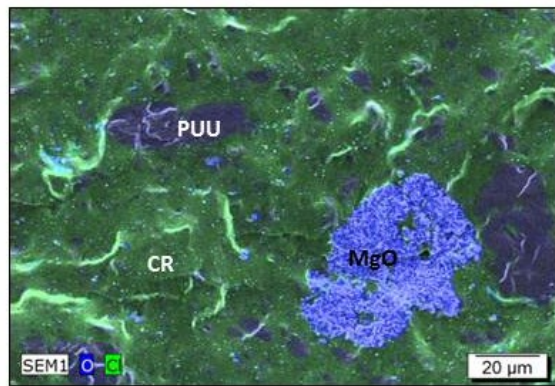
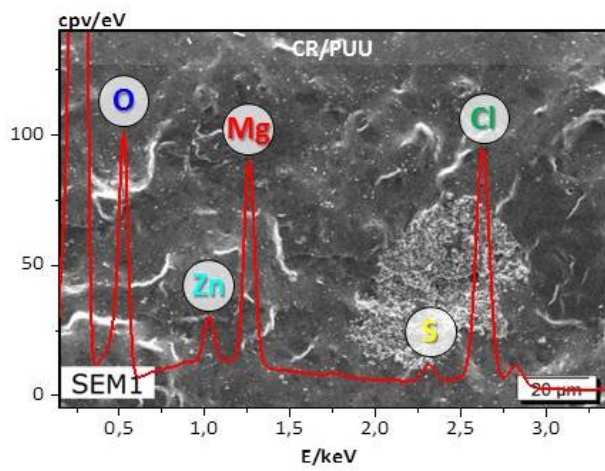
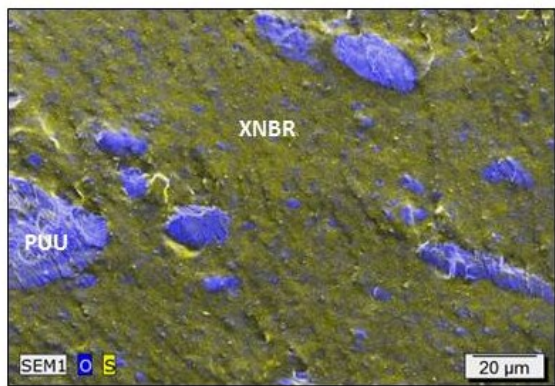
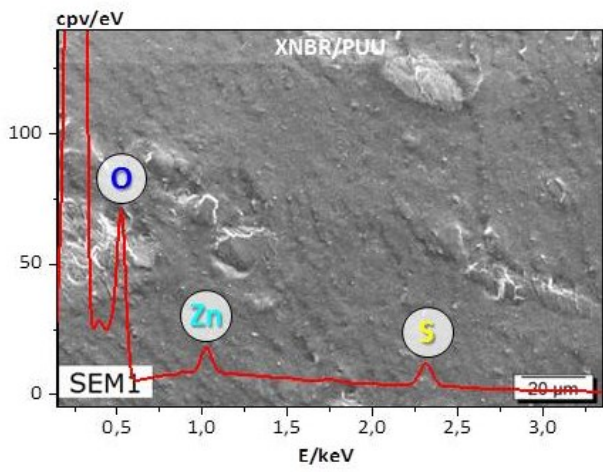
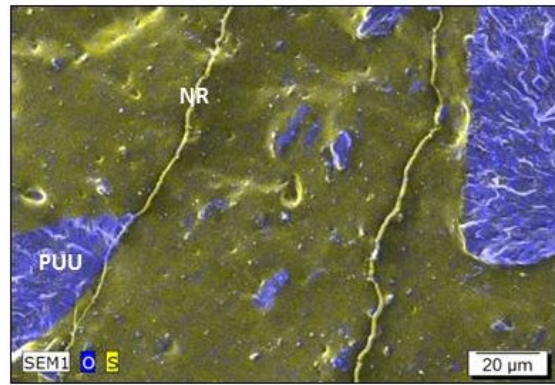
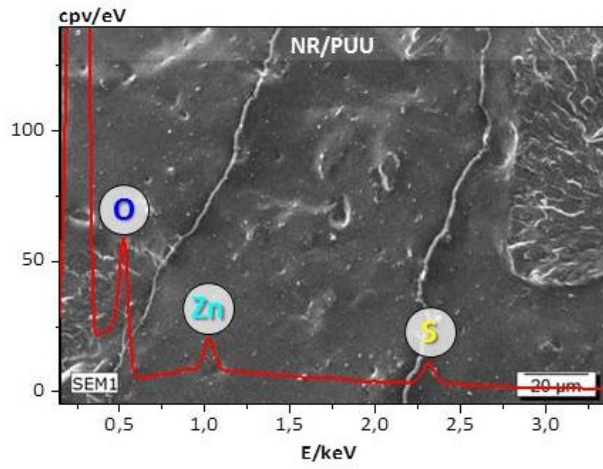


Figure 4.30 Raman spectra along with the corresponding Raman images as inset. **a).** EPDM/PUU, **b).** NR/PUU, **c).** XNBR/PUU, **d).** CR/PUU, **e).** sSBR/PUU blends. The continuous blue regions in Raman images represent rubber matrices (EPDM, NR, XNBR, CR, sSBR) and the dispersed red regions represent domains of *in-situ* synthesized PUU.

4.3.5 SEM-EDX analysis

The SEM images along with the elemental distribution over the surface of cryo-fractured blend specimens and the corresponding EDX spectra are shown in Fig. 4.31. The phases of a cryo-fractured blend specimens cannot be distinguished by SEM; however, an elemental oxygen analysis via EDX clearly identifies the oxygen-rich dispersed domains of PUU in rubber matrices. The corresponding EDX spectrum identifies the surface elements, including oxygen (O), Sulfur (S), Zinc (Zn), Magnesium (Mg) and Chlorine (Cl). Sulfur and ZnO are part of curative package to vulcanize NR, sSBR and XNBR therefore the elemental S and Zn peaks appear in their respective EDX spectra. The metal oxides (MgO + ZnO) are used as a curing package for the sulfur-modified CR and the characteristic elemental peaks of Zn, Mg, S and Cl are observed in the EDX spectrum of the CR/PUU blend. Also, agglomerates of MgO are identified in SEM-EDX images of CR/PUU blends. The presence of curing chemicals only in the rubber phase of blends is realized. This means that the stiff PUU domains inhibit the migration of the crosslinking chemicals into the PUU phase of the blends. The SEM-EDX images of the cryo-fractured specimens show that the interface between the *in-situ* PUU domains and the rubber matrix remains thoroughly intact. Irrespective of the polarity of rubber, the strong interfacial adhesion indicates the existence of an interpenetrated interfacial region.





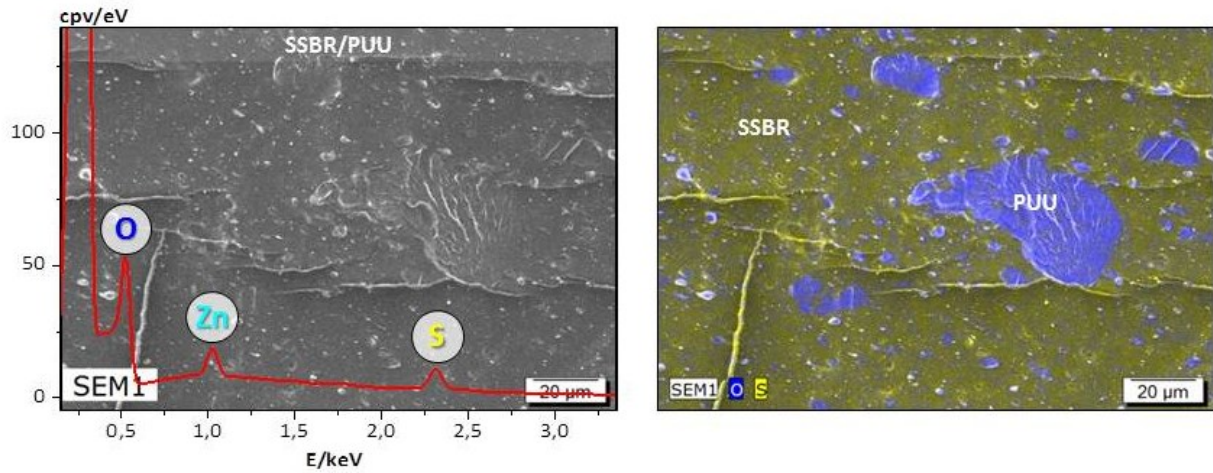


Figure 4.31 SEM-EDX images along with the respective EDX spectrum for EPDM/PUU, NR/PUU, XNBR/PUU, CR/PUU and sSBR/PUU blends. Elemental oxygen mapping identifies PUU domains in blends. In addition, mapping of elemental chlorine-Cl and Magnesium-Mg in CR/PUU, Sulfur-S in XNBR, sSBR and NR is considered.

4.4 Applications of Rubber/PUU blends

Carbon black (CB) and silica are the primary reinforcing fillers used in the rubber industry to produce products having the desired performance benefits. These fillers impart stiffness and strength to the rubber network. However, this reinforcement comes with the drawback of large energy dissipation, which build-up as heat in the rubber articles. If the energy dissipation potential of rubber article can be improved than the resistance to thermal degradation and operational life can be enhanced [105].

4.4.1 NR/PUU blend as tire tread material

Carbon black (CB), being the integral part of tire tread compounds, improves the strength and rolling resistance of on- and off-road pneumatic tires. However, this improvement is coupled with a drawback of large energy dissipation and heat buildup in a tire under conditions of continuously changing dynamic loads. If the energy dissipation potential of CB filled compound can be decreased than the tire life can be extended [105]. In this work, we replaced partially (50%) the carbon black in the NR based composite (NR-CB) by a certain amount of *in-situ* synthesized PUU to obtain a NR/PUU-CB composite of a shore A hardness similar to the reference NR-CB composite and compared their dynamic-mechanical responses. A typical bus/truck/aircraft tire tread formulation [106] is simplified to a model recipe for this investigation.

The N330 grade CB is widely used in the truck tire tread formulation to reinforce the mechanical and dynamic-mechanical response of compounds. The CB of grade N330 is partially replaced with the *in-situ* synthesized PUU to obtain composites having similar hardness.

4.4.1.1 Preparation of composites

The proposed reactive blending process is adapted to prepare CB filled NR and NR/PUU composites (see sub-chapter 4.3). The constituent structural components of the *in-situ* synthesized

PUU are the isocyanate-end capped prepolymer (MT2184) and 1,3-phenylene diamine (mPD). For the preparation of composites, the incorporation of CB succeeds pouring of premix for the *in-situ* synthesis of PUU in presence of NR in an internal mixer. The reactive blending process with an additional step of CB loading is shown in Fig. 4.32. The NR/PUU-CB and NR-CB composites are prepared under identical processing conditions.

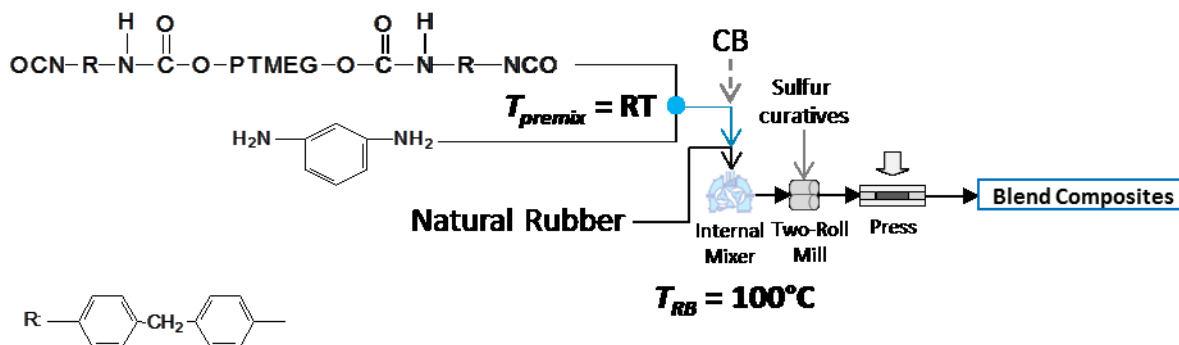


Figure 4.32 Reactive blending process to prepare CB filled composites based on NR and premix of PTMEG / MDI prepolymer and mPD. The temperatures of premixing and reactive blending are obtained from the chemo-rheological analysis (see section 4.1.1).

The recipe of compounds is given in Table 4.11. The unfilled compound, designated as NR, is used as a reference. The compound, designated as NR-CB, represents a simplified model truck tire tread formulation containing 40phr of CB. The 20phr of CB is replaced with 40 phr of *in-situ* synthesized PUU to obtain NR/PUU-CB composite of hardness similar to that of NR-CB composite.

Table 4.11 Recipe of compounds with quantities in parts per hundred parts of rubber

Ingredients	NR	NR-CB	NR/PUU-CB
NR	100	100	100
PUU	-	-	40
CB-N330	-	40	20
ZnO/Stearic Acid	3/2	3/2	3/2
DPG/CBS	2/1.5	2/1.5	2/1.5
Sulfur	1.5	1.5	1.5

4.4.1.2 Morphological investigation by TEM

The distribution of CB in composites is investigated by transmission electron microscopy (TEM). The TEM image of the NR-CB composite shows a rather homogeneous distribution of CB in NR, wherein the CB particles and aggregates can be seen (Fig 4.33 (a)). TEM image in Fig 4.33 (b) shows the distribution of nano-sized CB (black colour) and micro-sized PUU domains (light colour) in the NR matrix (dark colour) of the NR/PUU-CB composite. As expected, the nonpolar CB stays preferentially in a nonpolar NR matrix. CB is not present in polar PUU domains or close to the rubber-PUU interface. It is interesting to note that the PUU domains can be individually identified, and are not connected to each other in rubber matrix. As described in section 4.3.5 of sub-chapter 4.3, the scanning electron microscopy of the NR/PUU blends reveals a good interfacial adhesion between the NR matrix and the PUU domains. This refers to the fact that the interfacial region around PUU domains is generated from the mutual interpenetration of polymer chains as contrast to the bound rubber region, believed to be developed around particles/aggregates of CB.

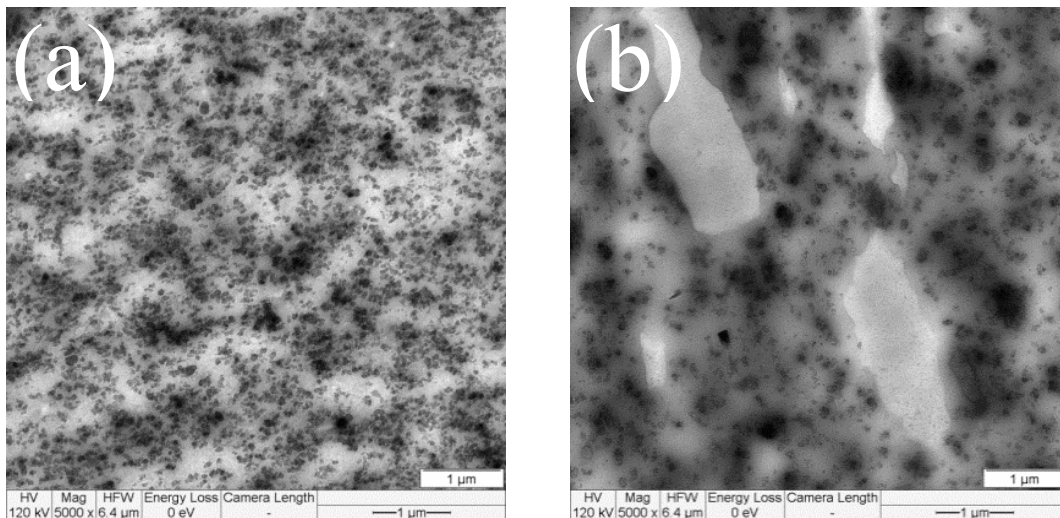


Figure 4.33 TEM micrographs of CB filled composites. a). NR-CB, b). NR/PUU-CB

4.4.1.3 Dynamic mechanical analysis

4.4.1.3.1 Temperature sweep test

The plots of storage modulus (E'), loss modulus (E'') and loss factor ($\tan \delta$) for the NR, NR-CB and NR/PUU-CB compounds as a function of temperature are shown in Fig. 4.34. The peak position of $\tan \delta$ curve is taken as the glass transition temperature, which is at about -47°C for NR ($T_{g,NR}$) in the unfilled and filled compounds (Fig. 4.34 (a)). The glass transition relaxation of NR overlaps with the relaxation (not observed) of soft segments of PUU phase in NR/PUU-CB composite. The NR-CB and NR/PUU-CB composites exhibit $\tan \delta$ peaks of equal height, which shows similar level of reinforcement by the CB and the CB/PUU dual-reinforcement inclusions.

In the rubbery plateau region, the NR-CB composite exhibits higher values of $\tan \delta$ (inset in Fig. 4.34(a)), loss and storage modulus (Fig 4.34(b)) than that of NR/PUU-CB composite. The higher level of loss modulus shows that the energy dissipation and heat build-up is higher in NR-CB composite as compared to the NR/PUU-CB composite. The values of $\tan \delta$ at 0°C and 60°C relate to the wet traction and rolling resistance of tires. Accordingly, the NR/PUU-CB composite offers lower rolling resistance than the NR-CB composite, at a similar level of wet traction.

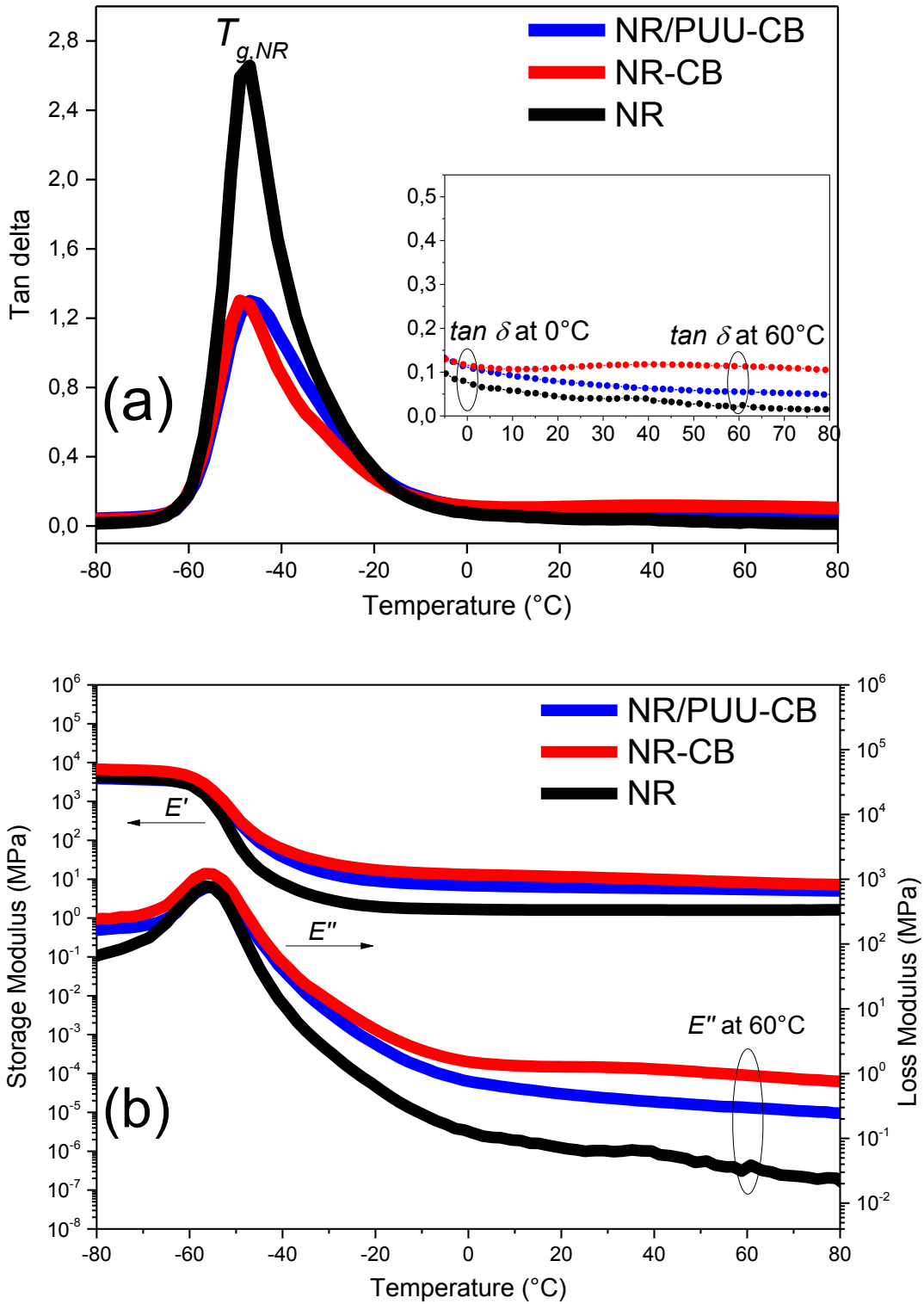


Figure 4.34 DMA curves of neat NR and its composites: NR-CB and NR/PUU-CB. **a)** Loss factor vs. temperature, **b)** loss and storage modulus vs. temperature curves

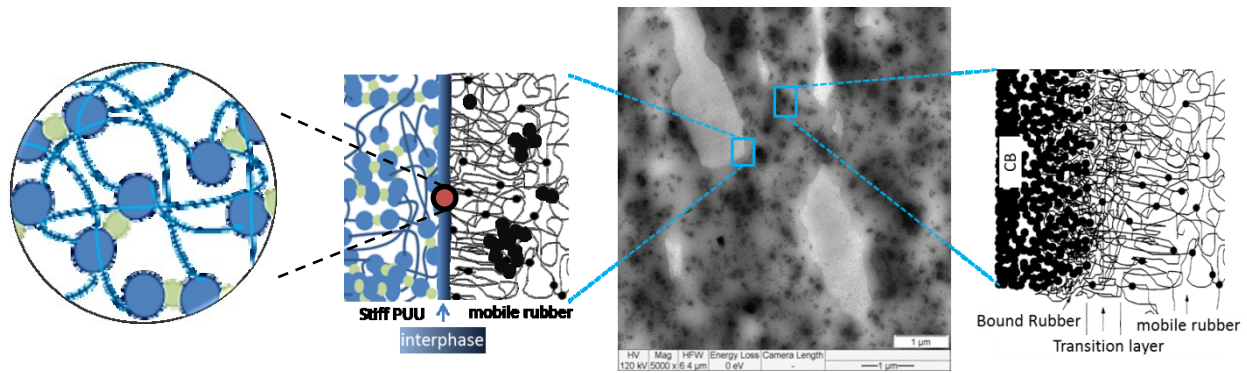


Figure 4.35 Graphical representation of interfacial interactions between NR and the reinforcing inclusions i.e. PUU and CB in NR/PUU-CB composite [107]

The higher heat build-up in NR-CB than NR/PUU-CB relates to a different nature of the interphase developed by CB and *in-situ* synthesized PUU with NR. The rubber chains close to CB particles/aggregates have a restricted mobility and are identified in bound rubber [108], salvation [109], insolubilization [110] and/or occluded rubber concepts [111]. The rubber chains are bound to the irregular surface of filler particles/aggregates mainly through physisorption and mechanical interlocking at the rubber-CB interface; though the chemisorptive mechanism of rubber-filler connection via free radical reaction has also been proposed [112-116]. In the bound rubber region, a large amount of the applied energy is dissipated to mobilize the restricted chains over one other and over the irregular filler surface. Accounting the elaborated models of the bound rubber concept [117] by Heinrich [107] and Fukahori [118], this sliding friction is considered to be more pronounced among the chains in the transition layer (sticky layer) instead of the bound rubber (glassy layer) chains penetrated into the nanostructures of CB aggregate/agglomerates. High CB loading leads to a large rubber-CB interphase, bound rubber region and high energy dissipation in NR-CB composite. Also, at higher loading, the possibility of friction loss amongst filler particles cannot be overruled.

In the NR/PUU-CB composite, the interfacial associations of mutually interpenetrated chains of *in-situ* synthesized PUU and NR phases are advantageous over CB (see Fig 4.35). In the NR-CB composite, the mobility of rubber chains relative to CB surface is possible, whereas the relative movement of mutually interpenetrated chains at the NR-PUU interphase seems not to be possible at low strain dynamic mechanical measurements.

It has been reported that the value of loss modulus at around 60 °C is inversely proportional to the adhesion (interfacial strengths) between the surface of reinforcing entities and the polymer [119] in constant strain DMA measurements. The level of loss modulus in Fig. 4.34 (b) indicates weak interfacial associations (bond strengths) between the CB surface and the NR chains in the NR-CB composite as compared to the strong associations of mutually interpenetrated chains of PUU and NR in the NR/PUU-CB composite. The strong adhesion between the reinforcing inclusions and rubber and the low rolling resistance are vital for better performance of a truck tire tread compound. Hence, in this prospect, the NR/PUU-CB prevails over the NR-CB compound.

4.4.1.3.2 Amplitude sweep test-Payne effect

The so-called Payne effect is measured from the nonlinear dependency of viscoelastic behavior of a filled compound on the amplitude of sinusoidal deformation [120-124]. It describes filler-filler networking, relates to energy dissipation and heat build-up in filled elastomers. Fig. 4.36 reflects that the initial (E'_0) modulus and final modulus (E'_∞) of the filled NR composites are higher as compared to unfilled NR. The unfilled NR exhibits a linear viscoelastic response with an increasing strain amplitude and shows similar values of E'_0 and E'_∞ . Both of NR-CB and NR/PUU-CB composites show a gradual decrease in storage modulus with increasing strain amplitude due to the breakdown of filler-filler networks. Higher loading of CB enhances the level of storage modulus (E'_0) and filler-filler networking for NR-CB composite [125]. The amplitude-

dependent decrease in storage modulus, known as the Payne effect ($\Delta E' = E'_0 - E'_\infty$), is extremely high for NR-CB (7.0 MPa) than that for NR/PUU-CB (4.1 MPa). The high level of the Payne effect reduces the mechanical efficiency of a composite. Consequently, the energy dissipation and the heat build-up are higher in NR-CB as compared to the NR/PUU-CB composite.

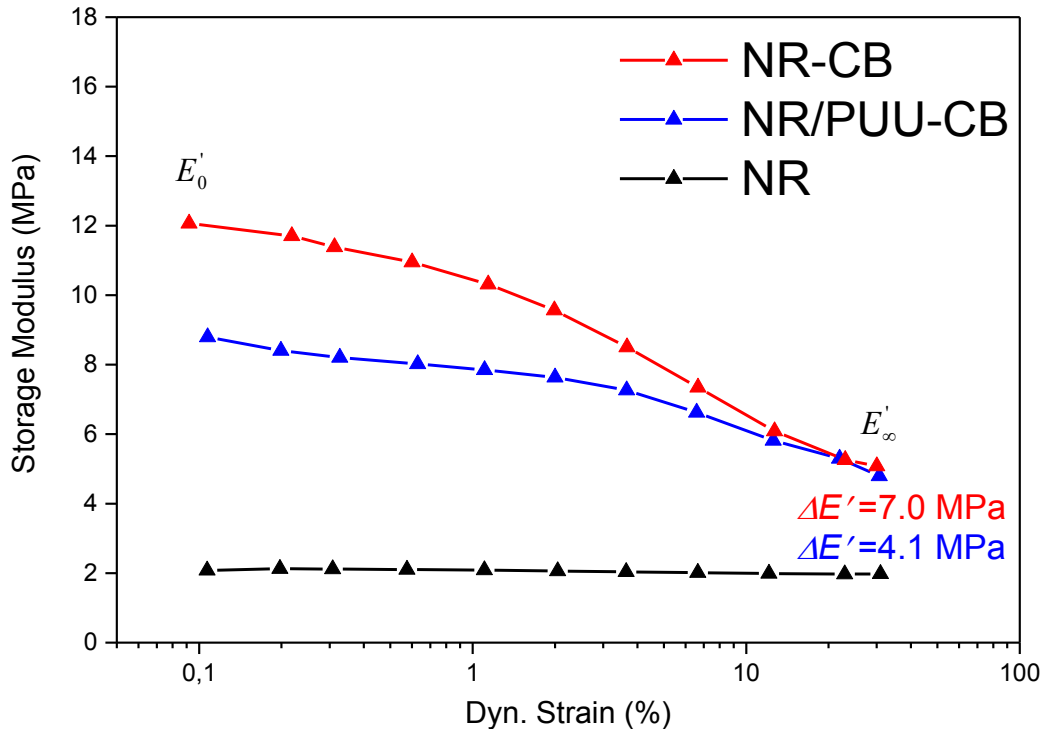


Figure 4.36 Dependence of storage modulus on strain amplitude for NR, NR-CB and NR/PUU-CB compounds

4.4.2 NBR/PUU blend as roller covering material

The reactive blending process is versatile with respect to the choice of rubber polymer, structural components of the *in-situ* synthesized polyurethane-urea and the ease of incorporating additives and auxiliaries typical to the rubber technology. Therefore, the prepared novel blends offer a wide range of performance benefits and application possibilities.

The application of NBR/PUU blends, obtained via the reactive blending process of Fig. 4.1, is tested as a roller covering material in this work. In order to prepare a prototype roller, the blend material in calendared form is wrapped around a shallow metallic roll and cured in a high pressure steam autoclave at Fender Gummiwalzen GmbH. The blend-covered roll is fixed with a roller shaft by Stark Gummiwalzen GmbH to obtain a finished NBR/PUU-covered roller, as shown in Fig. 4.37.



Figure 4.37 NBR/PUU blend-covered roller

The roller is tested on a lab-scale test rig (shown in Fig. 4.38) at the Institute of Process Engineering and Environmental Technology, Technische Universität Dresden. The heat build-up in a running NBR/PUU-covered roller and the sustainability of its structural integrity are tested.

The heat build-up in the NBR/PUU blend is also measured by a flexometer test and compared with a silica reinforced NBR composite of similar hardness. The recipe of the NBR/PUU blend and the NBR/Silica composite are given in Table 4.12.

Table 4.12 Formulation of compounds with quantities in parts per hundred parts of rubber

Ingredients	NBR/PUU	NBR/Silica
NBR	100	100
PUU	30	-
Silica (Coupsil VN3-gr)	-	33
Peroxide (Perkadox BC-40K-pd)	3	3
Coagent (Rhenogran TAC-50)	2	2

4.4.2.1 Experimental set-up and heat build-up test

Fig. 4.38 highlights the upper test roller and the lower drive roller on a test rig. The test rubber roller is mounted and pressed against the grooved metallic roller, which is driven at a desired rotational speed. The normal force of pressing two rollers together and the rotational speed are the main test parameters to assess the performance of rollers i.e NBR/PUU and NBR/Silica covered rollers.

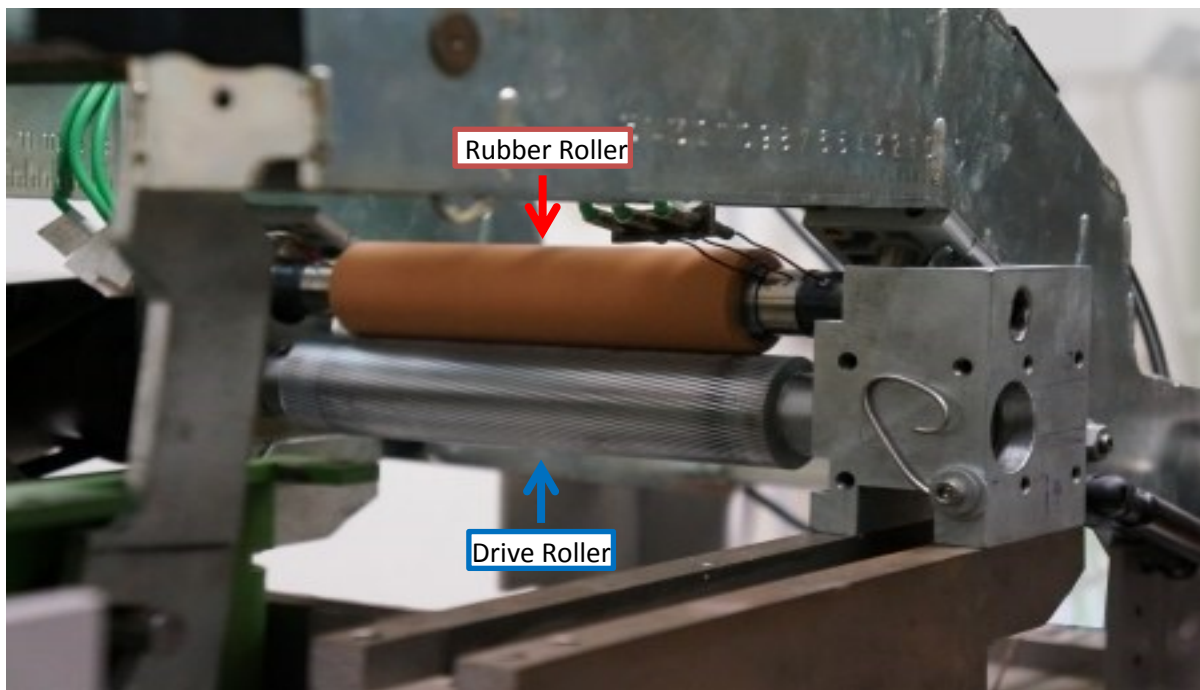


Figure 4.38 Experimental rig to examine thermo-mechanical behavior of NBR/PUU blend-covered roller. The upper test rubber roller and the lower corrugated drive roller are shown.

[Ref: <https://tu-dresden.de/ing/maschinenwesen/ifvu/evt/forschung/energiesystemtechnik/aktive-kuhlung-von-schnell-rotierenden>]

For a preliminary test, a normal force of 320 N and a rotational speed of 500 m/min are chosen as test parameters. The dissipated energy accumulates as heat and increases the temperature of the roller covering. This rise in surface temperature of the running roller is observed by an infrared camera and a thermal image at the steady-state running condition is taken to be shown in Fig 4.39.

The outcomes of the roller testing are consistent with the results of the flexometer test (see Fig. 4.40). It shows that the NBR/Silica specimen develops a steep temperature rise, a high steady-state surface and core temperature in comparison to the NBR/PUU specimen.

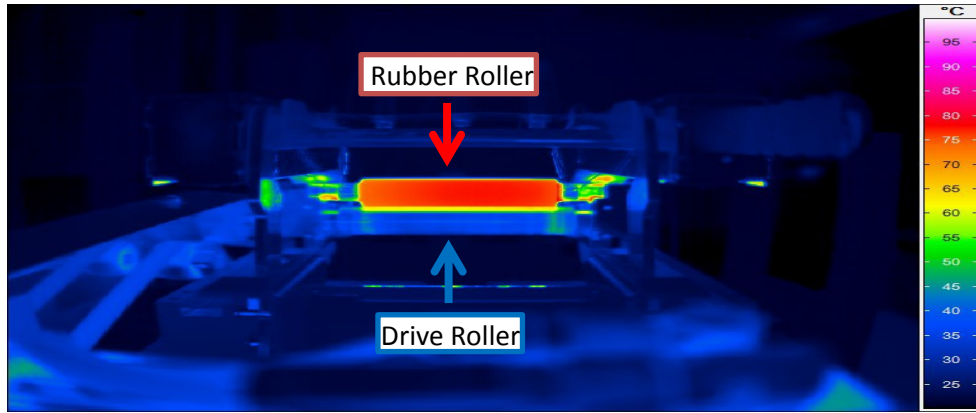


Figure 4.39 Thermal image of the running NBR/PUU roller is shown. Temperature distribution according to the color temperature scale in Celsius scale can be seen.

In the silica filled NBR composite, the strong filler-filler and weak rubber-filler interactions cause an excessive dissipation of applied energy as compared to a strong interphase of mutually interpenetrating chains in PUU filled NBR matrix (refer to section 4.4.1 for a detailed discussion).

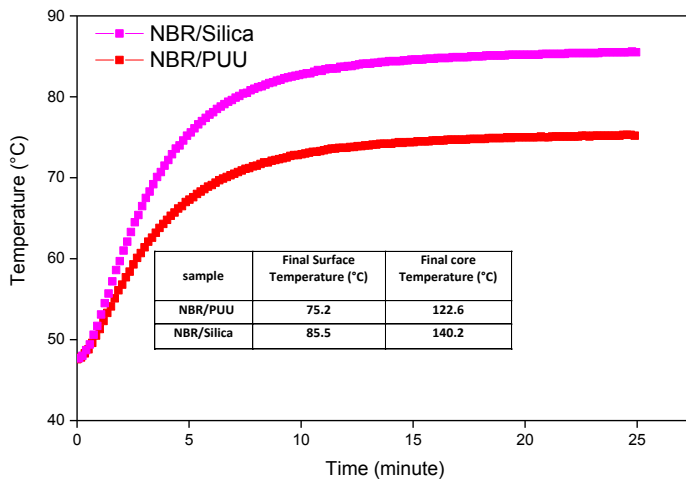


Figure 4.40 Curves of flexometer test. The final surface and core temperatures of specimens are as inset table. The core temperature is measured by using a thermocouple, as is shown in a photo of flexometer test setup.

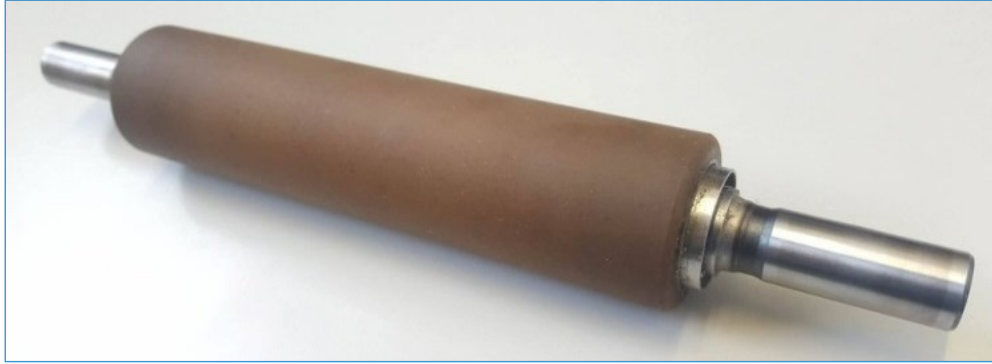


Figure 4.41 The tested NBR/PUU blend covered Roller. Roller retains integrity without any surface cracks.

The tested NBR/PUU blend-covered roller is shown in Fig. 4.41. The roller survives severe testing conditions on an experimental rig and retains integrity without any wear and tear on its surface. This shows that the PUU domains keep their stiffness, reinforcing tendency and strong interfacial adherence with the rubber matrix even under high temperature dynamic applications.

Conclusions

The blending of polar/nonpolar rubbers with structurally diverse polyurethane-ureas is investigated to obtain new functional elastomeric materials. The proposed process of reactive blending incorporates effectively the *in-situ* synthesized polyurethane-urea into rubbers for novel blends having unprecedented property profile and a broader temperature range of applicability.

In preliminary investigations, the polyurethane-urea (PUU) is synthesized via a prepolymer route during reactive blending with the nitrile butadiene rubber (NBR) in an internal mixer. The effectiveness of this prepolymer route to the *in-situ* synthesized polyurethane-urea is confirmed by the ^1H NMR spectroscopic analysis, which shows a high conversion ($\sim 87\pm 3\%$) of *m*-phenylenediamine during the polyaddition reactions with the 4, 4'-diphenylmethane diisocyanate (MDI) and poly(tetramethylene ether) glycol (PTMEG) based prepolymer. TEM measurements of the NBR/PUU blends verify the existence of a chain interpenetrated interfacial region (interphase) of about 30 nm between the NBR and the PUU phases. A SEM-EDX analysis verifies the presence of an interphase by depicting strong adhesion between the blend components. The stiff *in-situ* synthesized PUU is highly reinforcing and imparts remarkable improvements to the static- and dynamic-mechanical characteristics of NBR. Importantly, a dynamic-mechanical temperature sweep analysis shows that the incorporation of *in-situ* synthesized PUU decreases gradually the dissipation of applied energy in a stable rubbery plateau region of the blends. The *in-situ* synthesized PUU phase retains its stiffness due to the strong bidentate hydrogen bonding within the disorderly arranged hard segment domains as verified by the wide angle X-ray scattering measurements.

The reactive blending of four different kinds of *in-situ* synthesized PUUs with NBR is investigated, wherein the MDI-PTMEG prepolymer is chain extended with primary aliphatic and

aromatic diamines. 1,3-phenylenediamine (mPD), 1,4-Bis(aminomethyl)benzene (pXD), 4,4'-Methylene-bis(2-chloroaniline) (MBCA) and 4,4'-(m-phenylenediisopropylidene) dianiline (BisAM) were premixed with prepolymer for the *in-situ* synthesis of PUU-mPD, PUU-pXD, PUU-MBCA and PUU-BisAM, respectively, during blending with NBR in an internal mixer. The chemical structure of the *in-situ* synthesized polyurethane-urea influences the morphological, tensile and dynamic-mechanical characteristics of their blends with NBR. The tensile characteristics always improve on blending NBR with any kind of *in-situ* synthesized PUUs. The morphology of the dispersed PUU domains determines the ultimate level of tensile characteristics of the blends. The homogeneous dispersion of the spherical PUU-MBCA domains and the fibrillar PUU-BisAM domains offer a huge improvement in tensile properties, which are exceedingly superior to that of neat NBR. During the dynamic-mechanical testing, the storage modulus of the rubbery plateau region of the Blend-mPD, -pXD and -MBCA specimens remain stable and higher than that of neat NBR. The Blend-BisAM exhibits the best tensile response at room temperature and the worst dynamic-mechanical response in the rubbery plateau region due to the thermoplastic nature of the PUU-BisAM phase of blends.

The incorporation of *in-situ* synthesized PUU is equally effective in improving the low strain tensile and dynamic-mechanical response of both the polar (CR, XNBR) and nonpolar (NR, sSBR, EPDM) rubbers. Raman spectroscopy verifies a successful *in-situ* extension of the MDI-PTMEG based prepolymer chains with m-phenylenediamine in all five kinds of rubbers. Raman imaging structurally identifies the *in-situ* synthesized PUU as dispersed phase in the continuous rubber matrices. SEM-EDX micrographs conclude that the pre-polymer approach compatibilizes successfully the PUU with all used polar and nonpolar rubbers.

The use of novel Rubber/PUU blends in industrial applications is explored, such as in a model truck tire tread formulation and as a rubber roller covering material. In a simplified truck tire tread formulation, the reinforcing grade carbon black (N330) is partially (50%) replaced with an equivalent quantity of the *in-situ* synthesized PUU for a composite of similar hardness. The dynamic-mechanical investigation of these model compounds revealed that the partial replacement of CB by PUU offers a tread material with improved energy efficiency and rolling resistance without compromising the level of wet traction. In another application, the NBR/PUU blend is successfully tested as a roller covering material. The tested blend-coated roller retains structural integrity and exhibits lesser heat build-up than that of silica filled counterpart. This promises the suitability of the blend-covered rollers in commercial applications including film, printing and textile processing machinery.

The opted reactive blending process is very effective in blending polyurethane-ureas with rubbers. The process can readily be opted to generate different structures of polyurethane-ureas in different rubber. It offers potential of compatibilizing the polyurethane-ureas with any kind of rubber. The auxiliaries and additives typical for the rubber technology can readily be incorporated into blends via the opted process of reactive blending. Many applications of these novel blends can be envisaged including the high strength and mechanically efficient industrial wheels, belts or pump impellers.

Recommendations and Outlook

The proposed reactive blending process is a promising route to blend rubbers (or other polymers) with the *in-situ* synthesized polyurethane-urea.

The process, being simple and efficient, is attractive for scale up to industrial level. While scaling up, the temperature, residence time and shear rate, at the stages of premix preparation and reactive blending, need to be optimized. The optimization of the distributed blend morphology (generated primarily in a mixer chamber) is important to obtain product for better economic performance.

The isocyanate index, functionality, type and molecular weight of polyol, diisocyanate and chain extender are important parameters to obtain blends having the desired set of performance attributes.

The diamine based urea moieties tend to increase the polarity of polyurethane-urea chains, therefore, the polarity can be adjusted by combining diamine with diols (triggering the use of a catalyst) to better compatibilize the *in-situ* synthesized polyurethane-urea with nonpolar rubbers. A similar approach can be utilized in selecting the most suitable polyol. In addition, use of the unsaturated polyols can offer new set of interesting materials.

Aliphatic chain extenders are highly reactive and offer very little pot life during the premixing stage. However, their use can broaden the property spectrum of the *in-situ* synthesized polyurethane-urea based blend materials. The issue can be investigated by blocking the hydroxyl and amino reactive groups on the aliphatic chain extender in order to realize the deblocking at high temperature in the internal mixer during reactive blending.

References

- [1] L. A. Utracki, In: Commercial Polymer Blends, Eds. L. A. Utracki, 1st Edn., Springer, USA, 1998.
- [2] L. H. Sperling, R. Hu, In: Polymer Blends Handbook, Ed. L. A. Utracki, 1st Vol., Kluwer Academic Publishers, Dordrecht, Netherlands 2002.
- [3] J. W. Moore, C. L. Stanitski, P. C. Jurs, Chemistry: The Molecular Science, 4th Edn., Cengage Learning, USA, 2010.
- [4] G. Giancola, R. L. Lehman, J. D. Idol, Powder Technology 218 (2012) 18–22.
- [5] L. H. Sperling, Interpenetrating Polymer Networks and Related Materials, 1st Edn., Springer, New York, USA, 1981.
- [6] A. D. McNaught and A. Wilkinson., IUPAC Compendium of Chemical Terminology, 2nd ed. (the "Gold Book"), Compiled by Blackwell Scientific Publications, Oxford, UK, 1997.
- [7] L. D. Perez, L. Sierra, B. L. Lopez, Polym. Eng. Sci. 48 10 (2008) 1986–1993.
- [8] P. A. Marsh, A. Voet, L. D. Price, T. J. Mullens, Rubber Chem. Technol. 41 344 (1968).
- [9] J. G. Bonner, P. S. Hope, In: Polymer Blends and Alloys, Springer, The Netherlands, 1993.
- [10] L. A. Utraki, Polym. Eng. Sci. 35 (1995) 2-17.
- [11] M. Tahir, K. W. Stöckelhuber, N. Mahmood, H. Komber, G. Heinrich., Macromol. Mater. Eng. 300 2 (2015) 242-250.
- [12] M. Tahir, K. W. Stöckelhuber, N. Mahmood, H. Komber, P. Formanek, S. Wießner, G. Heinrich, Eur. Polym. J 73 (2015) 75–87.
- [13] Y. Berezkin, M. Urlick, ACS Symp. Ser. 1148 (2013) 65-81.
- [14] G. Oertal, Polyurethane Handbook, Hanser Publishers, New York, USA 1994.
- [15] Z. S. Petrovic, in: Handbook of Polymer Synthesis, Eds. H. R. Kricheldorf, O. Nuyken, G. Swift, 2nd edn., Marcel Dekker, Inc., New York, USA 2005.

- [16] G. Woods, *The ICI Polyurethane Book*, 2nd edn., JohnWiley & Sons, The Netherlands 1987.
- [17] A. Noshay, J. E. McGrath, *Block Copolymers: Overview and Critical Survey*, Academic Press, New York, USA 1977.
- [18] I. Dimitrievski, Z. Susteric, T. Marinovic, *Proc. 5th Eur Rheol Conf Slovenia (1998)* 73-74.
- [19] T. Tang, C. P. Hu, S. K. Ying, Y. X. Zhang, in *Advances in Polymer Blends and Alloys Technology*. 4th Vol. (Ed. K. Finlayson,), Technomic Publishing Co., Lancaster, UK, 1993, 1–10.
- [20] I. Dimitrievski, Z. Susteric, T. Marinovic, in *Advances in Polymer Blends and Alloys Technology*, 4th Vol. (Ed: K. Finlayson,), Technomic Publishing Co., Lancaster, UK, 1993, 11–28.
- [21] S. K. Singha Roy, C. K. Das, *Polym. Polym. Compos.* 3 6 (1995) 403-410.
- [22] M. Kotal, S. K. Srivastava, A. K. Bhowmick, *Polym. Int.* 59 1 (2010) 2-10.
- [23] J. H. Tan, X. P. Wang, J. J. Tai, Y. F. Luo, D. M. Jia, *Express Polym. Lett.* 6 7 (2012) 588-600.
- [24] N. Mahmood, A. U. Khan, Z. Ali, M. S. Khan, A. U. Haq, K. W. Stöckelhuber, U. Gohs, G. Heinrich, *J Appl. Polym. Sci.* 123 6 (2012) 3635-3643.
- [25] N. Mahmood, A. U. Khan, K. W. Stöckelhuber, A. Das, D. Jehnichen, G. Heinrich, *J Appl. Polym. Sci.* 131 11 (2014) 40341.
- [26] D. Xu, J. Karger-Kocsis, *J. Appl. Polym. Sci.* 115 3 (2010) 1651-1662.
- [27] H. A. Colvin, M. A. Alsamarraie, D. K. Parker, US5523351 A, 1996.
- [28] J. Karger-Kocsis, D. Felhös, D. Xu, *Wear* 268 (2010) 464-472.
- [29] U. Sebenik, J. Karger-Kocsis, M. Krajnc, R. Thomann, *J Appl. Polym. Sci.* 125 S1 (2012) E41-E48.

- [30] W. Pongdong, C. Kummerlöwe, N. Vennemann, A. Thitithammawong, C. Nakason, J. Polym. Environ. (2017) 1-15.
- [31] M. Szycher, Szycher's handbook of polyurethanes, CRC Press, USA, 2013.
- [32] C. Prisacariu, Polyurethane Elastomers: From morphology to mechanical aspects, Springer, New York, USA, 2011.
- [33] S. Desai, I. M. Thakore, A. Brennan, S. Devi, J Macromol. Sci. Pure Appl. Chem. A38 7 (2001) 711-729.
- [34] H. G. Im, K. R. Ka, C. K. Kim, Ind. Eng. Chem. 49 (2010) 7336-7342.
- [35] J. Karger-Kocsis, J. Gremmels, A. Mousa, Z. A. Mohd Ishak, Kaut. Gummi Kunstst. 53 9 (2000) 528-533.
- [36] A. Mousa, J. Karger-Kocsis, Plast. Rubber Compos. 30 7 (2001) 309-313.
- [37] Z. A. Mohd Ishak, P. Y. Wan, P. L. Wong, Z. Ahmad, U. S. Ishiaku, J. Karger-Kocsis, J Appl. Polym. Sci. 84 12 (2002) 2265–2276.
- [38] C. R. Kumar, J. Karger-Kocsis, Eur. Polym. J 38 11 (2002) 2231–2237.
- [39] S. Varghese, K. G. Gatos, A. A. Apostolov, J. Karger-Kocsis, J Appl. Polym. Sci. 92 1 (2004) 543–551.
- [40] G. C. Psarras, K. G. Gatos, J. Karger-Kocsis, J Appl. Polym. Sci. 106 2 (2007) 1405–1411.
- [41] S. Seingchin, J. Karger-Kocsis, G. C. Psarras, R. Thomann, J Appl. Polym. Sci. 110 (2008) 1613-1623.
- [42] G. C. Psarras, S. Seingchin, P. K. Karahaliou, S. N. Georga, C. A. Krontiras, J. Karger-Kocsis, Polym. Int. 60 (2011) 1715–1721.
- [43] M. Maity and C. K. Das, Polym. Int. 49 (2000) 757-762.
- [44] B. B. Khatua and C. K. Das, Polym. Int. 50 (2001) 495-502.
- [45] B. B. Khatua, C. K. Das, J Appl. Polym. Sci. 80 (2001) 2737–2745.

- [46] B. B. Khatua, M. Maity, C. K. Das, *J Appl. Polym. Sci.* 76 (2000) 1367–1376.
- [47] B. B. Khatua, C. K. Das, *J Appl. Polym. Sci.* 93 (2004) 845–853.
- [48] B. B. Khatua, C. K. Das, *Polym. Degrad. Stab.* 69 (2000) 381-386.
- [49] B. B. Khatua, C. K. Das, *J. Therm. Anal. Calorim.* 63 (2001) 565-576.
- [50] M. Maity, B.B. Khatua, C.K. Das, *Polym. Degrad. Stab.* 70 (2000) 263-267.
- [51] M. Maity, B.B. Khatua, C.K. Das, *Polym. Degrad. Stab.* 72 (2001) 499–503.
- [52] M. Maity, B.B. Khatua, C.K. Das, *Int. J Polym. Mater.* 49 4 (2001) 407-417.
- [53] B. B. Khatua, C. K. Das, P. K. Patra, M. S. Banerjee, W. Millins, *Int. J Polym. Mater.* 46 1-2 (2000) 347-360.
- [54] B. B. Khatua, C. K. Das, *J. Elastom. Plast.* 32 3 (2000) 231-247.
- [55] M. Maity, C. K. Das, *Polym Plast Technol Eng.* 40 1 (2001) 39-51.
- [56] M. Maity, B. B. Khatua, C. K. Das, *J. Elastom. Plast.* 30 3 (2001) 211-224.
- [57] K. Pal, R. Rajasekar, D. J. Kang, Z. X. Zhang, S. K. Pal, C. K. Das, J. K. Kim, *J. of Thermoplast. Compos. Mater.* 23 5 (2010) 717-739.
- [58] S. Pichaiyut, C. Nakason, N. Vennemann, *Iran Polym. J* 21 1 (2012) 65–79.
- [59] E. Kalkornsurapranee, N. Vennemann, C. Kummerlöwe, C. Nakason, *Iran Polym. J* 21 10 (2012) 689–700.
- [60] E. Kalkornsurapranee, C. Nakason, C. Kummerlöwe, N. Vennemann, *Adv. Mater. Res.* 626 (2013) 229-232.
- [61] S. Pichaiyut, C. Nakason, N. Vennemann, *Adv. Mater. Res.* 626 (2013) 240-244.
- [62] W. Pongdong, C. Nakason, C. Kummerlöwe, N. Vennemann, *Adv. Mater. Res.* 844 (2014) 140-143.
- [63] S. Pichaiyut, N. Vennemann, C. Nakason, *J. Elastom. Plast.* 47 1 (2015) 28–51.

- [64] S. Pichaiyut, C. Nakason, C. Kummerlöwe, N. Vennemann, *Polym. Adv. Technol.* 23 (2012) 1011–1019.
- [65] E. Kalkornsurapranee, C. Nakason, C. Kummerlöwe, N. Vennemann, *J. Appl. Polym. Sci.* 128 4 (2013) 2358–2367.
- [66] P. J. Thomas, P.A. Midgley. *Top. Catal.* 21 4 (2002) 109-138.
- [67] P. Matricardi, M. Dentini, V. Crescenzi, *Macromolecules* 26 (1993) 4386-4387.
- [68] P. J. Yoon, C. D. Han, *Macromolecules* 33 (2000) 2171-2183.
- [69] J. H. E. Hone, A. M. Howe, T. Cosgrove, *Macromolecules* 33 (2000) 1199-1205.
- [70] M. Daoud, *Macromolecules* 33 (2000) 3019-3022.
- [71] F. Tanaka, *Macromolecules* 31 (1998) 384-393.
- [72] M. Grisel, G. Muller, *Macromolecules* 31 (1998) 4277-4281.
- [73] C. Balan, K. W. Volger, E. Kroke, R. Riedel, *Macromolecules* 33 (2000) 3404-3408.
- [74] A. K. Bhowmick, H. L. Stephens, *Handbook of elastomers*, 2nd Ed., Marcel Dekker, New York, USA, 2001.
- [75] O. Bayer, E. Muller. *Angew. Chem.* 59 9 (1960) 257.
- [76] J. Mattia, P. Painter, *Macromolecules* 40 (2007) 1546-1554.
- [77] M. M. Coleman, K. L. Lee, D. J. Skrovanek, P. C. Painter, *Macromolecules* 19 (1986) 2149-2157.
- [78] M. M. Coleman, M. Sobkowiak, G. J. Pehlert, P. C. Painter, *Macromol. Chem. Phys.* 198 1 (1997) 117-136.
- [79] M. M. Coleman, D. J. Skrovanek, J. Hu, P. C. Painter, *Macromolecules* 21 1 (1988) 59-65.
- [80] N. P. Cheremisinoff, *Handbook of Polymer Science and Technology*, Vol. 2, CRC Press, New York, 1989.

- [81] E. L. Kay, K. B. Roskos, Nucleation of urethane compositions, EP 0199021 A2, Oct 29, 1986.
- [82] Z. Tadmor, C. G. Gogos, Principles of Polymer Processing, John Wiley & Sons, Inc., Hoboken, New Jersey, 2006.
- [83] A. N. Wilkinson, A.J. Ryan, Polymer Processing and Structure Development, Kluwer Academic Publishers, London, 1998.
- [84] L. A. Utracki, Polymer Blends Handbook, vol. 1, Kluwer Academic Publishers, Dordrecht, The Netherlands, 2002.
- [85] T. Whelan. Polymer Technology Dictionary, Chapman & Hall, London, UK, 1994.
- [86] F. Dimier, B. Vergnes, M. Vincent, Rheol. Acta 43 2 (2004) 196-202.
- [87] Y. Tanaka, Rubber Chem. Technol. 64 (1991) 325.
- [88] G. Wolfman, S. W. Hasenhidl, Kaut. Gummi Kunstst. 44 2 (1991) 118.
- [89] S. Toki, T. Fujimaki, M. Okuyama, Polymer 41 14 (2000) 5423-29.
- [90] K. Brüning, K. Schneider, S. V. Roth, G. Heinrich, Macromolecules 45 (2012) 7914-19.
- [91] K. Brüning, K. Schneider, S.V. Roth, G. Heinrich, Polymer 54 (2013) 6200-05.
- [92] L. Ibarra, A. Marcos-Fernández, M. Alzorriz, Polymer 43 5 (2002) 1649-55.
- [93] B. Hird, A. Eisenberg, Macromolecules 25 (1992) 6466– 6474.
- [94] H. P. Brown, Rubber Chem. Technol. 36 (1963) 931– 962.
- [95] K. Sunity, S. K. Chakraborty, S. K. De, Polymer 24 (1988) 1055– 1062.
- [96] N. D. Zakharov, Rubber Chem. Technol. 36 2 (1963) 568-574.
- [97] D. Basu, A. Das, K. W. Stöckelhuber, D. Jehnichen, P. Formanek, E. Sarlin, J. Vuorinen, G. Heinrich, Macromolecules 47 10 (2014) 3436–50.
- [98] W. R. Sorenson, J Org. Chem. 24 7 (1959) 978–980.

- [99] I. Franta, *Elastomers and rubber compounding materials*, Elsevier, Prague, Czechoslovakia, 1989.
- [100] N. Karak, *Fundamentals of Polymers: Raw Materials to Finish Products*, PHI publishers, Dehli, India 2009.
- [101] J. T. Maynard, W. E. Mochel, *J Polm. Sci. A Polym. Chem.* XIII (1954) 235-250.
- [102] B. Erman, J. E. Mark, C. M. Roland, *The Science and Technology of Rubber*, Academic Press, Oxford, UK, 2013
- [103] A. M. Stricher, R. G. Rinaldi, C. Barres, F. Ganachaud, L. Chazeau, *RSC Adv.* 5 (2015) 53713- 53725.
- [104] U. K. Mandal, D. K. Tripathy, S. K. De, *Plast Rubber Comp Proc. Appl.* 24 (1995) 19-25.
- [105] R. P. Brown, *Rubber Product Failure in Rapra review reports*, 13 (2002).
- [106] R. N. Datta, *Rubber Curing Systems in Rapra review reports*, 12 (2001).
- [107] G. Heinrich, T. A. Vilgis, *Macromolecules* 26 (1993) 1109-1119.
- [108] J. H. Fielding, *Ind. Eng. Chem.* 29 8 (1937) 880-885.
- [109] E. Guth, *J. App. Phys.* 16 (1945) 20-25.
- [110] B. Meissner, *J. App. Polymer Sci.* 18 8 (1974) 2483-2491.
- [111] A. I. Medalia, *Rubber Chem. Technol.* 47 2 (1974) 411-433.
- [112] R. L. Collins, M. D. Bell, G. Kraus, *Rubber World* 139 219 (1958).
- [113] G. Riess, J. -B. Donnet, In: *Physico-Chimie du Noir Carbone*, Edition du CNRS, Paris, 1963.
- [114] A. M. Gessler, *Proc. Fifth rubber technol. Conf.*, Maclaren & Sons, London, 1968.
- [115] A.M. Gessler, *Rubber Chem. Technol.* 42 (1969) 850-857.
- [116] G. Huber, T. A. Vilgis, *Eur. Phys. J. B* 3 (1998) 217-223.
- [117] P. B. Stickney and R. D. Falb, *Rubber Chem. Technol.* 37 (1964) 1299–1340.

- [118] Y. Fukahori, Rubber Chem. Technol. 80 (2007) 701-725.
- [119] K. W. Stöckelhuber, A. S. Svistkov, A. G. Pelevin, and G. Heinrich, Macromolecules 44 (2011) 4366–4381.
- [120] A. R. Payne, J Appl. Polym. Sci. 6 19 (1962) 57-63.
- [121] A. R. Payne, J Appl. Polym. Sci. 7 3 (1963) 873–885.
- [122] A. R. Payne, J Appl. Polym. Sci. 9 6 (1965) 2273-2284.
- [123] A. R. Payne, J Appl. Polym. Sci. 11 3 (1967) 383–387.
- [124] G. Heinrich, M. Klüppel, In: Filled elastomers drug delivery systems series: Advances in polymer science, ed.: K-S. Lee, Springer, Berlin, 2002.
- [125] J. Fröhlich, W. Niedermeier, H.-D. Luginsland, Compos. Part A Appl. S. 36 4 (2005) 449–460.

List of Figures

Figure 1.1 Process of reactive blending to obtain blend (-composite) based on rubber and <i>in-situ</i> synthesized PUU. Temperatures of premixing (T_{premix}) and reactive blending (T_{RB}) are obtained from the chemo-rheological measurements.....	4
Figure 2.1 A simplified representation of polymerization routes to polyurethane-urea: One-shot and prepolymer method [31].....	8
Figure 2.2 Main reactions of isocyanate with polyol and diamine to form polyurethane-urea via the prepolymer route	9
Figure 2.3 Graphical representation of morphologically diversified polyurethane-urea	10
Figure 2.4 Secondary addition reactions of isocyanate group with urethane- and urea-linkages of polyurethane-urea chains.....	10
Figure 3.1 Reactive blending process to prepare blend (-composite) based on rubber and <i>in-situ</i> synthesized PUU.	21
Figure 3.2 Internal mixer (Haake Rheomix 80ml), two roll mixing mill (Polymix 110 L) and compression moulding machine.....	22
Figure 3.3 ARES-G2 Rheometer showing parallel-plate test geometry	23
Figure 3.4 Rubber process analyzer: moving die rheometer (Scarabaeus SIS V50)	24
Figure 3.5 Transmission electron microscope (Libra 200 MC) by Carl Zeiss.....	25
Figure 3.6 Scanning electron microscope (NEON 40 EsB) by Carl Zeiss.....	26
Figure 3.7 Universal testing machine (Zwick 1456, Z010) by Zwick/Roell AG.....	27
Figure 3.8 Dynamic Mechanical Thermal Spectrometer (Eplexor 2000 N) by GABO Instruments	28
Figure 3.9 X-ray Diffractometer (XRD 3003 T/T) by GE Sensing & Inspection Technologies ...	29
Figure 3.10 Raman Imaging Microscope (alpha 300R) by WITec GmbH.....	29

Figure 4.1 Reactive blending process to prepare NBR/PUU blends. The temperatures of premixing and reactive blending are obtained from the chemo-rheological investigation of the premix.30

Figure 4.2 Storage modulus/ G' and loss modulus/ G'' versus temperature curves of a premix composed of PTMEG/MDI prepolymer and mPD chain extender.....31

Figure 4.3 Torque versus time curves of NBR and NBR/PUU blends reflect (I) the mastication of NBR, (II) the incorporation of premix and *in-situ* generation of PUU, and (III) the distribution of premix/*in-situ* generated PUU in rubber matrix, homogenization of blend components and steady level of final torque33

Figure 4.4 Overall reaction to the *in-situ* generated polyurethane-urea in presence of NBR in an internal mixer at 100°C and 70 rpm, $n=3.8$ (determined from ^1H NMR spectroscopy).34

Figure 4.5 ^1H NMR spectrum (region) of NBR/PUU 70/30 blend (solvent: DMSO- d_6) with formula of the PPU hard segment for signal assignment. PTMEG denotes the polytetrahydrofuran based soft segment. * marks the NBR signals.....35

Figure 4.6 TEM images of the NBR/PUU 70/30 blend. (a) Bright field image. (b) Carbon map. Note the thin dark borderline between the NBR and PUU phases, (c), (d), (e) amplitude, position and width of plasmon peak, respectively of the boundary region between the NBR.....37

Figure 4.7 SEM-EDX micrograph of NBR/PUU 70/30 blend.....38

Figure 4.8 Cure curves of NBR/PUU blends in comparison with neat NBR39

Figure 4.9 Stress-strain curves of neat NBR and its blends with *in-situ* synthesized PUU. The corresponding morphological sketches of the heterophase blends are also shown.40

Figure 4.10	Dynamic temperature sweep measurements reflect a concentration-dependent improvement in a) storage modulus/ E' and b) loss factor/ $\tan \delta$ of NBR/PUU blends	43
Figure 4.11	Hydrogen bonding interactions (mono- and bi-dentate) amongst segments of PUU phase in blends [84].....	44
Figure 4.12	X-Ray scattering scans of NBR/PUU blends in comparison with neat NBR.....	45
Figure 4.13	An exemplary TEM image (scale bar 500nm) of NBR/PUU 70/30 blend with the graphical representation of disorderly structured hard segment domains of <i>in-situ</i> synthesized PUU.....	46
Figure 4.14	Temperature-dependent viscoelastic response (storage modulus/ G' and loss modulus/ G'') of PP/MBCA premix	49
Figure 4.15	Temperature-dependent viscoelastic response (storage modulus/ G' and loss modulus/ G'') of PP/pXD premix	50
Figure 4.16	Development of viscoelastic response (storage modulus/ G' and loss modulus/ G'') during temperature ramp test of PP/mPD premix.....	51
Figure 4.17	Development of viscoelastic response (storage modulus/ G' and loss modulus/ G'') during temperature ramp test of PP/BisAM premix	52
Figure 4.18	Process of reactive blending to prepare blends from NBR and premixes of MDI/PTMEG prepolymer with mPD, pXD, MBCA and BisAM.....	53
Figure 4.19	Torque vs time profiles of a) Blend-MBCA, b) Blend-pXD, c) Blend-BisAM, d) Blend-mPD. The solid dot (●) and the asterisk (*) indicate pouring of premix and occurrence of polyaddition reactions respectively. The chemical structure and the characteristic features of the <i>in-situ</i> generated HS of PUU-mPD, -MBCA, -pXD	

	and –BisAM, as apprehended from the respective torque-time profiles, are also shown. The value of n is given in ^1H NMR section.	56
Figure 4.20	^1H NMR spectra (regions) of the PUUs extracted from a) Blend-mPD, b) Blend-BisAM, c) Blend-MBCA, and d) Blend-pXD. The top formula depicts the general PUU structure with different structures R depending on the used diamine. The formulas of the diamine-based end groups are given next to the spectrum. Hydrolysis of MDI results in the MDI end group (* marks 2'' (~6.5 ppm) and 3'' (~6.82 ppm)) which can react with MDI to form a MDI-NH-CO-NH-MDI urea bond (# marks the NH proton, overlapped in a) and b)). Solvent: DMSO- d_6 at 60°C.	60
Figure 4.21	Overall reaction to the <i>in-situ</i> synthesized PUUs in presence of NBR in an internal mixer. The value of n is given in table 4.6.	61
Figure 4.22	Cure curves of NBR and its blends with four different kinds of polyurethane-ureas	62
Figure 4.23	SEM images of the cryo-ultramicrotomed (smooth) and OsO $_4$ stained surfaces of blends (NBR is bright, PUU is dark) containing PUU-mPD, -pXD, -MBCA and -BisAM. The histogram of domain size distributions and the image of cryofractured surface are also shown as an overlay in the corresponding image. (The resolution of the images was reduced for publication. The original resolution is approx. 22 000 x 16 000 pixels ~ 350 megapixels for cryo-ultramicrotomed surfaces).	66
Figure 4.24	Stress-strain curves of NBR, Blend-mPD, Blend-pXD, Blend-MBCA and Blend-BisAM. The morphology of blends is graphically depicted.....	67
Figure 4.25	a) $\tan \delta$ versus temperature curves along with the glass transition region of soft segments (SS) and the order of structurally different PUUs with respect to chain	

flexibility, b) Storage modulus (E') vs temperature curves along with the photo of specimens after temperature sweep test.....	69
Figure 4.26 Wide-angle X-ray scattering scans of Blend-mPD, -pXD, -MBCA and -BisAM in comparison with NBR.....	70
Figure 4.27 Cure curves of neat rubbers and their blends with <i>in-situ</i> synthesized PUU. a) EPDM and EPDM/PUU, b) NR and NR/PUU, c) XNBR and XNBR/PUU, d) CR and CR/PUU, e) sSBR and sSBR/PUU.....	73
Figure 4.28 Stress-strain curves of compounds. a) EPDM and EPDM/PUU, b) NR and NR/PUU, c) XNBR and XNBR/PUU, d) CR and CR/PUU, e) sSBR and sSBR/PUU.	76
Figure 4.29 Temperature dependence of $\tan \delta$ and storage modulus. a). EPDM and EPDM/PUU, b). NR and NR/PUU, c). XNBR and XNBR/PUU, d). CR and CR/PUU, e). sSBR and sSBR/PUU.....	79
Figure 4.30 Raman spectra along with the corresponding Raman images as inset. a). EPDM/PUU, b). NR/PUU, c). XNBR/PUU, d). CR/PUU, e). sSBR/PUU blends. The continuous blue regions in Raman images represent rubber matrices (EPDM, NR, XNBR, CR, sSBR) and the dispersed red regions represent domains of <i>in-situ</i> synthesized PUU.	83
Figure 4.31 SEM-EDX images along with the respective EDX spectrum for EPDM/PUU, NR/PUU, XNBR/PUU, CR/PUU and sSBR/PUU blends. Elemental oxygen mapping identifies PUU domains in blends. In addition, mapping of elemental chlorine-Cl and Magnesium-Mg in CR/PUU, Sulfur-S in XNBR, sSBR and NR is considered.	86
Figure 4.32 Reactive blending process to prepare CB filled composites based on NR and premix of PTMEG / MDI prepolymer and mPD. The temperatures of premixing and	

reactive blending are obtained from the chemo-rheological analysis (see section 4.1.1).	88
Figure 4.33 TEM micrographs of CB filled composites. a). NR-CB, b). NR/PUU-CB	89
Figure 4.34 DMA curves of neat NR and its composites: NR-CB and NR/PUU-CB. a) Loss factor vs. temperature, b) loss and storage modulus vs. temperature curves	91
Figure 4.35 Graphical representation of interfacial interactions between NR and the reinforcing inclusions i.e. PUU and CB in NR/PUU-CB composite [107]	92
Figure 4.36 Dependence of storage modulus on strain amplitude for NR, NR-CB and	94
Figure 4.37 NBR/PUU blend-covered roller	95
Figure 4.38 Experimental rig to examine thermo-mechanical behavior of NBR/PUU blend-covered roller. The upper test rubber roller and the lower corrugated drive roller are shown.	96
Figure 4.39 Thermal image of the running NBR/PUU roller is shown. Temperature distribution according to the color temperature scale in Celsius scale can be seen.	97
Figure 4.40 Curves of flexometer test. The final surface and core temperatures of specimens are as inset table. The core temperature is measured by using a thermocouple, as is shown in a photo of flexometer test setup	97
Figure 4.41 The tested NBR/PUU blend-covered roller. Roller retains integrity without any surface cracks	98

List of Tables

Table 4.1 Formulations and designations of compounds are given. Quantities of curatives are in parts per hundred parts of blend.	30
Table 4.2 Mechanical properties of compounds with and without in-situ synthesized PUU	42
Table 4.3 Dynamic mechanical characteristics of NBR and NBR/PUU blends as obtained from the storage modulus/tan δ vs temperature curves.....	44
Table 4.4 Composition of compounds along with the stoichiometric quantities of prepolymer and diamine*	47
Table 4.5 Characteristic temperatures obtained from the chemo-rheological investigation of PP/mPD, PP/pXD, PP/MBCA and PP/BisAM premixes.....	52
Table 4.6 Summary of GPC and ¹ H NMR analysis	59
Table 4.7 Recipe ingredients of compounds in parts per hundred parts (in weight) of rubber (phr)	71
Table 4.8 Cure characteristics of compounds as obtained from their respective cure curves.....	74
Table 4.9 Tensile characteristics of neat rubbers and their blends with in-situ PUU, The modulus values represent stresses at X% deformation.	77
Table 4.10 Dynamic-mechanical characteristics of compounds as obtained from their respective temperature sweep test.	80
Table 4.11 Recipe of compounds with quantities in parts per hundred parts of rubber.....	88
Table 4.12 Formulation of compounds with quantities in parts per hundred parts of rubber	95

Publications

Patents:

- **Tahir M**, Mahmood N, Stöckelhuber KW, Heinrich G, Das A, Jurk R. Blends of thermoplastic polyurethanes and rubbers and process for producing same, Publication No. WO 2015032681 A1, 2015.
- **Tahir M**, Stöckelhuber KW, Wießner S. Partikelförmiges Kohlenstoffmaterial herstellbar aus nachwachsenden rohstoffen und Verfahren zu dessen Herstellung. German patent application together with SunCoal Industries GmbH, submitted (2016).

Journal Articles:

- **Tahir M**, Stöckelhuber KW, Mahmood N, Komber H, Heinrich G. Reactive Blending of Nitrile Butadiene Rubber and In situ Synthesized Thermoplastic Polyurethane-Urea: Novel Preparation Method and Characterization. *Macromol Mater Eng* 2015; 300: 242-50.
- **Tahir M**, Stöckelhuber KW, Mahmood N, Komber H, Formanek P, Wießner S, Heinrich G. Highly reinforced blends of nitrile butadiene rubber and in-situ synthesized polyurethane-urea. *Eur Polym J* 2015; 73:75-87.
- Le HH, Das A, Barak S, **Tahir M**, Wießner S, Fischer D, Reuter U, Stöckelhuber KW, Bhowmick AK, Do Q K, Heinrich G, Radosch H J. Effect of different ionic liquids on the dispersion and phase selective wetting of carbon nanotubes in rubber blends. *Polymer* 2016; 105: 284-97
- Tiwari A, Dorogin L, Bennett AI, Schulze KD, Sawyer WG, **Tahir M**, Heinrich G, Persson BNJ. The effect of surface roughness and viscoelasticity on rubber adhesion. *Soft Matter* 2017; 13: 3602-3621.

Oral Presentations:

- Stöckelhuber KW, **Tahir M**, Das A, Mahmood N, Heinrich G. Enhanced Mechanical and Dynamic-Mechanical Properties of Blends Composed of Nitrile Butadiene Rubber and in-situ Synthesized Polyurethane-urea via Precursor Route. POLYCHAR 22 World Forum on Advanced Materials, 7-11 April 2014, Stellenbosch, South Africa

- **Tahir M**, Stöckelhuber KW, Mahmood N, Komber H, Heinrich G. Novel blends and Blend Nano-composites Based on in-situ Synthesized Thermoplastic Polyurethane-urea and Nitrile Butadiene Rubber. Nanostruc, 20-21 May 2014, Madrid, Spain
- **Tahir M**, Stöckelhuber KW, Mahmood N, Heinrich G. Characterization and properties of novel blends composed of nitrile butadiene rubber and in-situ synthesized thermoplastic polyurethane-urea. 27th International Symposium on Polymer Analysis and Characterization, 16-18 June 2014, Les Diablerets, Switzerland
- **Tahir M**, Stöckelhuber KW, Mahmood N, Heinrich G. Novel preparation method and properties of the blends based on nitrile butadiene rubber and in-situ synthesized thermoplastic polyurethane-urea. PolyMerTec, 25-27 June 2014, Merseburg, Germany
- **Tahir M**, Stöckelhuber KW, Mahmood N, Heinrich G. A new method of preparation and properties of blends based on in-situ synthesized thermoplastic polyurethane-urea and nitrile butadiene rubber. 11th Fall Rubber Colloquium, 26-28 November 2014, Hannover, Germany
- **Tahir M**, Stöckelhuber KW, Mahmood N, Wießner S, Heinrich G. Highly reinforced blends based on in-situ synthesized polyurethane-urea and nitrile butadiene rubber, 187th Technical Meeting, ACS, 28-30 April 2015, Greenville, SC, USA
- **Tahir M**, Stöckelhuber KW, Wießner S, Heinrich G. Novel blends of rubber and in-situ polyurethane-urea: Role of structure of chain extender, Type of rubber and Carbon black Loading, Eurofillers Polymer Blends, 23-27 April 2017, Crete, Greece.

Poster Presentations:

- **Tahir M**, Stöckelhuber KW, Mahmood N, Heinrich G. Blends of in-situ synthesized Thermoplastic Polyurethane-Urea and Nitrile Butadiene Rubber. 4. Dresdner Werkstoffsymposium 2013: Verbundwerkstoffe und Werkstoffverbunde, 18-19 Nov. 2013, The Westin Bellevue Hotel, Dresden, Germany.
- **Tahir M**, Stöckelhuber KW, Mahmood N, Heinrich G. Novel Blend Nano-Composites based on in-situ Synthesized Thermoplastic Polyurethane-urea and Nitrile Butadiene Rubber, Turkey-Germany Workshop on Polymeric Nanocomposites, 29-31 August 2014, ITU, Istanbul, Turkey
- **Tahir M**, Stöckelhuber KW, Mahmood N, Heinrich G. Characterization of Nitrile Butadiene Rubber/ in-situ polyurethane-urea blends: Mechanical, structural and Morphological Aspects. European Polymer Congress, 21-26 June 2015, Dresden, Germany